UNIVERSITY OF CAPE TOWN
IYUNIVESITHI YASEKAPA • UNIVERSITEIT VAN KAAPSTAD

Implementation of a Fully Variable Valve Actuation Valvetrain

Author:
Mr. Steven Jaffa

Supervisor:
Dr. Gareth Floweday

Co.Supervisor:
Prof. Andrew Yates

A dissertation submitted to the Department of Mechanical Engineering, University of Cape Town, in partial fulfilment of the requirements for the degree of Master of Science in Engineering.

May 25, 2011

Acknowledgments

The author would like to extend his thanks to the following people for their contributions and assistance in this project:

Dr. Gareth Floweday – Project Supervisor

Prof. Andrew Yates – Co-supervisor

Mr. Paul Jaffa – Editor (Father)

Mr. Nicholas Savage – Sasol Advanced Fuels Laboratory

Mr. Mark Wattrus – Sasol Technology

Mr. Gavin Tomlinson – Sasol Advanced Fuels Laboratory

Workshop Staff – University of Cape Town

Sasol Technology – Sasol Advanced Fuels Laboratory

Plagiarism Declaration

1. I am aware that plagiarism is wrong. Plagiarism is using someone else's work and pretending it is one's own.
2. I have used the IEEE convention for citation and referencing. Each significant contribution to and quotation in this report, which has been taken from the work or works of other people, has been attributed, cited and referenced.
3. This project and report is my own work.
4. I have not allowed, and will not allow, anyone to copy my work with the intention of passing it off as his or her own work.

Author:
Steven Jaffa

May 25, 2011

Executive Summary

In January 2008 the Sasol (Pty) Ltd Advisory Board identified that the Sasol Advanced Fuels Laboratory's (SAFL) single cylinder research engine was not in line with the current engine technologies, in particular Fully Variable Valve Actuation (FVVA). This project represented the first stage of the engine upgrade, which was to modify the current single cylinder engine to interface with pneumatic valve actuators and a fully configurable Engine Control Unit (ECU).

The engine that was used for the development of the FVVA valvetrain was the single cylinder Ricardo Hydra research engine. The Cargine actuators were pneumatic-hydraulic actuators, which were electrically controlled via the Field-Programmable Gate Array (FPGA) ECU and computer.

A custom mounting was fabricated to mount the FVVA actuators, sensors and related systems to the cylinder head. A new dummy camshaft was designed to facilitate the use of the original engine phase sensor and was operated using the original cambelt and pulley configuration. In addition, new valve springs and spring retainers had to be designed to fit inside the FVVA valvetrain. Custom software was written, which enabled the operator to use a computer to control and monitor the engine, FVVA valvetrain and their subsystems.

The commissioning of the engine was divided into the following three stages: commissioning of the FVVA valvetrain, commissioning of the Hydra engine without FVVA, and running the engine with the FVVA valvetrain. The following conclusions were drawn from the results of the experimentation and commissioning of the FVVA engine.

- The FVVA valvetrain and its subsystems were successfully implemented and incorporated with the single cylinder Ricardo Hydra engine en-

abling the Hydra engine to operate in compression ignition, spark ignition or Homogeneous Charge Compression Ignition (HCCI) combustion.

- The FVVA valvetrain was effectively used to demonstrate the advantages of FVVA technology using different valve timing strategies and to produce an optimised power and torque curve for the SI engine configuration.
- HCCI combustion was successfully achieved with the aid of the FVVA valvetrain and the use of Early Inlet Valve Closing (EIVC) to capture hot residual in-cylinder gas. As part of the HCCI validation, a number of specific points in the HCCI operating envelope were defined.

Table of Contents

List of Figures

List of Tables

List of Symbols

Symbol	Detail
ABDC	After Bottom Dead Centre
ATDC	After Top Dead Centre
AFR	Air/Fuel Ratio
BBDC	Before Bottom Dead Centre
BTDC	Before Top Dead Centre
BDC	Bottom Dead Centre
bsfc	break-specific fuel consumption
CAD	Crank Angle Degree
CAT	Crank Angle Tick
CC	Constant Current
CI	Compression Ignition
CIDI	Compression Ignition Direct Injection
CO	Carbon Monoxide
CO_2	Carbon Dioxide
CV	Constant Voltage
DBTDC	Degrees Before Top Dead Centre
DI	Direct Injection
ECU	Electronic Control Unit
EGR	Exhaust Gas Recirculation/Re-breathing
EEVC	Early Exhaust Valve Closing
EEVO	Early Exhaust Valve Opening
EIVC	Early Inlet Valve Closing
EIVO	Early Inlet Valve Opening
EVO	Exhaust Valve Opening
EVC	Exhaust Valve Closing
FIFO	First In, First Out
FPGA	Field-Programmable Gate Array

Symbol	Detail
FVVA	Fully Variable Valve Actuation
GUI	Graphical User Interface
HC	Hydrocarbon
HCCI	Homogeneous Charge Compression Ignition
HRR	Heat Release Rate (J/CAD)
I/O	Input/Output
IC	Integrated Circuit
IVO	Inlet Valve Opening
IVC	Inlet Valve Closing
LEVC	Late Exhaust Valve Closing
LEVO	Late Exhaust Valve Opening
LIVC	Late Inlet Valve Closing
LIVO	Late Inlet Valve Opening
NO	Nitric Oxide
NOx	Nitrogen Oxides
OEM	Original Equipment Manufacturer
P	Cylinder Pressure (bar or kPa)
PC	Personal Computer
PID	ProportionalIntegralDerivative
PM	Particulate Matter
REG	Residual Exhaust Gas
RON	Research Octane Number
RPM	Revolutions Per Minute
RT	Real-Time
sfc	Specific Fuel Consumption (g/kW.h)
SI	Spark Ignition
SIDI	Spark Ignition Direct Injection
TDC	Top Dead Centre
V	Volume (m^3)
VI	Virtual Instrument
VVA	Variable Valve Actuation
VVT	Variable Valve Timing
WOT	Wide Open Throttle
η	Efficiency
Δ**T**	Temperature Change
λ	Air/Fuel Ratio
ϕ	Fuel/Air Ratio

Glossary of Terms

Air/Fuel Ratio (AFR): The ratio between the air mass flow $\dot{m}_a$ and the fuel mass flow $\dot{m}_f$, which is used to define the engine's operating conditions. The inverse of this is the Fuel/Air Ratio.

$$Air/FuelRatio(A/F) = \frac{\dot{m}_a}{\dot{m}_f}$$

$$Fuel/AirRatio(F/A) = \frac{\dot{m}_f}{\dot{m}_a}$$

Auto-ignition: The spontaneous combustion reaction of a fuel and an oxidiser which is not initiated by any external mechanism.

Engine Knock: This refers to the spontaneous ignition of a portion of the unburned end-gas air and fuel in the combustion chamber. This causes high pressure shock waves that propagate through the combustion chamber, which can seriously damage the engine. The name is derived from the "pinging" or "hammering" sound that can be heard through the engine's structure.

Equivalence Ratio (ϕ): The ratio between the F/A ratio at operating conditions and F/A ratio of a stoichiometric mixture. $\phi = 1$ indicates a stoichiometric fuel/air ratio. $\phi < 1$ indicates excess air and $\phi > 1$ indicates excess fuel.

$$\phi = \frac{F/A_{acutal}}{F/A_{stoichiometric}}$$

λ is the inverse of the equivalence ratio ϕ where the A/F ratio is used instead for the calculation.

$$\lambda = \frac{A/F_{acutal}}{A/F_{stoichiometric}}$$

Exhaust Re-compression: This refers to a valve timing technique that is used to trap exhaust gas and reduce exhaust emissions. The exhaust valve is closed early in the exhaust stroke, which causes the trapped exhaust gas to be compressed during the final portion of the exhaust stroke. The gas is then expanded during the intake stroke and mixes with the fresh charge of mixture.

Exhaust Re-breathing: This refers to a valve timing technique that is used to trap exhaust gases and reduce exhaust emissions. The inlet valve is opened early in the exhaust stroke, which allows exhaust gas to flow into the inlet manifold. Then, in the following cycle the exhaust gas is "re-breathed" into the combustion chamber with a fresh charge of mixture.

Heat Release Rate (HRR): This is defined as the amount of energy released every CAD, or second, due to combustion (J/CAD or J/s).

Homogeneous Charge: A mixture of air and fuel, which has a uniform composition throughout the mixture.

Ignition Delay: The time taken from the point of the fuel injection to the point when ignition occurs, which is measured in CAD or ms.

Mean Effective Pressure (MEP): A theoretical average pressure that if applied over the engine's cycle, will produce the same amount of work. This is a useful method to compare the effectiveness of engines of different sizes.

$$mep(kPA) = \frac{Pn_R}{V_d N}$$

Miller Cycle: In a Miller Cycle engine the inlet valves are only closed well into the compression stroke. This reduces the effective compression ratio of the engine as some of the fresh charge will be expelled back into the inlet manifold.

Stoichiometric Mixture: A mixture of air and fuel with the correct ratio of reactant that will combust to completion, whereby all reactants are consumed.

Volumetic Efficiency: Volumetric efficiency is a parameter that is used to measure the effectiveness of an engine's induction process and is defined as the mass of air inducted into the engine's combustion chamber per engine cycle. The volumetric efficiency of an engine can be reduced by the air filter, carburetor, intake manifold, intake ports and intake valves. The following equation defines the volumetric efficiency as the volume flow rate of air into the cylinder divide by the maximum theoretical rate at which the piston displaces volume, where m_a is the mass flow rate of air, $\rho_{a,i}$ is the inlet air density, V_d is the displaced cylinder volume and N is the engine speed.

$$\eta_v = \frac{2m_a}{\rho_{a,i} V_d N}$$

Chapter 1

Introduction

1.1 Background

Over the past 20 years, engine manufacturers and fuel producers have been put under intense pressure by legislators to reduce vehicle emissions, while still satisfying consumers' desires for fast, high power vehicles. In addition, the increasing price of fuel and the threat that crude derived fuels will run out in the near future, have further intensified pressure to reduce fuel consumption. These opposing requirements have forced engine OEMs (Original Equipment Manufacturer) to devise various after-treatment systems to reduce emissions and to improve the in-cylinder combustion processes. One of the possible solutions is an advanced combustion process called Homogeneous Charge Compression Ignition (HCCI).

HCCI combustion has offered the possible solution of concurrently reducing exhaust emission and fuel consumption. However, there are various challenges in controlling the combustion of an HCCI engine. The composition of the fuel being used for HCCI has been identified as a promising method for combustion control. Being a synthetic fuel producer, Sasol (Pty) Ltd is in a unique position to specifically design the composition of its fuel to aid with the control of auto-ignition and combustion phasing.

In January 2008 the Sasol Advisory Board identified that Sasol Advanced Fuels Laboratory's (SAFL) single cylinder research engine was not in line with the current engine technologies that were incorporated in modern day vehicles. As a result, it would not be possible to perform respectable future

orientated fuels research without the latest engine technologies. HCCI is accepted to be a vital part of the future of internal combustion engines and was therefore targeted for the hardware upgrades. Since "off the shelf" solutions were found to be prohibitively expensive, a cost effective solution had to be found. One of the technologies that the engine was lacking was Fully Variable Valve Actuation (FVVA). FVVA is a powerful mechanism for controlling engine breathing and combustion, which in turn can reduce exhaust emissions, improve fuel consumption and increase engine torque.

FVVA offers the following advantages over standard camshaft operated valves [1]:

1. Optimization of the valve event timing, duration and lift over the entire engine speed range to improve the engine's power output (Volumetic Efficiency).
2. Variable effective compression ratio (Miller Cycle).
3. Internal exhaust gas recirculation for emissions control (Exhaust Rebreathing or Re-compression).
4. Reduced flow losses by eliminating the need for a throttle valve (variable lift height).

The first stage of the proposed engine upgrade was to combine the current single cylinder engine with pneumatic valve actuators from Cargine Engineering AB and a configurable Electronic Control Unit (ECU) system from National Instruments Corporation and Drivven, Inc. The valve actuators were not purchased with a control system, so this stage of the upgrade included developing the system integration of the Hydra engine, the valve actuators and the control hardware and software.

1.2 Objectives

The following objectives were outlined for this project:

1. Conduct a detailed literature review on variable valve timing technologies and HCCI combustion.

2. Design and fabricate suitable modifications to the engine to mount the valve actuators.
3. Set up the services (air, lubrication, etc.) required by the actuators.
4. Replace the current ECU with a customizable CompactRIO FPGA ECU and set up the control hardware required for the actuators.
5. Incorporate existing hardware requirements into the new control system (e.g. fuel injection and spark timing).
6. Design a user interface for the control system.
7. Configure the control hardware and software.
8. Program a "simulation mode" operation to enable testing of the valvetrain (on the cylinder head) without running the engine.
9. Set up safety measures in the control system to prevent user error resulting in damage to the valvetrain or engine.
10. Perform maintenance and repairs on the current single cylinder test engine and test cell.
11. Commission the FVVA valvetrain and subsystems and integrate the valvetrain with the Ricardo Hydra test engine.
12. Perform validation testing of the valvetrain and demonstrate its capabilities for SI operation.
13. Operate the FVVA engine in HCCI mode and demonstrate its usefulness for HCCI combustion control.
14. Write a user manual on the operation of the valvetrain control system.

1.3 Thesis Outline

This report begins with a detailed literature review on variable valve timing and valve strategies. The literature review also contains a brief description of HCCI combustion, outlining the advantages, disadvantages and control methods. There follows a description of the engine and the test cell's subsystems, including the FVVA valvetrain. Chapter 4 covers the process of

designing the new systems and the modification to the engine that were required to implement the new FVVA valvetrain. Chapter 5 explains the process of commissioning the FVVA valvetrain, overhauling the Hydra engine, integrating the new valvetrain and FPGA ECU with the engine and finally running the engine in SI and HCCI mode. The chapter following is a comprehensive discussion on the results that were obtained from commissioning the valvetrain and from the SI and HCCI testing. Finally, conclusions are drawn from the results of the engine and valvetrain commissioning and testing, and a number of recommendations are put forward with respect to the outcomes of this project and any future work.

The following appendices appear at the end of this dissertation as additional information: Appendix A covers the operation of the Cargine actuators, the way they work, the way in which they were controlled, and the required subsystems for their operation. Appendix B is an explanation of the custom LabVIEW control software and ECU. Appendix C covers in detail the various subsystems that make up the test cell and experimental apparatus. Appendix D is a user manual for the operation of the FVVA valvetrain and Hydra engine. Appendix E lists safety precautions that were taken during experimentation. Finally, Appendix F contains the technical drawings for the FVVA valvetrain, Cargine Actuators and MicroStrain sensors.

Chapter 2

Literature Review

2.1 Fully Variable Valve Actuation

2.1.1 Introduction to FVVA

In general, the inlet and exhaust valves of internal combustion engines are actuated via camshafts, which have fixed profiles and are linked to the crankshaft with a belt or chain drive. Thus the valves have a predetermined lift height and opening and closing points in relation to the crankshaft's rotation. The cam profiles are typically optimised for the engine speed that is most frequently used and for the purpose of the engine [2]. As a result, a compromise has to be made in order to maintain stable operation during idling, and good performance at high engine speeds. Hong *et al.* provides an extensive review of this subject [1].

From the earliest internal combustion engines, it was known that having fixed cam profiles was not an efficient method of operation, and that the most advantageous solution would be the ability to control all aspects of the valves' actuation at any engine speed [3]. This lead to the concept of Fully Variable Valve Actuation (FVVA), which is the ability to control and adjust the lift height, timing, phasing and rate of actuation of the valves. However, only since the 1980s has this vision been realised with breakthroughs in computing power, electronic engine control, machining and various other technologies [4].

The motion of valves (timing, height, etc) has a significant effect on the engine's efficiency and exhaust emissions [5], and therefore the ability to control the actuation of an engine's valves offers several advantages over conventional engines with fixed camshaft and profiles. FVVA allows the engine to be optimised for the engine's entire speed and load range which results in increased fuel efficiency, low-end torque, high-end power and lower exhaust emissions [1].

2.1.2 Advantages and Disadvantages of VVA

A key advantage that VVA has over a conventional spark ignition (SI) engine is the reduction in pumping losses [1, 6]. Pumping losses occur when a fluid flowing though a pipe is forced around a bluff body inside the pipe. In the engine cycle this occurs during the intake stroke, when sub-atmospheric pressure gas is inducted into the engine, and during the exhaust stroke, when exhaust gas is expelled out of the combustion chamber. The amount of energy lost is dependent on the position of the throttle valve and thus the degree to which the throttle valve impedes the gas flow. At WOT the losses are low as the valve is only a small obstruction. However, the losses are at a maximum during idling when the throttle is almost closed [1, 7]. VVA allows for the elimination of the throttle valve as the inlet and exhaust flow can easily be regulated by changing the lift height or duration of the valves. The inlet valve timing is the most important factor for optimising the volumetric efficiency of the engine [1, 6, 8, 9].

Another significant advantage of VVA is the ability to control the Residual Exhaust Gas (REG) and thus greatly reduce exhaust emissions, particularly Nitrogen Oxide (NOx) emissions. REG is controlled by the exhaust valve timing and the amount of overlap between the exhaust and inlet valves [1, 6].

Despite the benefits that VVA offers, there are a number of difficulties with its implementation, which have been discussed in various references [1, 4, 6, 10]:

1. High power consumption.
2. Accuracy and repeatability at high engine speeds.
3. Weight and packaging.
4. Increased engine noise compared to cam operated valves.
5. Very high cost.
6. Possibility of engine damage in the case of electrical control or power failures.

2.1.3 Methods for Achieving VVA

There are a number of different methods for achieving VVA and controlling the different parameters: valve event timing, duration, and lift height. These systems can be divided into two primary categories: camshaft driven and camless VVA. The website Autozine.org provides a comprehensive review and discussion of the various systems that are being used by vehicle manufactures [4].

Camshaft Driven VVA

Engine manufacturers currently employ a number of camshaft driven methods (mechanical system) as these are the cheapest and easiest systems to implement [4]. However, these systems have the least amount of flexibility in terms of variable lift height, timing and duration [11]. The camshaft driven systems can be further separated into cam-phasing and cam-switching technologies.

Cam-phasing uses a hydraulic valve gear to rotate the camshaft relative to the crankshaft, which changes the phase angle of the camshafts [6, 12]. This allows for the valves to be opened earlier (advanced timing) or later (retarded timing) and also to increase or decrease the amount of valve overlap. The first instances of cam-phasing, such the BMW VANOS, were only applied to the inlet valve camshaft and had two or three fixed angles. However, they have since been further developed so that the phase angle of both the inlet and exhaust camshafts can be infinitely varied according to the engine's speed, load and acceleration requirements (e.g. Toyota VVT-i and BMW Double VANOS) [4].

Cam-phasing is the most widely used mechanical method of VVA as it is the simplest and cheapest of all the systems to implement[4]. This is because only one hydraulic actuator is needed for each camshaft. However cam-phasing offers the least gain in performance compared to the other systems. The significant limiting aspect of the system is that it cannot change the maximum valve lift or the duration of the valve events. Figure 2.1 shows the cam-phasing system of the BMW Double VANOS.

As the name suggests, the cam-switching mechanism has a number of cam profiles that it is able to alternate between, depending on the engine

speed. The cam profiles are optimised over a small speed range and are generally configured to switch at a particular engine speed. In the Honda VTEC system this is done by locking/unlocking the cams together using hydraulically actuated pins.

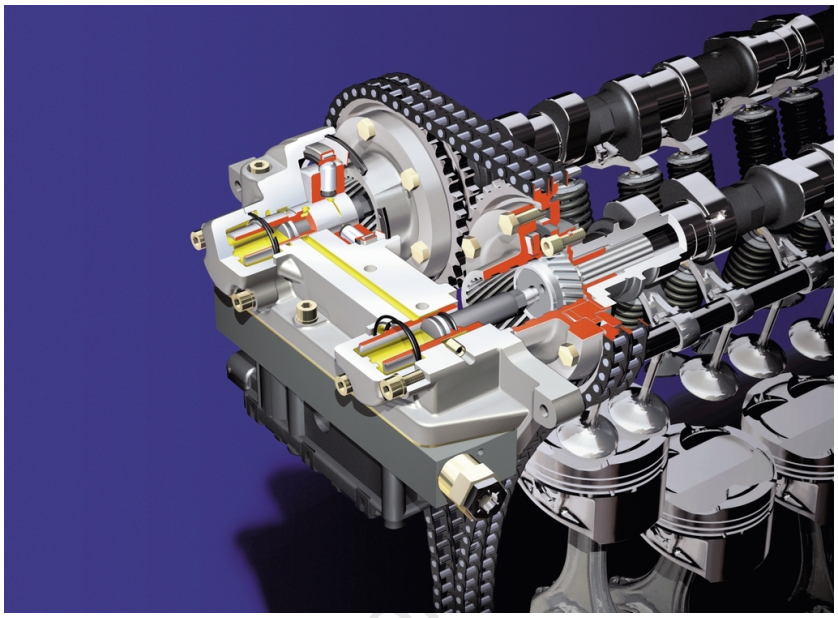

Figure 2.1: Internal Mechanism of BMW's Double VANOS Cam-Phasing System [13].

Honda first introduced their VTEC system in the 1980s. The VTEC system had two different cam profiles for the inlet valves, which the ECU could switch between at 4500 rpm [4, 11]. Honda have since improved their system to have three cam profiles: slow engine speed and low lift, slow engine speed and medium lift, and fast engine speed and high lift.

The main advantage of this system is that it can significantly increase peak power output. However, these systems are very complex and they are not continuously variable. They also take up a large amount of space on the cylinder head [12].

Honda and Toyota have subsequently combined each of their cam-phasing and cam-switching technologies, which are respectively called i-VTEC and VVTL-i. These systems offer continuous cam-phasing, 2-stage variable valve lift and opening duration and are applied to both the inlet and exhaust valves [14, 15]. The "i" in the naming of the technologies stands for "intelligent", which means that the ECU determines the optimal cam profiles and cam-

phasing based on the engine's speed, load and acceleration requirements. These systems are consequently even more expensive and complicated to implement [4, 14, 15].

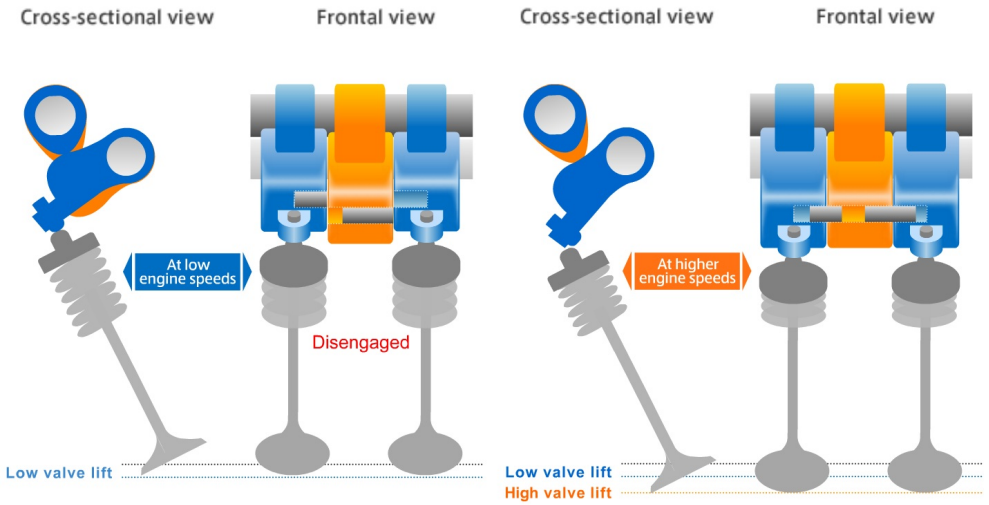

Figure 2.2: Internal Mechanism of Honda's VTEC Cam-Switching System [16].

The latest camshaft driven VVA system is termed Continuous Variable Valve Lift (CVVL). BMW call their system Valvetronic, and in 2001 they were the first to release this type of system. Subsequently, Nissan and Toyota each released their own versions called Variable Valve Event and Lift (VVEL, 2007) and Valvematic (2008) respectively [4]. Each system uses an eccentric cam and lever mechanism as an intermediate system between the camshaft and valve lifter to vary the maximum valve lift [4, 15]. Figure 2.3 shows a diagram of the Toyota Valvematic system.

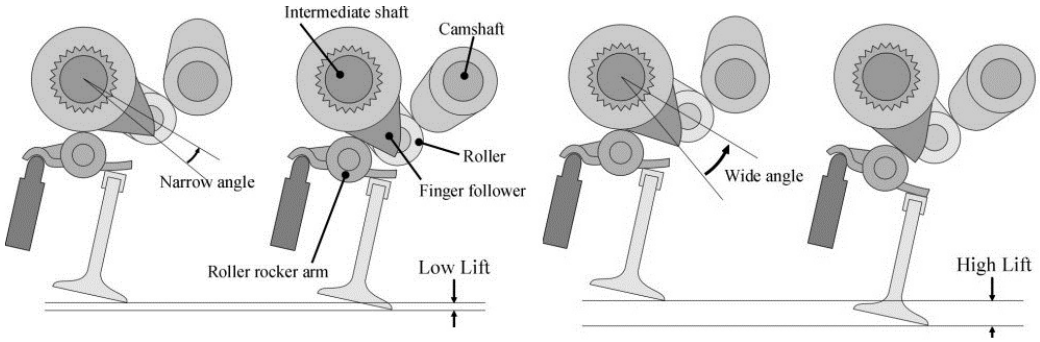

Figure 2.3: Internal Mechanism of Toyota's Valvematic System [4].

The Toyota Valvematic is the most advanced of the three systems, and in addition, incorporates Toyota's VVT-i system on both the inlet and exhaust valves for extra versatility. Valvematic is able to vary the maximum lift from 0.97 mm to 11 mm [4, 17]. Valvematic has the following advantages: very compact design (BMW's Valvetronic occupied a lot of space over the cylinder head), increased engine power output, reduced fuel consumption (elimination of throttle valve reduces pumping losses), and its mechanism is significantly less complicated than that of the Valvetronic and VVEL systems [4, 17].

Camless VVA

There are two main types of camless VVA systems: electromagnetic and electrohydraulic. These technologies have more versatility over camshaft driven VVA. However, they are generally more complex systems, very expensive and require a lot more power (additional pumps, compressors, solenoids and electrical hardware) [6, 12]. They also have their own specific challenges.

Electromagnetic VVA systems generally use solenoids or piezo actuators in conjunction with springs and highly complex control software to actuate the poppet valves [11]. Some of the challenges associated with these systems are: implementing variable lift (generally not possible), accurate timing of valve events, and high valve seating velocity [11, 12]. In addition, electromagnetic VVA systems create a lot of electrical noise and are limited by their minimum valve opening duration and a maximum engine speed of 7000rpm. This is due to the amount of time it takes for the actuator to charge and discharge [11].

Electrohydraulic VVA systems use a hydraulic piston and fluid to actuate the poppet valves, which are returned to their seats using valve springs. The flow and pressure of the hydraulic fluid is controlled using high speed solenoids, check valves and special control software.

Electrohydraulic VVA has the highest flexibility it terms of variable lift height, duration and timing, when compared to camshaft driven and electromagnetic systems [12, 18]. These systems are also the most complicated and expensive to implement. The hydraulic servo is the most expensive part of the system, and they are therefore prohibitively expensive for commercial engine applications [18].

2.1.4 Intake and Exhaust Timing Strategies

The following section describes the valve events that occur during a four-stroke SI (see Figure 2.4) engine cycle and the various intake and exhaust timing philosophies that are possible with FVVA.

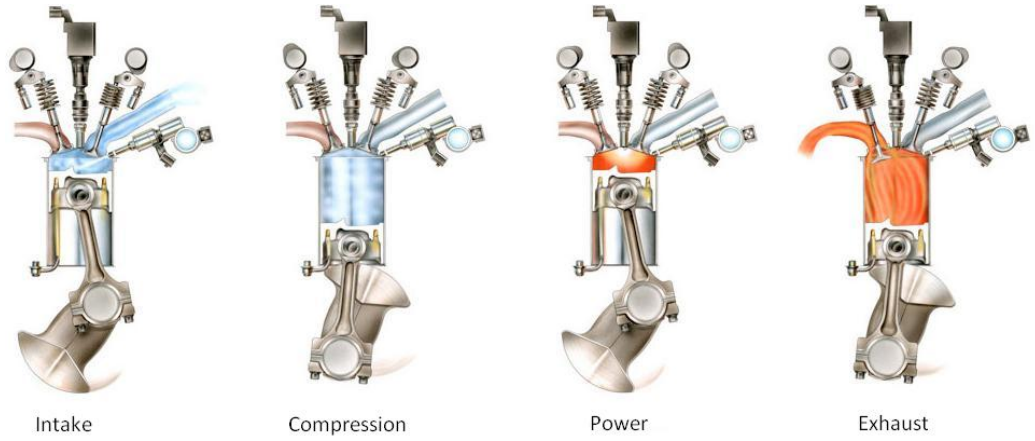

Figure 2.4: Four-Stroke Cycle of a Spark Ignition Engine [19].

Valve Events

Inlet Valve Opening (IVO) is the point at which the inlet valve opens for the induction phase of the engine cycle where a fresh charge of air and fuel is drawn into the cylinder. It also signifies the start of the inlet and exhaust valve overlap. IVO generally takes place 10° to 20° before TDC (Top Dead Centre) during the exhaust stroke [20].

Exhaust Valve Closing (EVC) occurs once most of the exhaust gas has been expelled from the combustion chamber. This is the point at which the exhaust phase and valve overlap ends. EVC generally takes place 10° to 30° after TDC during the intake stroke [20].

Inlet Valve Closing (IVC) is the point at which the inlet valve closes, and signifies the end of the induction phase and the beginning of the compression phase. IVC generally takes place 50° to 70° after BDC (Bottom Dead Centre) during the compression stroke [20]. The valve is closed during the beginning of the compression stroke in order to maximise the amount of fresh charge that is inducted into the combustion chamber. Even though the piston is

moving upwards, the cylinder's pressure is relatively low at the beginning of the stroke and so the momentum of the gas can drive extra charge into the cylinder before the cylinder's pressure increases and starts pushing the gas back out.

Exhaust Valve Opening (EVO) designates the end of the combustion phase and the start of the exhaust phase. EVO generally takes place 40° to 60° before BDC during the combustion stroke [20].

The following figure shows a standard valve timing diagram in relation to the PV diagram for a conventional SI engine.

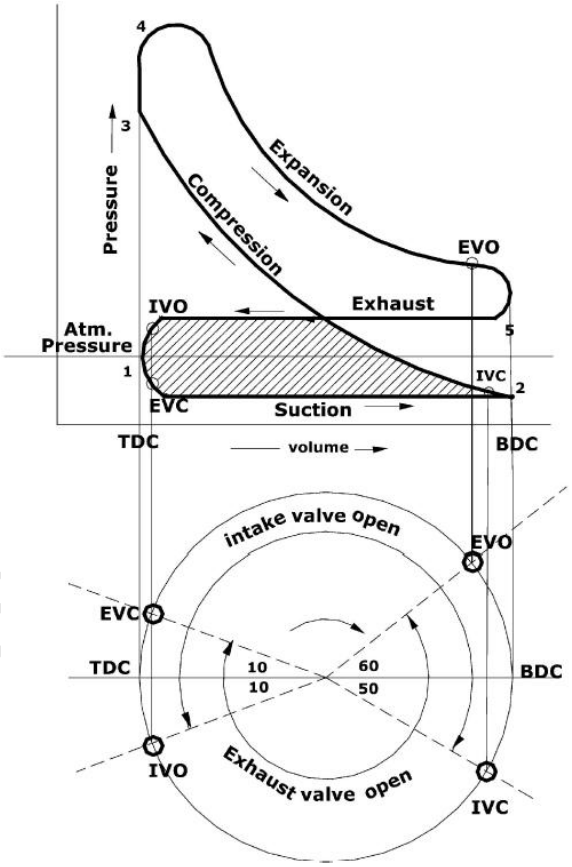

Figure 2.5: Valve Timing Diagram in Relation to a PV Diagram for a Conventional SI Engine [1].

Late Inlet Valve Closing (LIVC)

In conventional SI engines the inlet valve is normally closed at the beginning of the compression stroke. However, in the LIVC strategy, the inlet valve is closed slightly later in the compression stroke and results in some of the air/fuel mixture being pushed back into the inlet manifold. This increases the pressure inside the manifold, and consequently it will be slightly higher than atmospheric pressure. Therefore, when the air/fuel mixture is re-entrained during the next cycle it will be at a higher than normal pressure. The pumping losses will be reduced because the engine creates less of a vacuum while sucking the mixture into the combustion chamber. LIVC has shown to reduce pumping losses by 40% and nitric oxide (NO) emissions by 24% during partial load [1].

Over the years, a substantial amount of research has been carried out in the area of LIVC strategy. In these particular cases LIVC was not achieved by using VVA, but instead by driving the camshaft using a variable geometry timing belt, fitting additional camshafts, physically changing the camshafts or by some other mechanical solution. The following list summarises the various observations and conclusions that were presented in the research papers.

IVC is the most sensitive parameter for changing the breathing characteristics of an engine [8]. LIVC increases the volumetric efficiency at high engine speeds because the high flow-momentum of the mixture continues to fill the combustion chamber during the compression phase. However, LIVC will reduce the volumetric efficiency at low engine speeds because the inlet manifold and combustion chamber have the same pressure at BDC. Consequently, this will allow the air/fuel mixture to be pushed back into the inlet manifold during the compression phase [8, 21]. Therefore, the timing of IVC is very important in regulating the amount of fresh charge trapped in the cylinder, and will have a significant effect on engine performance and fuel efficiency [6].

The following advantages can be gained by using LIVC: the engine's specific fuel consumption (sfc) can be reduced, NOx production reduced, and both fuel conversion efficiency and combustion efficiency improved [22, 23]. In addition exhaust gas recirculation can be used to help reduce NOx, unburned hydrocarbon (HC) emissions and pumping losses. In a four valve per cylinder engine, tumble can be induced inside the combustion chamber by having symmetric valve events, and swirl can be induced by having asymmetric valve events [24].

Early Inlet Valve Closing (EIVC)

By employing the EIVC strategy, it is possible to eliminate the inlet throttle valve and still operate an SI engine throughout its speed and load range. During low-load and low-speed operation the inlet valve is closed before the piston reaches BDC at the end of the induction stroke. This limits the quantity of mixture that is inducted into the combustion chamber. Once the inlet valve is closed the cylinder is isolated and trapped gas will act as a gas spring, whereby most of the work performed by the piston in expanding the gas will be recovered at the beginning of the compression stroke. Not all the energy can be recovered because of heat loss, and due to the fact that the expansion is not reversible [1].

As with the LIVC strategy, EIVC also induces higher manifold pressure in multi-cylinder engines. This is caused by suddenly closing the inlet valve while the air/fuel mixture is still flowing into the combustion chamber. The inertia of the flow creates a pressure build-up in the inlet manifold. The higher pressure can inhibit fuel vaporization. However, EIVC engines can overcome this problem because they have a higher inlet velocity, which increases turbulence and actually promotes fuel vaporization [1].

Many of the papers reviewed in [1] found that EIVC substantially reduced pumping losses, fuel consumption and NOx at part-load conditions. Sellnau and Rask stated that pumping losses are reduced with EIVC because the cylinder gases undergo expansion and re-compression at a lower effective compression ratio [25]. This results in the mixture having a lower average pressure and temperature and helps to reduce NOx emissions.

For certain engine loads fuel efficiency can be increased by combining EIVC with a small amount of valve overlap. Gray theorised that this might be because the small valve overlap results in reduced residual gases in the cylinder [26].

Late Inlet Valve Opening (LIVO)

As stated previously, IVO takes place at around 10° before TDC and signifies the start of the induction phase and valve overlap period. LIVO causes the pumping losses to increase because the cylinder pressure is greatly reduced in the first part of the intake stroke, although this does not negatively impact

on the volumetric efficiency. This is because during the final portion of the induction stroke the air/fuel mixture enters the combustion chamber at a higher velocity. The higher velocity increases turbulence, which promotes good mixing and combustion. This is considered to be a good technique to reduce unburned HC emissions [1].

Early Inlet Valve Opening (EIVO)

EIVO strategy results in the inlet valve being opened some time before the end of the exhaust stroke and increases the amount of valve overlap. This allows some of the exhaust gas to be expelled into the inlet manifold and re-breathed during the induction phase [1, 6]. This is known as internal exhaust gas recirculation (EGR) and can greatly reduce NOx formation and improve part-load efficiency [6]. This is because the exhaust gas acts as an inert diluent and reduces the combustion temperature.

This strategy also reduces pumping losses because the internal EGR results in less exhaust gas being expelled during the exhaust stroke. However, EIVO can reduce the engine's performance at full load because the EGR will reduce the amount of fresh charge inducted by the engine [6].

Early and Late Exhaust Valve Closing (EEVC and LEVC)

The exhaust valve is normally closed a few degrees after TDC, which concludes the exhaust phase and the valve overlap period. The timing of EVC has a significant effect on the amount of exhaust gas left in the combustion chamber and can allow backflow of exhaust gas from the exhaust manifold into the combustion chamber [1, 6]. EEVC can be used to prevent the combustion gases from being exhausted from the cylinder. This would reduce the intake of fresh mixture and also reduce the need for the throttle valve. Consequently, pumping losses will be lowered and part-load efficiency will be increased [6].

LEVC increases the valve overlap duration. At high speed, increased valve overlap can assist with scavenging residual gas, and as a result increase the engine's power output. But this can also reduce the engine's volumetric efficiency [1]. Too much overlap is detrimental at low load and engine speed because EGR reduces the concentration of fresh charge in the cylinder and

too much EGR will cause the combustion to become unstable [6]. It was also noted that LEVC is less effective in reducing HC emissions when compared to EEVC [27].

Early and Late Exhaust Valve Opening (EEVO and LEVO)

The exhaust valve is usually opened towards the end of the power stroke. The timing of EVO is important because the exhaust valve must be opened as late as possible so that the maximum amount of work can be performed by the expanding combustion gases. It is also important that the pressure inside the combustion chamber is allowed to drop to the lowest possible value in order to reduce exhaust back pressure and therefore the amount of pumping work required to exhaust the gas [6].

In the case of EEVO strategy, the exhaust valve is opened well before the end of the power stroke. If the valve is opened too early it could cause a reduction in the engine's power. However, EEVO provides better scavenging of burned gases [1]. EEVO also helps to reduce the pumping work that is required to expel the exhaust gas from the combustion chamber as there will be less exhaust gas in the combustion chamber. Therefore, the piston would need to do less work in order to evacuate the remaining exhaust gas.

LEVO also reduces the power output of the engine because the pumping losses are increased, which means that the exhaust stroke has to perform more work to exhaust the burned gas from the combustion chamber. HC emissions are also affected by the EVO timing. LEVO provides more time for the gases to blow-down and fully oxidise [28].

2.2 HCCI Technology

2.2.1 Introduction to HCCI Combustion

Homogeneous Charge Compression Ignition (HCCI) is an alternative combustion process whereby a premixed charge of air and fuel is compressed until auto-ignition occurs spontaneously at multiple points in the mixture. Auto-ignition occurs when a fuel and an oxidising agent spontaneously ignite as a result of the mixture being held at a sufficiently high temperature and pressure for a certain period of time. The engine is then able to use the increased gas pressure and temperature from this exothermic reaction to perform work [29, 30].

This process is different to a gasoline or diesel engine where ignition only proceeds when the spark plug is discharged or as fuel is directly injected into the combustion chamber, respectively.

When the spark plug is discharged in an SI engine a flame-front propagates through the mixture of air and fuel and is characterised as a slow burn where only a fraction of the mixture is burning at any point in time. The efficiency of an SI engine is lower than HCCI or diesel because its compression ratio is limited by the possibility of auto-ignition of the unburned mixture (knocking). However, SI engines are able to operate with stoichiometric or slightly rich mixtures and therefore have a high power-to-weight ratio. Additionally, SI engines have lower exhaust emissions than diesel engines because operating with a stoichiometric air/fuel ratio allows for the implantation of a three-way catalyst, which is highly effective at converting HC, CO and NOx into less toxic products [7].

Compression Ignition (CI) engines use compression to increase the pressure and temperature of the air inside the combustion chamber so that combustion occurs as the fuel is injected into the cylinder. As a result, CI engines have very high compression ratios and are significantly more efficient than SI engines. Combustion occurs at the interface layer between the compressed air and the injected fuel. Therefore, combustion is limited by the fuel droplet evaporation, mixing and diffusion [7]. This can result in locally fuel rich zones, even though the overall air/fuel ratio is lean. Consequently, the rich combustion zones lead to increased formation of particulate matter (PM) from incomplete combustion of the fuel. In addition, there is greater nitrogen oxide formation from high local combustion temperatures [31]. Exhaust

gas after-treatment methods for CI engines are very complex and expensive to implement because of the overall lean air/fuel mixture [32].

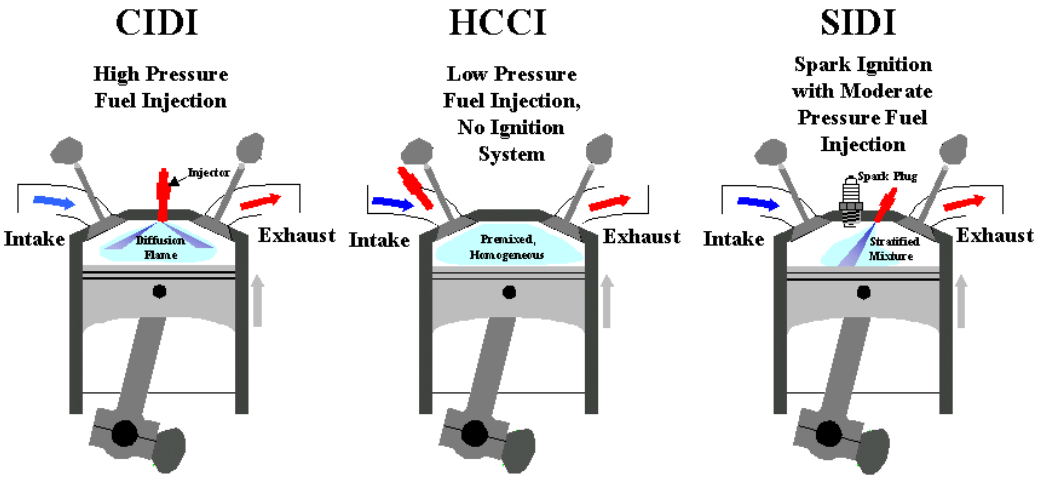

Figure 2.6: Comparison of Combustions Methods: Compression Ignition Direct Injection (CIDI), HCCI and Spark Ignition Direct Injection (SIDI) [33].

2.2.2 Advantages of HCCI

The reason why so much time and effort has been put into HCCI combustion research is because it offers the possibility of combining both the emissions benefit of the gasoline engine and high efficiency of the diesel engine [33]. HCCI operation has the following important advantages over SI and CI engines:

- HCCI engines, which are based on the Otto Cycle, are able to achieve a higher thermodynamic efficiency than an SI engine because they operate at higher compression ratios and do not require a throttle valve, which reduces an engine's volumetric efficiency. In addition, lean-burn operation and rapid heat release contribute to further increase the thermodynamic efficiency [29, 30].
- The lean homogeneous mixture produces less NOx and PM than diesel combustion and it also creates a more efficient combustion process. NOx formation is reduced because the combustion temperature is lower and particulate emissions are reduced because there are no locally rich fuel zones to promote PM formation [7].

- HCCI engines are able to achieve combustion using a variety of different fuels, which include gasoline, diesel, n-heptane and most alternative fuels [29, 30].
- HCCI engines are more fuel efficient than SI or CI engines and can have up to 20% better sfc [29, 30].

2.2.3 Challenges with HCCI

The following is a list of challenges associated with HCCI combustion technology:

- There is significant difficulty in controlling the combustion phasing as there are no direct control mechanisms as in SI and CI engines. This is especially challenging during transient operation [30].
- HCCI engines have a very narrow operating range, which is limited by the fuel's lean auto-ignition time at low loads and peak pressures at high load. Increasing the fuel content would cause faster heat release rates and higher peak pressures, which can damage the engine. The engines must be structurally strong enough to withstand the high peak pressures and due to the limitations described above, HCCI engines have a low specific power output [29, 30, 34].
- HCCI engines can have high HC and carbon monoxide (CO) emissions. HC emissions are caused by fuel being trapped in small crevice volumes and CO emissions are caused by in-cylinder temperatures being too low to complete the CO to carbon dioxide (CO_2) oxidation reaction [29, 30, 35].
- Transient dynamic operation is one of the most challenging aspects of HCCI combustion and is the primary limiting factor for the reason why HCCI engines have not been adopted in modern vehicles [29, 36]. It is relatively easy to run an HCCI engine at a fixed speed and load point. However, quickly changing from one speed-load point to another, which is required by a vehicle, requires that the control mechanisms are able to maintain the correct combustion phasing [29, 30].
- The complex electronic control systems, engine hardware and the associated development make HCCI engines prohibitively expensive when

compared to SI or CI engine and their exhaust gas treatment systems [30].

- The rapid heat release of HCCI combustion can be very noisy and would be unpleasant for a vehicle owner [30].

2.2.4 Basic Methods of HCCI Combustion Control

Unlike SI or CI engines, HCCI engines are challenging to control because auto-ignition occurs entirely from the compression of the mixture and there is no direct method for controlling the point of ignition. Therefore, combustion is controlled by the chemical kinetics of the fuel and the mixture's temperature and pressure history after IVC. This lack of direct combustion control makes applying HCCI combustion technology in a production engine challenging [33].

The following methods are commonly employed to control the point of auto-ignition during HCCI operation [29, 30]:

- Temperature control of the intake mixture.
- Charge boosting to control the mixture's pressure at the start of compression.
- Air/Fuel ratio of the homogeneous charge.
- Exhaust Gas Recirculation (EGR) for heating or diluting the charge.
- Variable compression ratio.
- Variable valve actuation.
- Custom designed fuel compositions.

As there is no throttle valve the engine load control is achieved by varying the amount of fuel injected and with charge boosting. In-cylinder pressure sensors are used in conjunction with the advanced control mechanisms for closed-loop control of the combustion phasing [37].

2.2.5 Operational Limits

HCCI engines have a very narrow operating range where combustion can occur with regard to engine speed and load [29, 30]. The area between the speed and load limits is known as the operating envelope and is defined by the following limits:

- Low Speed: A relatively slow engine speed compared to the fuel's auto-ignition delay can advance the combustion phasing. This can cause high peak pressure rise rates and damage the engine.
- High Speed: A relatively high engine speed compared to the fuel's auto-ignition delay can retard the combustion phasing. This can cause the engine to misfire or cut-out completely.
- Low Load: At low loads the combustion is very lean. Lean operation has a lower combustion temperature, which can lead to misfiring or stalling.
- High Load: Too much fuel can cause very rapid combustion, which results in dangerously high heat release rates and peak pressures that can damage the engine.

Figure 2.7 shows a comparison between the load and speed ranges for HCCI, SI and CI engines.

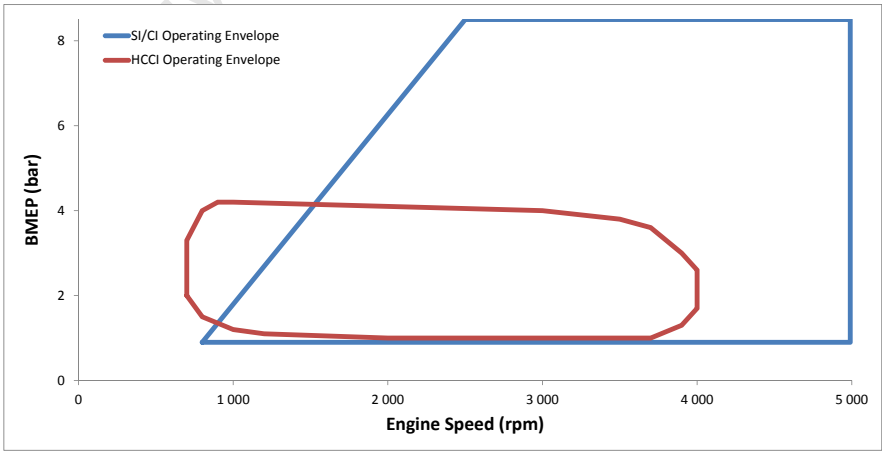

Figure 2.7: HCCI, SI and CI Load and Speed Ranges (Adopted from [38]).

2.2.6 Implementation of HCCI

Instead of pure HCCI engines, many OEMs and researchers are trying to implement mixed-mode HCCI engines as an alternative. These engines incorporate many of the above-mentioned control methods and are able to switch from HCCI to either spark ignition or diesel operation. This allows the engine to expand its operating range to areas that are generally impossible for HCCI operation, while retaining the benefits of HCCI combustion. An example of this is the Mercedes-Benz DiesOtto concept, which is a gasoline SI-HCCI engine that uses direct injection, variable compression ratio, variable valve timing, variable geometry turbocharging and is spark assisted [39]. Unfortunately, these engines are highly complex and thus significantly more expensive than even the most advanced SI or CI engine.

Chapter 3

Experimental Apparatus

The following chapter is a summary of the main elements of the experimental apparatus, which includes the Hydra engine, FVVA valvetrain and the FPGA ECU.

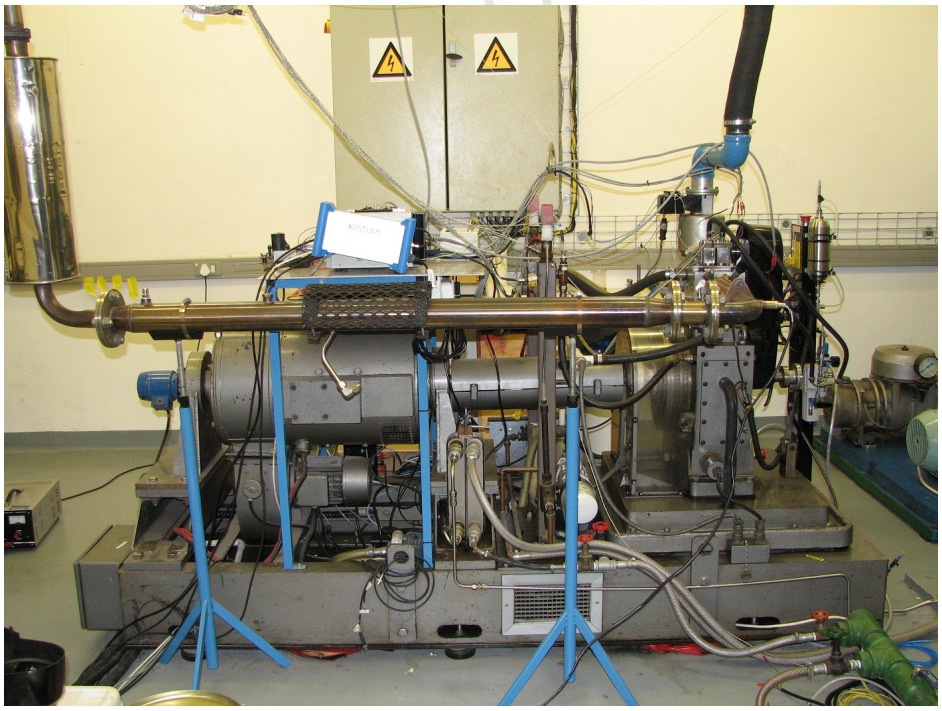

Figure 3.1: SAFL's Hydra Engine Test Cell.

3.1 Hydra Engine

The engine used for the development of the Fully Variable Valve Actuation system was the Ricardo Hydra Research Engine. The Hydra was a single cylinder engine with a 0.45 L swept volume. The engine was named after the Greek mythical beast, the Lernaean Hydra, which had many heads. As its name states, the engine had many different cylinder heads, which allowed the engine's compression ratio to be changed and made it capable of operating as a diesel or spark ignition engine. The compression ratio was determined by the clearance volume in the cylinder heads. This made the engine highly versatile and perfectly suited for this particular project.

The following section lists the general specifications of the engine and the possible setups:

Table 3.1: **Hydra Engine – General Specifications.**

Specification	Value
Bore	80.26 mm
Stroke	88.90 mm
Swept Volume	0.45 L
Maximum Speed	Gasoline - 5400 rpm
	Diesel - 4500 rpm
Maximum Power	Gasoline - 15 kW
	Diesel - 8 kW

Table 3.2: **Hydra Engine – Possible Compression Ratio Setups.**

Mode	Compression Ratio
Gasoline	8:1
	9:1
	11:1
	13:1
Diesel	20:1
	21:1

Table 3.3: **Hydra Engine – Standard Valve Timings.**

Valve Timing	Gasoline	Diesel
Inlet Open	12° BTDC	10° BTDC
Inlet Close	56° ABDC	42° ABDC
Exhaust Open	56° BBDC	58° BBDC
Exhaust Close	12° ATDC	10° ATDC

3.2 Dynamometer and Controller

The Ricardo engine test stand was supplied with a regenerative motor-dynamometer, which was capable of motoring the engine during start up and absorbing the engine's power during operation. The dyno was controlled using a thyristor drive, which regulated the AC supply to provide variable DC voltage. It also allowed for the power generated by the engine to be sent back into the mains electrical grid.

The dyno controller was located in the control room. A number of its circuits became obsolete because they were replaced by the computer/FPGA system, for example the control of the fuel injection. However, all the pumps, heaters, the mass flow meter, thermocouples and the emergency stop were all controlled by the panel. The engine's speed was also controlled via a dial on the panel. Figure 3.2 shows the dynamometer, thyristor drive and dyno controller.

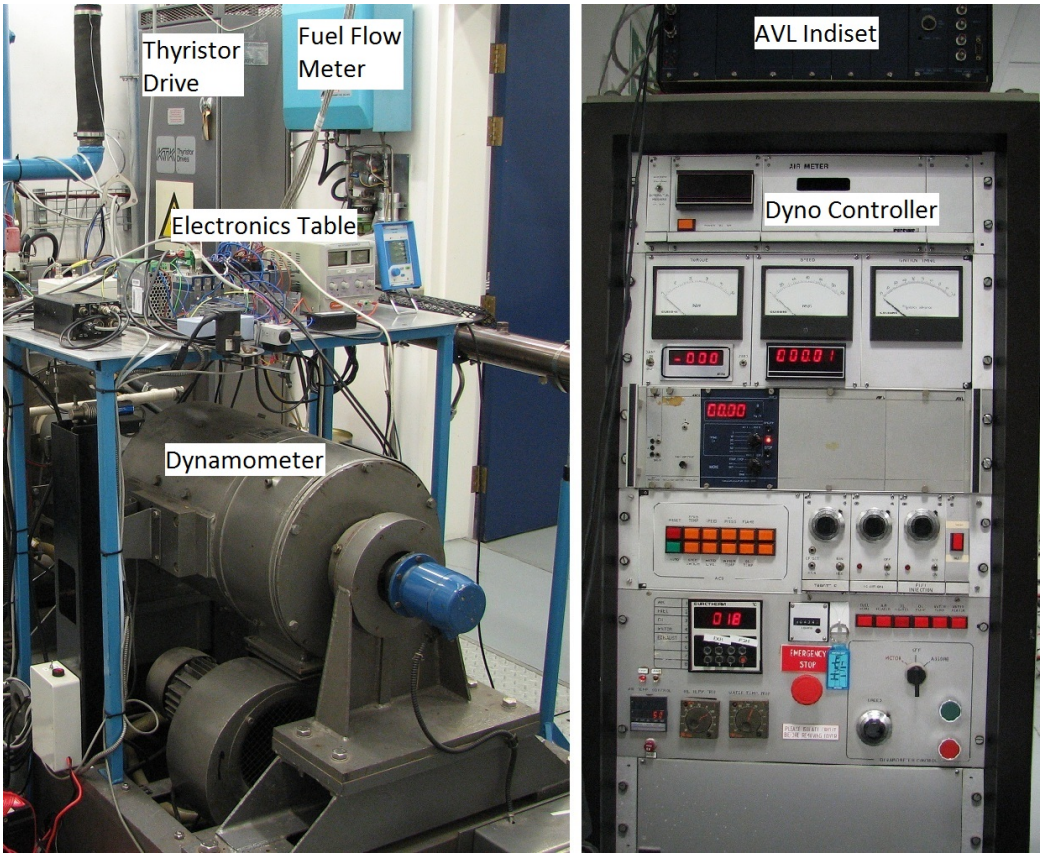

Figure 3.2: Dynamometer, Thyristor Drive and Dyno Controller.

3.3 Electrical Systems - ECU/FPGA

The engine's electrical and control systems were mounted on an aluminium table that was situated above the dyno. This table is shown below in Figure 3.3 where the following items can be seen: FPGA, power supplies, shaft encoder module, opto-couplers, solenoid driver circuit and charge amplifier.

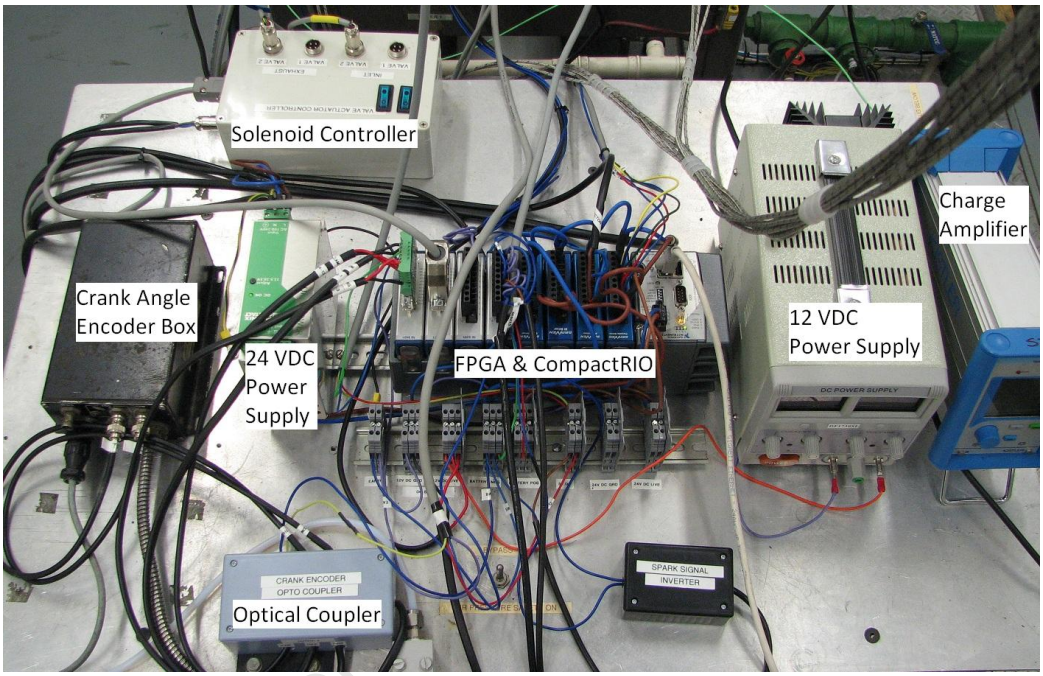

Figure 3.3: Electrical Systems - FPGA, Solenoid Drivers and Power Supply.

The engine was completely controlled by a National Instruments CompactRIO Real-Time controller and FPGA chassis. The chassis has a 40 MHz processor that allowed for extremely accurate timing of the executed commands. The FPGA chassis is made up of special logic blocks that can be fully configured and adapted by the user. This allows the user to quickly produce and modify complex logic circuitry without the need of a soldering iron. The user controlled the chassis via a LabVIEW interface on a computer. However, the CompactRIO and FPGA were able to run independently of the user or PC (Personal Computer). This means that if the computer had crashed, the chassis would continue to run and the hardware would not crash as well.

The user controls the engine from a PC, where the user can read dials and gauges and input his commands in the LabVIEW front panel. The computer

transfers information between the CompactRIO through a TCP/IP connection. The real-time controller on the CompactRIO controls and communicates with the FPGA, transferring user inputs and retrieving data. Finally, the FPGA interfaces with the various modules that are connected to it. It uses these modules to read data from sensors such as thermocouples and transducers, or to control objects such as solenoids and relays.

The 8 modules that were used on the FPGA and their applications are listed in the following table:

Table 3.4: **List of FPGA Modules and Their Applications.**

Module	Application
Throttle Driver	Control throttle bodies
PFI Driver	Port Fuel Injector Control
DI Driver	Direct Fuel Injector Control
Spark Driver	Control spark plug
4 Channel Analog Input	Read valve lift sensor data
8 Channel Analog Input	Not Used
8 Channel High Speed Digital IO	Control actuator solenoids
8 Channel High Speed Digital IO	Read crank and cam encoders

3.4 FVVA Valvetrain

Fully Variable Valve Actuation was accomplished by utilizing pneumatic-hydraulic actuators which were electrically controlled via the FPGA and computer. The actuators were supplied by Cargine, who developed the actuators for the Koenigsegg supercar [40, 41]. Solenoids were used to regulate pressurised air into to the actuators, which allowed for the timing, open duration and lift height of the valves to be precisely controlled. This allowed the valve events to be optimised over the entire speed and load range of the engine in order to achieve maximum power output in conjunction with significant reduction in fuel consumption and exhaust emissions.

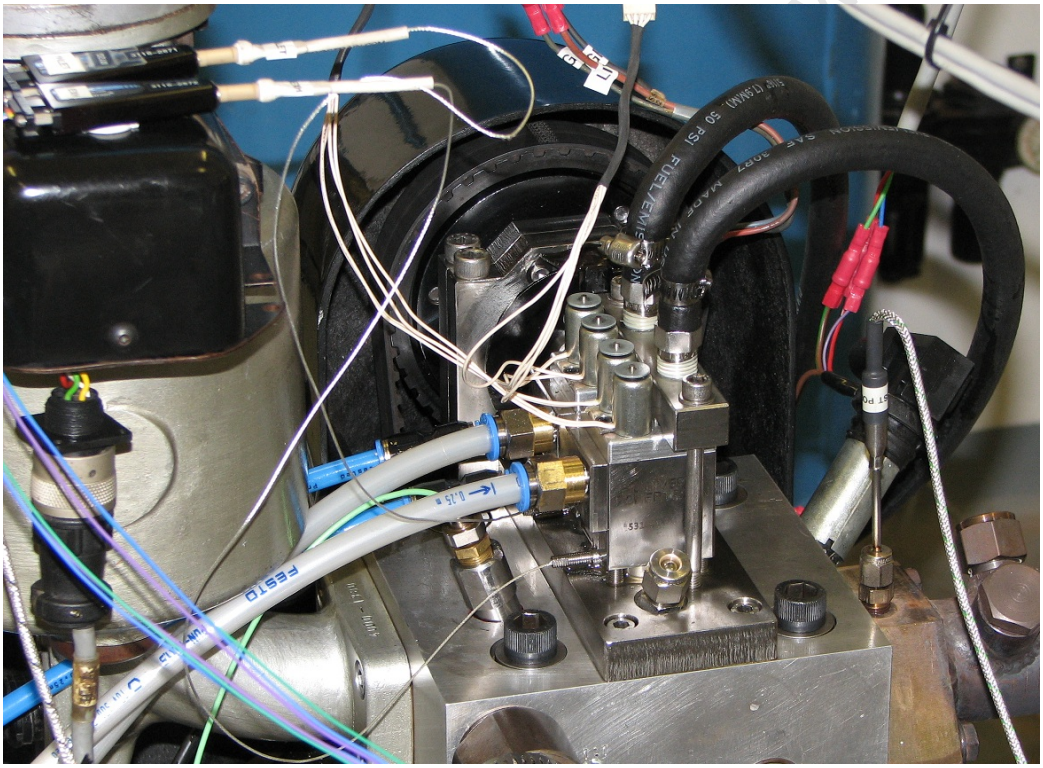

Figure 3.4: FVVA Valvetrain and Subsystems.

Figure 3.4 shows the FVVA valvetrain installed on the hydra engine and the various systems that were needed for the actuators to operate. These systems are: the cam pulley and cam encoder, pneumatic lines, hydraulic lubrication lines and lift sensors. These systems and their functions are covered in detail in Appendix A.

Chapter 4

Design and Setup of the FVVA Valvetrain

4.1 Actuator Mounting and Camshaft Pulley

As the aim of this project was to replace the camshaft driven valvetrain with a pneumatic FVVA valvetrain, a special mounting plate had to be designed that would enable the new FVVA valvetrain to be attached to the cylinder head in place of the camshaft assembly. The FVVA system that was implemented replaced the standard valvetrain components, including the camshaft, camshaft housing and cam-pulley assembly.

The space that was available on the engine head for mounting the actuators and TDC Phase Encoder was very limited. In order to mount the actuators and phasing pulley accurately, whilst ensuring that there were no interferences between the various parts, the cylinder head, actuators and custom parts were modelled in a 3D Computer-Aided Design software package called PTC Pro Engineer. This enabled all the parts to be assembled virtually to verify that they fitted together correctly. This also allowed changes and refinements to be implemented quickly. Figure 4.1 shows the 3D Pro Engineer rendering of the FVVA valvetrain assembly and its various components.

There were a number of important factors that had to be taken into account when designing the mounting plate for the actuators. The first design consideration was to ensure that the actuators were mounted at the

correct height above their respective valves so that the tappet clearances were correct. The clearance that was specified in the Ricardo Hydra's engine manual was 0.3-0.4 mm. Once all the components of the valvetrain were modelled and assembled in Pro Engineer, the thickness of the mounting plate and valve shims were adjusted to 15.0 mm and 1.7 mm respectively in order to achieve the specified clearance. Each actuator had four threaded holes in each corner of its base which were used to fasten the actuators to the mounting plate. The technical drawings for the design can be seen in Appendix F.

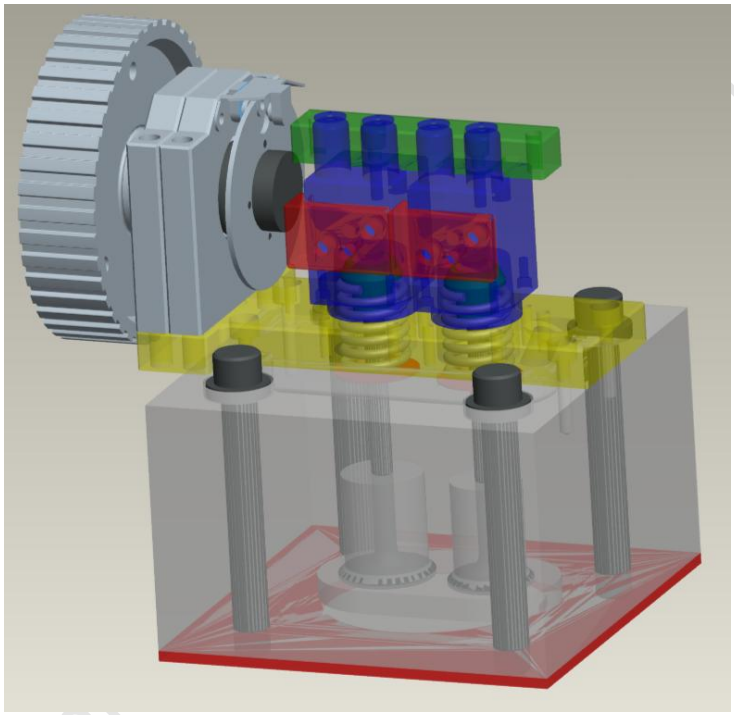

Figure 4.1: Pro Engineer 3D Rendering of The Cylinder Head and FVVA Valvetrain Assembly (Excluding Fasteners).

The original camshaft had an optical sensor attached to its free end, which is called a Camshaft TDC Phase Encoder. The function of the sensor was to determine the phasing of the engine. The sensor consisted of a light emitter, an optical pickup and a disc with a small notch cut out of it. This disc rotated at half the speed of the engine, and with every second crankshaft revolution the gap in the disc passed the sensor, which allowed a light beam to be picked up by the sensor. This enabled the control system to calculate when one full engine cycle had been completed. Naturally, the engine control system was unable to function without the Camshaft TDC Phase Encoder.

The second design consideration was to minimise the extent of the alterations made to the engine and to also ensure that the FVVA valvetrain could be easily disassembled for maintenance. Therefore, the reduced camshaft and TDC Phase Encoder assembly were mounted in the same position as the original camshaft, and the original bolt holes in the cylinder head were used to affix the mounting plate. This also allowed for the original timing belt and belt cover to be used in the new setup.

The new pulley shaft was essentially a free-running shaft with almost no bending moments other than that caused by the belt's tension and no torsion was applied to the shaft. The pulley shaft was designed to be as compact as possible in order to minimise any bending moments and reaction forces, and so that the pulley could be kept in its original location on the engine.

A simple bending moment calculation was performed on the reduced camshaft in order to verify that the tension in the timing belt would not overload the bearings. The maximum possible timing belt tension was determined by calculating the belt angles and then using trigonometry to calculate the belt tension. Figure 4.2 shows the valvetrain's timing belt, belt tensioner and pulleys, which were used to drive the TDC Phase Encoder. The relevant belt angles are also shown in this figure. The free-body diagram that was used for the bending moment calculation can be seen in Figure 4.3.

In order to tension the timing belt the tensioning pulley had to be physically pushed and held in place without any levers or aids, and then locked in its position with a cap screw. Therefore, it was assumed that a person would not be able to apply more than 500 N of horizontal force to the tensioning pulley. This resulted in a maximum belt tension of 4843 N. In addition, the belt manufacturer specified that when the belt is correctly tensioned it should be able to be twisted by 90° , which would prevent the belt from being over tensioned and the bearings being overloaded.

It can be seen in Figure 4.3 that the tension in the timing belt makes the camshaft want to pivot about point b and thus the radial force Fb on this bearing was the limiting variable. Taking moments about point a and summing the forces along the vertical axis resulted in force $Fb = 14157$ N and force $Fa = 9314$ N.

Based on the calculations above and the design requirements the bearings sealed roller ball bearings from NSK were selected. The bearings could withstand radial forces of 53 kN, axial forces of 15 kN, and were rated to

a maximum speed of 10000 rpm. Therefore, the safety factor for the radial force on bearing b was 3.74. In order to overload the bearing a horizontal force of more than 1872 N would have to be applied to the tensioning pulley, which is physically impossible for a person to apply. The selected bearings did not require any form of additional lubrication or cooling for them to operate continuously at their rated speed. According to the NSK website, "the limiting speed of the bearings is an empirically obtained value for the maximum speed at which the bearings can be continuously operated without failing from seizure or generation of excessive heat." [42]

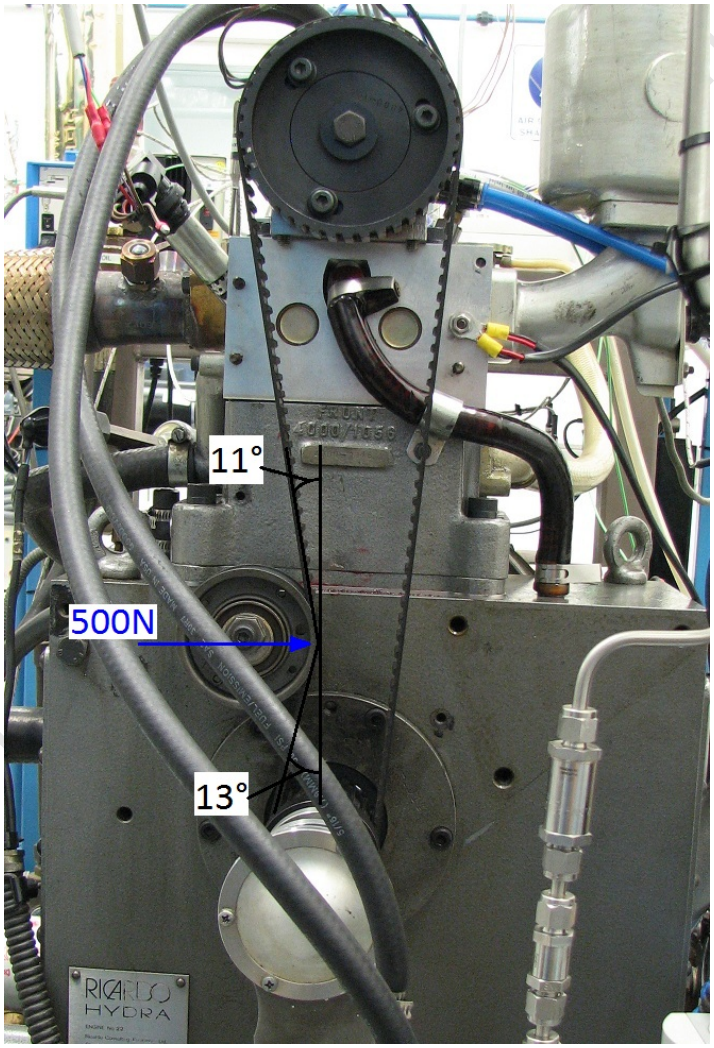

Figure 4.2: FVVA Valvetrain: Timing Belt, Belt Tensioner, Pulleys and Crankshaft Encoder.

The design of the mounting plate and reduced camshaft included packaging the assembly so that it occupied minimal space and did not interfere with the cylinder head bolts or other parts of the engine. This was important because it allowed the FVVA valvetrain to be attached quickly to any of the cylinder heads and it also meant that no modifications had to be made to any of the original engine parts. Therefore, if required, the engine could be converted back to cam-operated valves.

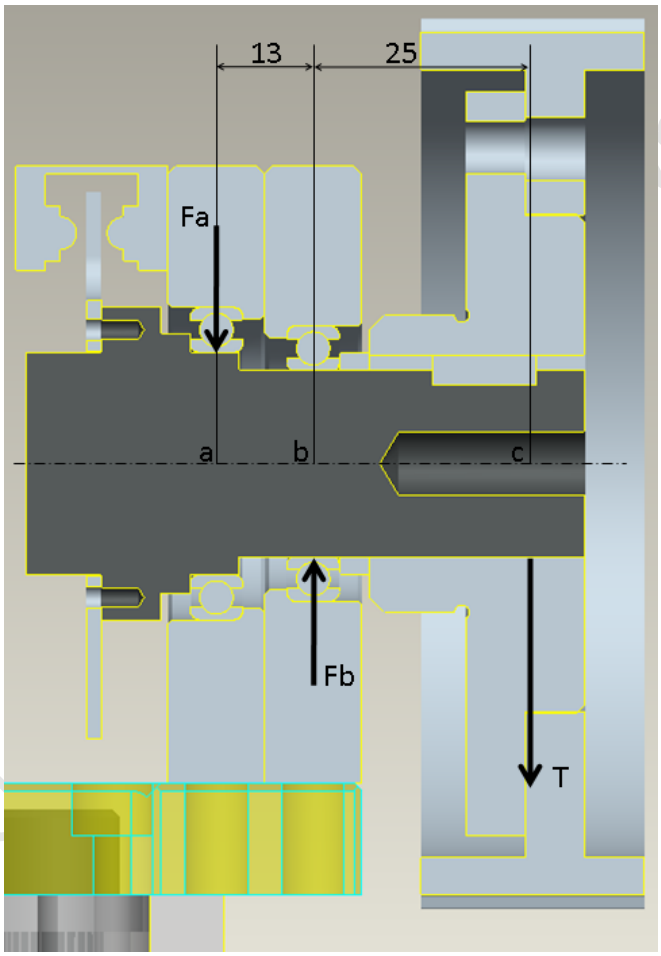

Figure 4.3: Free-body Diagram of The Phase Encoder Shaft Assembly.

The pneumatic and hydraulic systems were attached to the actuators using special mounting plates, which were clamped onto the actuators and used O-rings to provide the necessary sealing. The pneumatic lines were connected to their mounting plates with 3/8" quick-connectors and the hydraulic lines were connected with 1/4" hose fittings.

4.2 Spring Design

New springs had to be designed for the FVVA valvetrain because the original Hydra springs had an outer diameter that was too large to fit inside of the actuator pistons, which tapered from 28.8 mm at the rim to 26.9 mm at the base. The outer diameter of the Hydra springs was 29.8 mm. The new springs were designed to have the same length, spring constant and pre-load force as the original springs. However, the outer diameter was reduced to 22.6 mm so that they could fit inside the actuator piston. It was calculated that the original springs had a pre-load force of 200 N and a spring constant of 28 N/mm. In order to achieve the same specifications as the original springs, the number of coils for the new valve springs were increased.

During testing, two failures occurred with the custom manufactured springs. It was discovered that the springs could not handle the high stresses and dynamic loading because the incorrect material was used. It was not possible to acquire locally the special valve spring steel that was required to manufacture the springs. Valve springs that closely matched the new springs (reduced diameter) had to be used from another engine. The springs were replaced with new springs from the EA111 engine of the 2010 VW Polo 1.4. Figure 4.4 is a graph of the spring constant and displacement versus force for the new VW springs, which was supplied by VW. Table 4.1 lists the specifications of the original Hydra springs and the new springs.

Table 4.1: **Table of Valve Spring Specifications.**

	Original	VW EA111
Length (mm)	50.0	48.0
Wire Diameter (mm)	3.85	3.0
Outer Diameter (mm)	29.8	23.0
Spring Constant k (N/mm)	26.5	25.1

The EA111 valve springs were slightly shorter than the original springs and had a slightly lower spring constant. As a result they had a lower pre-load force. It is important that the spring's pre-load force is high enough to prevent valve bounce. Valve bounce describes the situation where the valves do not stay seated after valve closure. In this case it was not an issue as the engine was limited to low speed operation where valve bounce is not prevalent. In addition, the pre-load force was approximately 150 N, which was within the acceptable pre-load range.

One of the requirements for Cargine's pneumatic actuators was that there was a physical stopper to prevent the actuator piston from over extending. If the actuator piston was allowed to move more than 14 mm, it would come out of the actuator housing and the piston and piston ring could be damaged when returned by the valve spring. The new spring retainer, which was designed to fit the smaller valve springs, was designed with an elongated inner section that was long enough to touch a raised section around the valve's stem. This prevented the actuator piston from extending further than 13 mm. The spring retainer and raised section can be seen as a Pro Engineer rendering of the Hydra head assembly in Figure 4.5 or in the manufacturing drawing Figure F.2 in Appendix F.

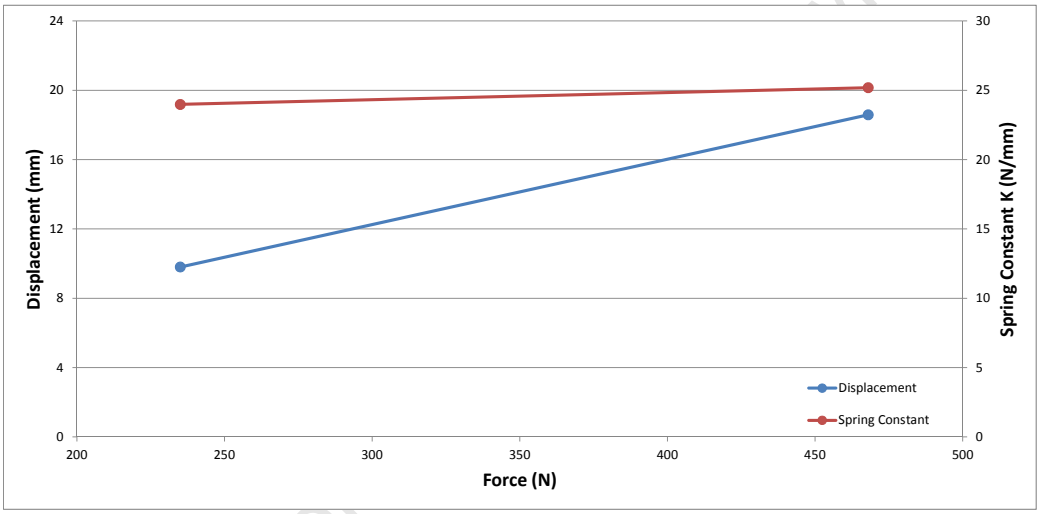

Figure 4.4: Graph of Displacement and Spring Constant vs. Force for VW EA111 Springs.

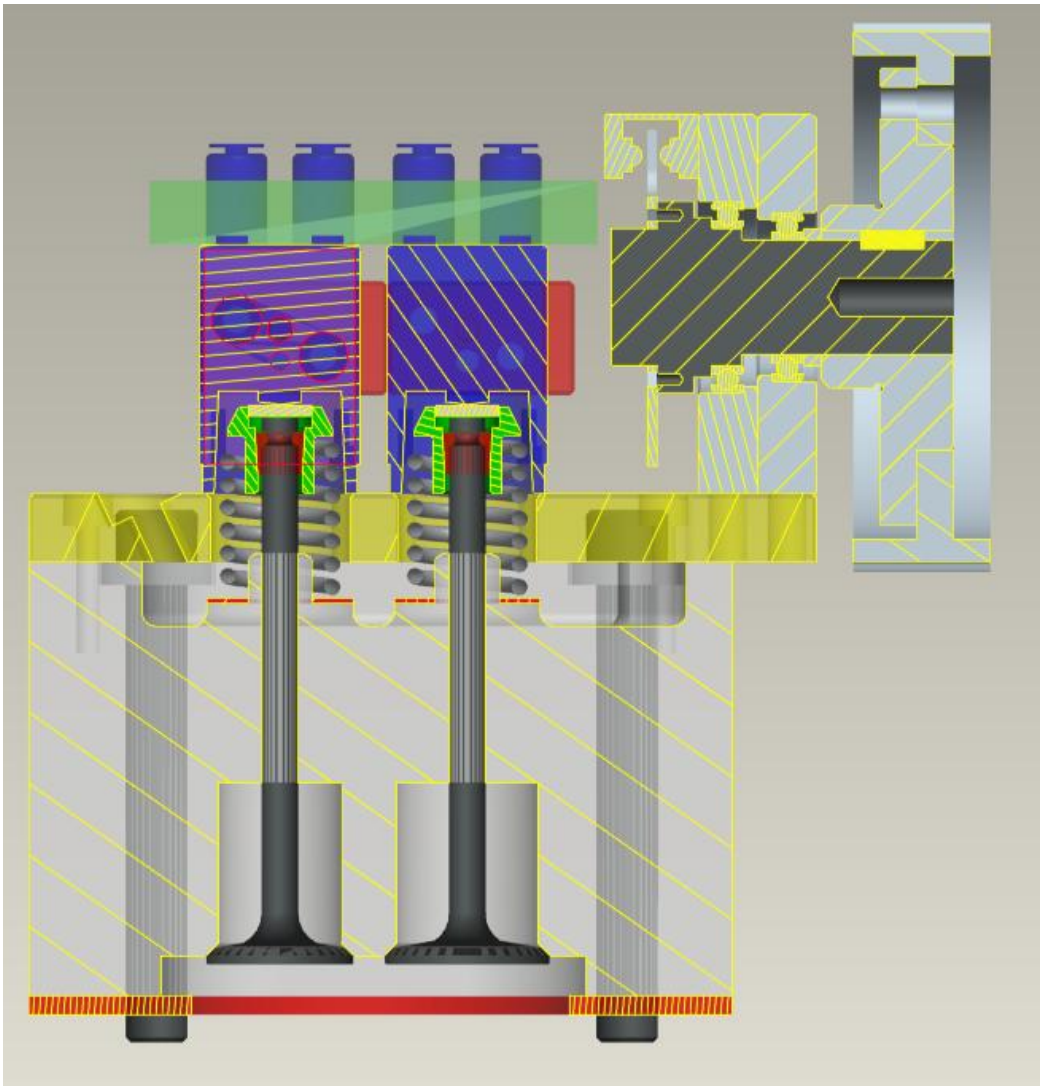

Figure 4.5: Pro Engineer Cross-Sectional Rendering of The FVVA Valvetrain.

Chapter 5

Commissioning of the Actuators and Hydra Engine

5.1 Introduction

This chapter addresses the process of commissioning the FVVA valvetrain and engine, as well as noting a number of mechanical and electrical failures and difficulties, and how they were overcome. This portion of the project was divided into three stages. The first stage was the commissioning of the FVVA valvetrain, the second stage was the commissioning of the Hydra engine without FVVA, and the final stage was the running of the engine with the FVVA valvetrain.

5.2 FVVA Valvetrain Commissioning

It was decided that before the new valvetrain could be incorporated with the engine, it should be developed and commissioned separately from the engine. The prime reason for this decision was that this was a new field of exploration for SAFL, which meant that there was a possibility that the engine or valvetrain could be damaged during the development process.

The FVVA valvetrain and its subsystems were able to be operated independently from the Hydra engine. Therefore, the valvetrain commissioning began by mounting the actuators onto one of the SI cylinder heads and then fastening it to a table next to the engine. Following which the hydraulic and pneumatic systems were connected to the actuators. Figure 5.1 shows the Hydra head and setup that was used for the FVVA valvetrain commissioning.

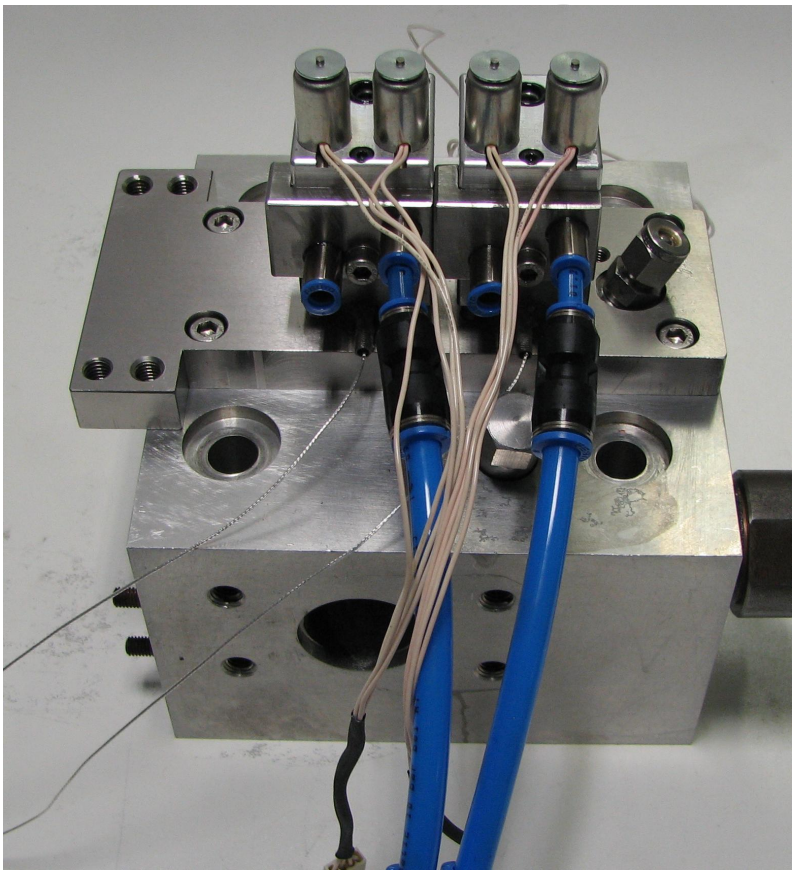

Figure 5.1: Setup Used for The FVVA Commissioning.

In order to be able to test and commission the FVVA system, special control software had to be written. The control software was written in LabVIEW, which allows for rapid development and refinement of the software. The software was designed to simulate the crankshaft encoder signal, which was used to control the points where the valves opened and closed and the maximum height of the valve lift. Appendix A provides details on how the actuators are controlled and Appendix B provides an explanation of the control software.

The commissioning of the valvetrain involved two tasks. The first was to test the mechanical systems, and the second was to test the electrical systems and control software. The two mechanical systems that needed to be tested were the lubrication/hydraulic latch and the pneumatics system.

The lubrication system was first checked to make sure that it was assembled correctly. This was important because the Swagelok filter and check valve were almost identical in appearance and could be easily confused. The filter had to be placed directly after the oil reservoir in order to stop particles greater than 10 μm travelling through the actuators. If this should happen the actuators could be damaged and they would then need to be sent back to Cargine in Sweden for repairs.

In addition, it was important that the check valve was positioned directly after the filter so that the filter did not act as a positive displacement pump when the valves were actuated. This was possible due to the construction of the filter. Figure 5.2 shows the layout of the hydraulic system. Route "a" in the figure is the correct assembly and route "b" is the incorrect assembly. Because the filter was essentially a piston and spring, the pressure waves that were created in the hydraulic lines from damping the actuators caused the filter element to oscillate. In assembly "b" the check valve is positioned before the filter and, therefore, the oscillation of the filter opened the valve and allowed additional pressurised oil into the hydraulic lines. The oil continued to be pumped into the lines until the rubber hose could no longer absorb any more and became extremely stiff. This pressure build-up in the hydraulic lines inhibited the hydraulic latch from being properly evacuated causing the valves to be stuck open. In assembly "a" the check valve prevented the oscillations from reaching the filter, preventing the filter from pumping additional oil into the hydraulic lines.

While trying to repair a leak in the lubrication supply lines to the valvetrain, this issue was inadvertently demonstrated. The hydraulic system was

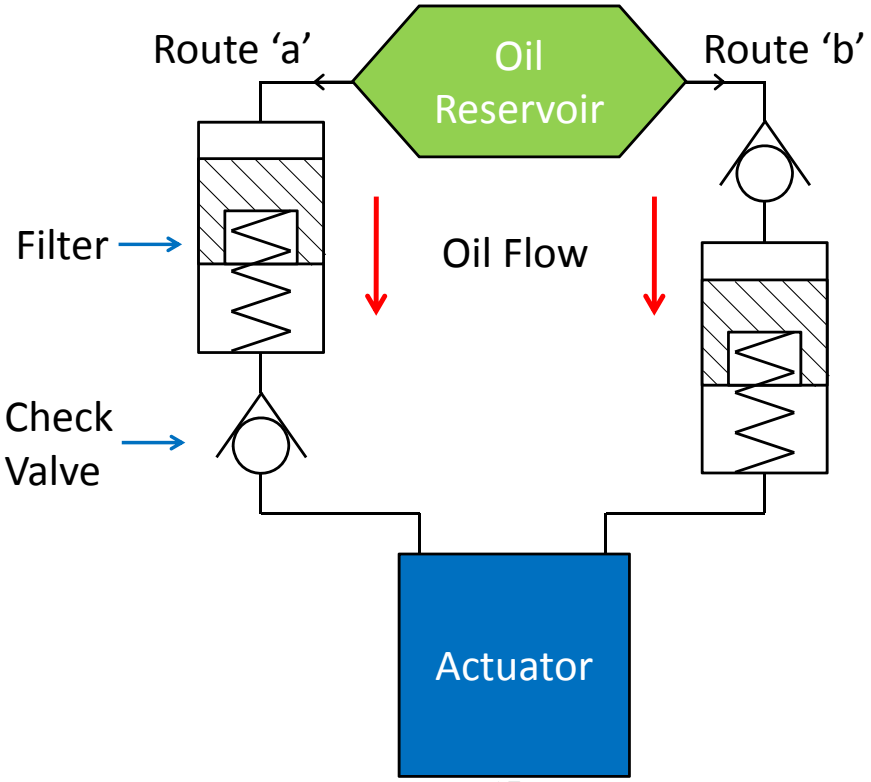

Figure 5.2: Diagram of The Correct Assembly of The Hydraulic System.

taken apart, and during reassembly the filter was incorrectly positioned after the check valve. After approximately 10-15 cycles of operation the valves failed to close and the oil had to be drained from the lines before the valves could be closed. This highlighted the importance of assembling the hydraulic system correctly, failing which could lead to the valves and actuators being damaged by the engine's piston.

Testing the pneumatic system involved operating the actuators with compressed air at the correct pressure and at a high enough flow rate, and then energizing the timing solenoids with a 12 V analogue electrical pulse. In order to test whether the supply flow rate was adequate, the lift profiles at the maximum possible engine speed of 5400 rpm were compared to the lift profiles at 500 rpm, which was the lowest possible motoring speed. It was crucial that the actuators were able to maintain the same lift height and open duration throughout the speed range. Testing showed that the actuators were not receiving sufficient air flow at high rpm. This was evident as the valve lift would start to drop after 2000 rpm, and at 5400 rpm

the valves could only achieve around 4 mm of lift instead of the usual 12 mm. It was determined that the diameter of the pneumatic lines was too small which restricted the flow of air into the actuators. This problem was remedied by increasing the size of all the fittings and pneumatic lines. The pneumatic mounting plates had to have their threads re-tapped so that the larger fittings could be accommodated.

Once the mechanical systems had been debugged, the control software had to be debugged. This entailed manual experimentation with combinations of lift strategy, valve timing, valve overlap and negative overlap at different engine speeds in order to make sure that the software or user could not damage the valves or cause the software to crash. One of the main difficulties with the software was to control the point of activation of the timing and height of the solenoids. This was because the relative activation times and activation durations of the solenoids were controlled in nanoseconds (FPGA has a 40 MHz processor), whilst the engine operated in crank angle degrees (CAD) from 0 to 720 CAD (two revolutions of the engine's crankshaft). The most challenging control situation occurred at high engine speeds because the actuators were open for such a short period of time, although the actual duration of CAD that the valves were open remained constant throughout the speed range.

In conjunction with the precise timing, the engine speed had to be compensated for as the speed was increased by pre-empting the activation of the solenoids so that the points at which the valves opened and closed remained constant in relation to the crankshaft's rotation. As it took 4-5 ms (120-150 CAD at 5000 rpm) from when the activation signal was generated to when a valve began opening, it was possible that the activation signal needed to be generated on the preceding engine cycle. Also, with relatively long activation signal durations, the signal might only need to be terminated on the following engine cycle. This could cause the valves to be either permanently opened because the signal was not terminated properly, or the valves might not open early enough because the signal was not generated on the preceding cycle.

The former situation is obviously the more dangerous of the two, and this actually occurred while the software was being tested. One of the solenoids was not deactivated properly, which caused the solenoid to be held open for too long. Consequently the solenoid overheated and burnt out. All the wires connected to the solenoid melted because the solenoid was drawing too much current from the 12 V car battery. Fortunately this problem occurred

during the valvetrain commissioning as this could have led to the actuator and engine being severely damaged if the valvetrain had been on the engine while the engine was operating. The rig was easily fixed by swapping out the solenoid, replacing the wires and changing the faulty code.

One of the challenges encountered during the commissioning of the valvetrain was a significant amount of electrical noise on the lift sensor signal, the cause of which could not be established. However an electrical ground loop was discovered while commissioning the Hydra in SI engine mode, which helped to reduce some of the electrical noise on the lift sensor signal. A ground loop can occur when two circuits are at different potentials and share a common ground [43]. In such a case, one circuit will impart a current or noise onto the other circuit. The discovery and elimination of the ground loop will be discussed in more detail later in this chapter.

While solving the noise problem, a new DC power supply was purchased so that the lift sensors would have a dedicated power source. The new power supply had a very low level of noise (Constant Voltage (CV) 0.5 mV rms and Constant Current (CC) 3 mA rms) and very good voltage regulation (CV 110^{-4}+2 mV and CC 210^{-3}+3 mA). When this did not significantly improve the signal noise, a software low pass filter was applied to the sensor signal as it was read into the FPGA. This reduced a large portion of the noise on the signal. However, a balance had to be settled on because too much filtering would degrade the accuracy of the lift trace. In addition, the amount of noise on the signal now fell within the measurement uncertainty of the sensors, so there was no appreciable benefit in trying to smooth the signal any further.

Another electrical issue was the electrical "floating" of the lift sensor signal. This was exhibited when the portion of the lift trace where the valves were closed "floated" off the zero line. However, the actual lift trace did not show any change in shape or in relative magnitudes. When an electrical signal floats around it is generally because the sensor has not been grounded properly. This effectively means that the sensor does not have a definitive point to assign as the zero point and from which to reference the magnitude of the signal. This was of significant importance to the software control because the opening and closing points of the valves were calculated using the lift traces.

While addressing this issue, the sensors were electrically isolated from all the other systems and all the electrical connections where checked. In addition, a number of electrical experts at UCT (University of Cape Town)

and Cargine were consulted. Eventually it was realised that when displacements of such small magnitude are being analyzed, the surface finish of the material, imperfections in the circular geometry of the actuator piston, the rotation of the actuator piston and mechanical free play all have an effect on the accuracy of the measurements. The linear transducer sensors have a sensing range of 1 mm and were reading minute fractions of a millimetre.

Consequently, the solution was to create a special routine in the control software that automatically zeroed the entire lift trace after every engine cycle. This was achieved by calculating the average lift height over the duration of the trace where the valve was closed, and then subtracting this value from the entire lift trace. This method worked fairly well. However, there were times when the auto-zeroing did not work and the lift trace would again start to "float". However, after a short time the lift trace zeroed again. It was felt that this occurred when the sensor encountered a portion of the actuator piston that was either scratched or slightly dented, and the control software could not react fast enough.

5.3 Commissioning of Hydra Engine

The Hydra engine had not operated for a very long time, and the next stage of the schedule was to ensure that the engine and its subsystems were functioning. Part of the engine upgrade was to replace the old ECU with a National Instruments FPGA ECU and custom engine control software. Consequently, all the old monitoring and control systems had to be rewired and integrated into the new FPGA ECU. As the engine was already assembled to run as a diesel engine, the Hydra was first commissioned as a diesel engine before it was converted to operate in SI mode, and finally HCCI.

The following subsystems and items had to be repaired or replaced for the commissioning of the engine:

- Low pressure pump, rubber hoses and various fittings for the fuel system.
- New oil and fuel filters.
- New thermocouples.
- Rewired all electrical devices and sensors.
- New power supplies/sources for the new hardware and sensors.

The new FPGA ECU was designed to be very simple to implement and it had all the interfaces that were required to control the three modes of engine operation. This gave extra versatility to the FPGA ECU. One of the commissioning tasks was connecting the following items to the new FPGA ECU:

- Diesel Injector
- Pressure Relief Valve
- Rail Pressure Sensor
- Camshaft Encoder
- Crank Angle Encoder

The final task that needed to be performed before the engine could be started was to update the standard LabVIEW ECU software that runs on the FPGA and controls the engine. The company that developed the modules for the FPGA provided the LabVIEW code for controlling their modules. This was to assist users so they only need to change a few settings for their particular setup. However, there were a number of challenges in making the hardware and software communicate correctly with each other.

One of the challenges was to resolve how the program interpreted the analogue signals from the crankshaft and camshaft encoders. The first problem encountered was with the analogue signals, and how the program combined the signals from crankshaft encoder and camshaft encoder in order to determine an accurate TDC point for 0 CAD. Without the correct signals the ECU software was unable to determine the engine speed and it would not allow the engine to start.

During every revolution, the crankshaft encoder sent out a short "high" signal when the TDC marker was encountered. Because the camshaft rotates at half the engine's speed, it sends out a long duration signal that goes "low" every second revolution, which signals the start of a new engine cycle. When a signal voltage switches to its maximum value it is described as going "high". Conversely when the signal voltage switches to its base value it is described as going "low".

When these two signals are added together they should produce a single accurate pulse that indicates that the engine is at 0 CAD and is starting a new 4-stroke cycle. However, the LabVIEW software required a signal that went "high" once every second revolution when the TDC marker was encountered and only one of the signals generated went "high". This was discovered after connecting the two encoder signals to an oscilloscope and analyzing their outputs while motoring the engine. Once the signal requirements were understood, the problem was rectified by utilizing an inverter in the software to invert the camshaft signal. After combining the two signals with an "AND" gate, this gave the correct output.

The next issue to overcome was to make sure that the number of "teeth" the encoder was outputting matched up with the number of "teeth" the program was expecting. The program has a safety feature that shuts down the engine if the TDC marker is not picked up or if a "crank tooth" is missed during one crankshaft revolution. If not enough "teeth" are counted between consecutive TDC marks or if too many are counted, the safety circuits in the

software will trip and shut down all the engine's systems.

The challenge with this was to determine how many "crank teeth" the encoder was generating for each revolution, as this was not explicitly stated, and then to change the program to expect that many "crank teeth" for every engine cycle. In addition, the software had a number of variables that were used to calculate the number of "crank teeth", but they were located in different sections of the software. The crankshaft encoder disc had 180 divisions etched onto its surface, which were detected by a sensor. Every time the signal went "high" or "low" the program registered it as a "crank tooth". This produced a square wave signal which amounted to 360 "teeth" per revolution. The encoder could also interpolate a designated number of fractions between each tooth, which increased the resolution of the crankshaft encoder. It was calculated that the encoder generated 5760 "crank teeth" per revolution, which gave a resolution of 1/8th of a degree per tooth, and thus the program was set to expect 5760 encoder pulses per engine cycle.

The final challenge for this stage was to resolve the electrical noise on the encoder signals. This was an intermittent problem which was initially not identified as electrical noise. The engine would operate reliably for some minutes, and then suddenly shut down because of a missed TDC marker or missed "crank tooth" error flag. After checking all the software and then analyzing the signal again on the oscilloscope, it was discovered that there was noise on the encoder signal which occasionally spiked so high that the noise spike would be registered as either an extra "crank tooth" or an early TDC marker. Once this was discovered it was resolved by adding a software low pass filter to both encoder signals as they were read into the FPGA.

Once all the mechanical, electrical and software problems had been resolved, the engine was able to run as a diesel engine, which allowed for the next stage of the project to commence.

5.4 Running Hydra with FVVA

5.4.1 SI Operation

For the final stage of the project, the new valvetrain was fitted to the Hydra engine and together they were converted to run as a FVVA spark ignition engine. Before the engine was converted the following tasks were performed:

1. All fuel and liquids were drained from the engine and the various systems.
2. The top works of engine was disassembled and the components (piston, liner, conrod, etc.) were thoroughly cleaned to ensure that no dirt was lodged between the moving parts.
3. The cylinder liner was honed.
4. The fuel and oil filters were replaced.
5. The O-rings and gaskets were replaced.

A number of parts were common to both engine setups, although some had to be exchanged for SI parts, while others were not required for the SI setup. The two main parts that had to be exchanged for SI parts were the piston and cylinder head. The diesel piston was exchanged for a flat-topped SI piston, although the connecting rods for both setups were identical. The SI cylinder heads were very different from the diesel heads. Most noticeably the SI head had a large bowl in it for the clearance volume, which gave the head used a compression ratio of 11:1. This compression ratio head was selected because it was in the best physical condition and no valves or springs were missing (unlike the other SI heads). In addition, it was planned to use the high compression ratio for HCCI operation. The SI head also had fittings for a spark plug and pressure transducer. However, it did not have an injector fitting like the diesel head because the engine used port fuel injection for SI operation.

When the engine was reassembled, a 3 mm spacer plate was placed between the crankshaft housing and the cylinder block in order to increase the distance between the valves and the piston. The purpose of this was to prevent any possibility of catastrophic collisions. The spacer effectively allowed

the valves to be opened to their maximum lift heights without the valves hitting the piston when the piston was at TDC. However, as a result the compression ratio was reduced and calculated to be 8.48:1.

A special intake manifold designed specifically for SI operation, was fitted to the engine. This manifold had three distinct features that the diesel manifold did not have, these being, a fitting for the port fuel injector, a plenum and a throttle body.

The FVVA valvetrain was the final system that was attached to the engine. The valvetrain included the entire actuator assembly, actuator lubrication system, pneumatic system and a new mounting for the camshaft pulley. The camshaft pulley was still required to drive the camshaft encoder at half the engine's speed because it was used by the FGPA ECU to determine the engine's phasing and TDC point. On the diesel setup, the high pressure injector pump was used to drive the half-speed TDC encoder. However, because the high pressure pump was not required for petrol injection, the cam pulley was used to drive the TDC encoder.

Once the engine was fully assembled the new electrical systems were connected to the FPGA and powered with the correct voltages. The pressure relief valve and rail pressure sensor from the diesel setup were no longer required and were removed with the high pressure fuel rail. The throttle and port fuel injector were connected to the Drivven modules on the FGPA that have the same respective names. A VW pencil igniter (spark ignition module) was used for the ignition system instead of a typical ignition coil. This was because the pencil igniter created less electrical noise than an ignition coil, and the control system had shown to be very sensitive to electrical noise.

When trying to start the engine for the first time in SI mode, the difficulty that was experienced with the camshaft encoder while commissioning the diesel setup, again caused the safety circuits to trip. The encoder safety circuits tripped the moment the ignition system was turned on. It was assumed that this was a similar problem where electrical noise was confusing the software. However, the problem persisted even when the filter levels on the encoder signals were increased. All the sensor and ignition cables were replaced with shielded cables and shields were connected to earth. But this did not solve the problem. This led to the realization that the noise was already on the lines and originated from one of the power supplies.

A ground loop was discovered between all of the power supplies and it was decided that the power supply for the encoders should be completely isolated from all other systems. However, the crankshaft encoder could not be isolated from the battery voltage because of the design of its metal housing. The noise on the encoder signals was eliminated by using an optical isolator (opto-coupler) to electrically isolate all the encoder signals before they were connected to the FPGA for processing.

Because an opto-coupler uses light to transmit a signal between circuits, there was no need for a physical electrical link between the two circuits. What remained were two separate circuits, one with a very clean and stable line, and the other with a dirty (noisy) line that would no longer interfere with the sensitive signal analysis. The signal from the encoder was a 5 V analogue signal, which powered the LED in the opto-coupler. A clean power supply was then used to power a photo-diode that picked up the flashes from the LED and converted them into a noise free 5 V analogue signal. In addition, any high frequency noise is eliminated because the response time for the opto-coupler is a lot slower than the frequency of the noise. However, it is fast enough to pick up all the "crank teeth" at the maximum engine speed. This gave a satisfactory solution to the problem of the excessive noise and the ground loop.

5.4.2 HCCI Conversion and Operation

Once all the systems were functioning and the engine was running reliably as an SI engine with the FVVA valvetrain, the engine was converted to run in HCCI mode. After the valve spring and actuator failures, and control challenges, it was decided that it would be safer to keep the 3 mm spacer plate and maintain the engine's compression ratio at 8.48:1.

Initially, it was thought that even with this relatively low compression ratio and running on 100% n-heptane, the engine would be able to achieve auto-ignition fairly easily. Consequently, the engine was converted to operate in HCCI mode by draining all the fuel, replacing the fuel filters and then priming the system with n-heptane.

Before the engine was started, it was motored with the heaters and pumps for water and oil switched on. This was done to preheat the engine so that some of the energy from the cylinder could be transferred to the air/fuel mixture. If the engine had not been preheated, the cold cylinder would

have taken energy away from the air/fuel mixture and reduced the mixture's temperature and the chance of auto-igniting.

Initially, the exact HCCI operating envelope of this engine was unknown. Therefore, to begin with the engine was motored at the lowest possible speed while the fuel injection duration was gradually increased. A full speed and injection duration sweep was performed in an attempt to find the HCCI combustion zone relative to engine speed and load. This process was repeated a number of times. However, HCCI combustion could not be initiated.

It was thought that the engine could first be started up in SI mode, and then once the engine was warm enough, the spark plug could be turned off and the engine would continue to run in HCCI. The spark plug was turned on at various engine speeds and air/fuel ratios. However, when the air/fuel ratio was within its flammability range the heat release rates were extremely high and the engine would knock. As a result, the spark plug had to be turned off immediately.

Up until this stage the engine was motored with the standard valve timing that was recommended in the engine manual. Once it was established that the engine was unable to start with the standard setup, the valve strategy of early exhaust valve closing (EEVC) was employed. This strategy effectively trapped some of the hot exhaust gas inside the cylinder and preheated the fresh air/fuel mixture. Because there was no actual combustion taking place, the fresh mixture's temperature was only slightly increased by the mixture that was compressed and expanded in the previous cycle. Consequently, even extreme EEVC of 50 CAD did not facilitate combustion.

There were a number of likely reasons why the fuel would not auto-ignite. It was possible that the compression ratio was either too low, the starting temperature of the fuel was not high enough, or the fuel was losing too much heat to the cylinder wall. The engine was fitted with systems for inlet heating and boosting, which increases the temperature and pressure of the air/fuel mixture before the compression stroke commenced. These were the most efficient methods of increasing the likelihood of the fuel auto-igniting.

First the inlet heating was engaged because it was possible to control it from inside the control room while the engine was running, and it had finer control than the boosting system. Once again the engine was motored and the engine speed and injection duration were gradually swept through the typical HCCI operating envelope. After 30 min of motoring the engine

with EEVC, the inlet temperature reached a maximum of 50°C. However, the engine would not start in HCCI mode.

The next process was to turn on the inlet boosting system in conjunction with the inlet heating. The inlet boosting was increased in steps of 3 psi (20 kPa) to the roots blower's limit of 15 psi (103 kPa). With the inlet boosting set to 15 psi, the inlet temperature increased to around 65°C, and 50 CAD of EEVC, there was still no sign of auto-ignition at any point in the HCCI speed and load envelope.

The last option was to add a cetane improver to the n-heptane, namely isopropyl nitrate. The cetane improver is highly reactive and therefore increases the reaction rate of the fuel, thereby promoting faster auto-ignition. The fuel line, filter and pump were completely drained and then 2.5% by volume was added to the fuel tank and thoroughly mixed. Once the mixture was considered to be homogeneous, the fuel system was re-primed. Only a small amount of cetane improver was added to the fuel because too much would make the fuel auto-igntie too easily and would be very difficult to control.

Finally, at around 1000 rpm small puffs of smoke were emitted from the exhaust, which signalled that the fuel was only partially auto-igniting. After about 15 min of operation and with 15 psi of boost pressure, the inlet temperature reached about 90°C. The exhaust valve timing was adjusted to 30 CAD of EEVC and at 1000 rpm the air/fuel mixture was able to auto-ignite and the engine started to run in HCCI mode.

5.4.3 Actuator Operational Issues and Failures

During the commissioning and testing of the engine and valvetrain, there were a number of mechanical failures. Some of these incidents were covered earlier in this chapter and also in Chapter 4. However, the three major failures related to new valve actuators.

The first failure occurred with the timing spool valve of the inlet valve actuator. The failure was first noticed because of the presence of an uncharacteristic oscillation in the lift trace while the valve was closing. During the troubleshooting process, the valvetrain was manually tested before it was disassembled. The timing solenoid was lightly depressed to open the valve, but instead of remaining open while the solenoid was held down, the valve

fluttered open and closed.

When the actuator was disassembled it was seen that side of the inlet port valve cap had cracked and the base had almost been completely broken off. Figure 5.3 shows the sheared inlet port valve cap. The port valves are small caps, which sit on the spool valves and move up and down to open or close a port in the actuator's piston chamber. These ports allow compressed air into and out of the cylinder, which controls the motion of the actuator piston. The valve caps oscillate between 4 and 45 times a second, depending on the engine speed.

Figure 5.3: Inlet Port Valve Failure of The Cargine Pneumatic Actuator.

Initially, it was not known exactly why the inlet port valve caps failed after only 12-16 hr of operation. The actuators were supplied with 8 bar air pressure, which was well within the 16 bar limit, and the spool valve was also adequately lubricated from the oil mist lubricator in the supply air. In addition, the engine was never run higher than 4000 rpm, which was significantly lower than the advertised range of 12000 rpm, and most of the operation was between 1000 rpm and 2000 rpm. The failure was apparently due to fatigue, which was caused by the valve cap hitting the spool valve when it was opened and the high frequency cyclic operation. The valve cap was replaced with another one from a spare actuator. That valve cap also failed in a similar operating time. After this failure occurred, the manufacturers were contacted to establish if they had encountered similar problems or if they could shed any light on the matter. Cargine requested that the actuators be returned to them for analysis and maintenance. Their final report was that they had used inferior quality material for the valve caps and they subsequently replaced all the valve caps with others of better quality.

The next mechanical problem concerned wear that occurred at the in-

terface between the actuator pistons and valve shims where the stem of the actuator piston was being eroded away. The wear was initially observed when the actuators were disassembled to investigate the first port valve cap failure. The wear appeared to be caused by the natural rotation of the actuator piston, and at the time it was thought that the amount of wear was normal and insignificant. After the engine testing had been completed, when the valvetrain was disassembled, it was observed that there was substantial wear on the actuator piston.

It was subsequently established that the valves' shims and interfaces were being sufficiently lubricated from oil leakage past the actuator's piston, and from oil splashing from the movement of the valve spring. Therefore, the only possible explanation for the unusually high amount of wear was that the incorrect material had been used in the manufacture of the valve shims or the actuator piston. The shims were fabricated from hardened steel and the surfaces were ground. It is not known what material the stem of the actuator's piston was made from, but it was assumed also to be from hardened steel. When the actuators were sent to Cargine for the analysis of the valve cap failure, Cargine also examined the wear. They concluded that the actuator piston had not been properly hardened. The wear on the stem of the actuator piston can be seen in Figure 5.4.

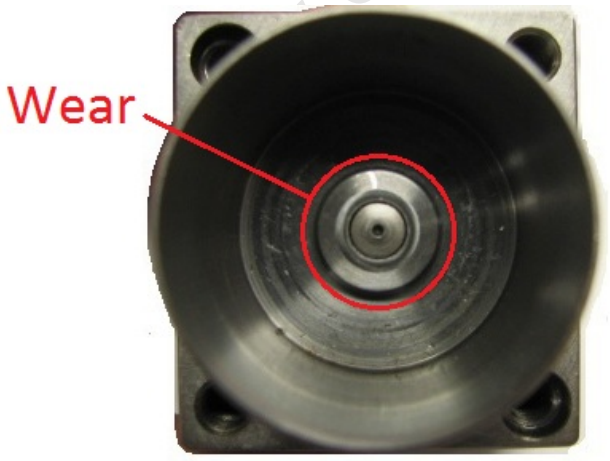

Figure 5.4: Wear on The Piston of The Cargine Pneumatic Actuator.

The last major mechanical failure that occurred was with the engine valve springs. This happened towards the end of the SI testing. This failure was discovered after unusual lift traces were observed. When consulting with various spring manufacturers, it was established that engine valve springs are

generally made from high strength chrome-vanadium steel, and the springs that were installed were made from regular spring steel. As a result, the springs failed because they could not cope with the high stresses and dynamic loading.

It also became apparent that this special valve spring steel is expensive to import, and consequently no one in South Africa imports this quality steel. Therefore, replacement springs could not be manufactured, and ready-made springs would have to be sourced from a scrap yard or a vehicle manufacturer. New springs were obtained from the EA111 engine of the 2010 VW 1.4 Polo, which was still to be launched in South Africa. This was fortunate because until then every other spring that was assessed had too large a diameter to fit inside the cup of the actuator's piston. A list of the specifications for the EA111 valve springs can be seen in Chapter 4 as well as a graph showing the spring constant and displacement vs. force.

Chapter 6

Experimental Results and Discussion

The following chapter presents the results that were obtained from testing the FVVA system and Hydra engine. This chapter is divided into three sections. The first section contains the results from the valvetrain commissioning, the second section covers testing the SI engine, and the final section presents the results of the HCCI testing.

6.1 Testing the FVVA Valvetrain

The final testing of the FVVA valvetrain was performed once development of the control software and FGPA ECU had been completed. The reason for carrying out these tests was to perform a final safety check to confirm that the actuators and software were functioning correctly, and also to document the full capabilities of the system.

Figure 6.1 shows the standard valve timing profiles and the generated solenoid pulses. The profiles show the maximum possible valve lift at 2000 rpm. Once the timing and duration of the solenoid pulses had been set, the repeatability of the entire lift profile was very good. It was observed that cylinder pressure and engine speed have the greatest effect on the profiles and their repeatability. This is because the valves are not mechanically driven and any variance in the engine's cylinder pressure affects the resultant force

on the face of the valves, and consequently its acceleration.

Additionally, it can be seen in the figure that the tops of the lift profiles are almost perfectly flat. This is because the measurement limit of the lift sensors had been reached. If the range of the lift sensors had been greater then the profiles would have had a more parabolic shape, similar to the profiles of camshaft driven valves. Alternatively, when the lift height was limited by the timing of the height solenoid, a sinusoidal oscillation was present at the flat peak of the lift.

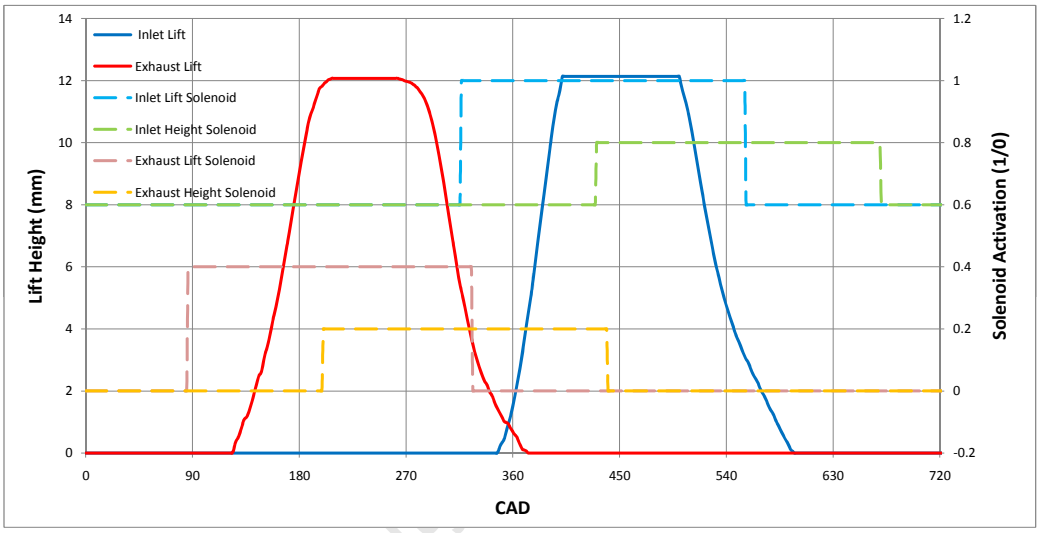

Figure 6.1: Standard Valve Lift Profiles at 2000 rpm with Standard Timing and Maximum Lift.

There was a temporal delay in the FVVA system from when a signal was generated to when the actuator actually responded. This meant that when the timing solenoid was activated or deactivated it took approximately 3-4 ms for the valve either to start opening, or for the valve seat to close. The height solenoid was typically activated 5-10 ms after the timing solenoid had been activated, depending on the desired lift height. It was only deactivated a few milliseconds after the valve had completed its movement for that particular engine cycle. It was found that for a given lift height when the engine speed was varied, the time delay between the activation timing solenoid and the activation of the height solenoid, was relatively constant. However, the time delay that was required to maintain a desired lift height changed significantly when the duration of the valve lift was changed.

The relationship between the valve lift height, lift duration, engine speed

and the various CAD offsets was very complex. After analysing the variables that affected the lift height it was determined that a number of multidimensional look-up tables would have been required to control the valve lift height, which would have been very complicated and time-consuming to implement. Therefore, it was concluded that the easiest method was to set the desired valve lift height manually by visually inspecting the actual lift profile graph and then adjusting the variables until the desired profile and lift height was achieved.

The figure below shows a graph of various lift profiles, which illustrates how the valve lift height can easily be manipulated by changing the time delay between the activations of the two solenoids. The control software was able to maintain the opening and closing points fairly accurately throughout the range of the lift with only a slight variance in the closing point. The maximum possible lift that the sensors could measure was just less than 12 mm although the physical limit of the valves' lift was 13 mm. The absolute minimum valve lift was 0.4 mm. This was the physical limit of the actuators and was defined by the activation time of the solenoids, which was a minimum of 2 ms. Therefore, the solenoids could not actuate and compressed air was not admitted into the actuators.

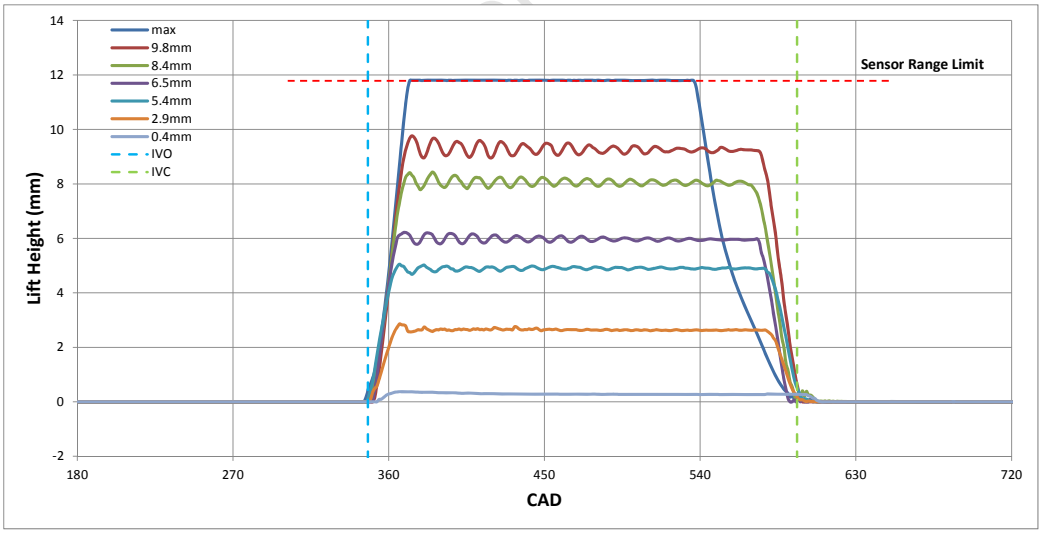

Figure 6.2: Inlet Varied Valve Lift Profiles at 1000 rpm with Standard Timing.

The graph shows a high frequency oscillation at the peak of the lift profile. This was due to the dampening effect of the hydraulic latch. The valve vibration was expected to occur under normal operating conditions and had

no noticeable effect on the intake air or exhaust flow. It can be seen that the valve oscillations were reduced as the lift height was reduced. This was because the valve's maximum velocity was also lowered when the lift height was reduced. Therefore, the required deceleration was also reduced and the hydraulic dampening had a more immediate effect.

It can be seen in Figure 6.2 that the valve's closing rate for the maximum lift trace was more gradual than that of the other traces, which all have fairly similar and steep closing rates. This was because at maximum lift the valve's motion was not restricted by the timing of the height solenoid and therefore the valve was allowed to move in a parabolic motion.

Figure 6.3 shows how the lift profile was affected by the speed of the engine. The valve typically took 2 ms to reach its maximum lift height from a fully seated position, and 2 ms to close. Therefore, as the engine's speed was increased the rise rate seemed to decrease. However, this only appears so because the graph was plotted in CAD. The rise rate actually remained fairly constant when compared with respect to time. In this figure the valve oscillation can only be seen on the profile trace for 3000 rpm because the tops of the other profiles were cut off when the lift sensor reached its maximum range. The slight deviation between the maximum lift height for 500-2000 rpm was caused by the material imperfections in the actuator's piston, which is covered in Chapter 5.

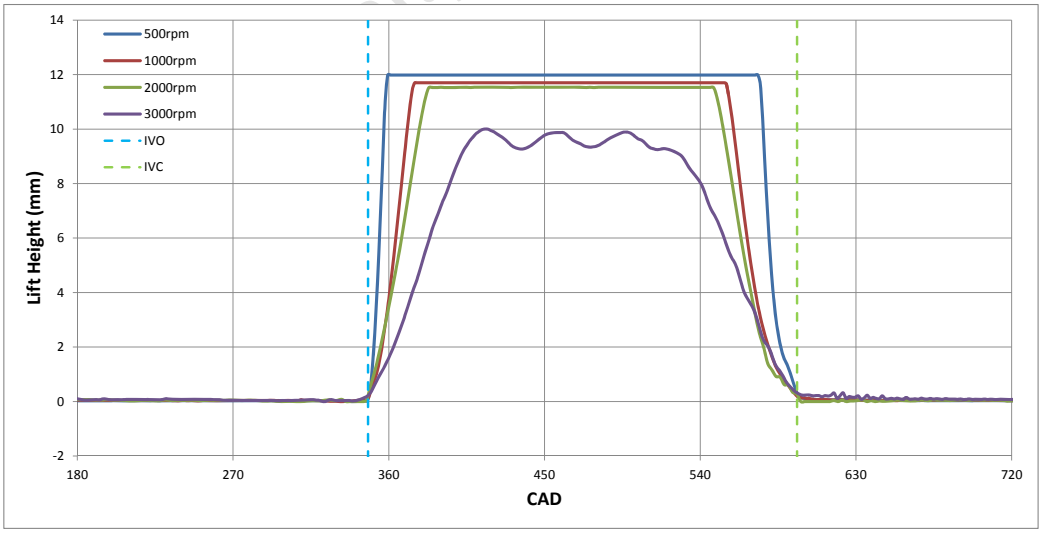

Figure 6.3: Maximum Inlet Valve Lift Profiles at Different Engine Speeds with Standard Timing.

6.2 FVVA SI Engine Testing

SI operation was used as the exploring grounds for FVVA because it guaranteed that combustion could be achieved relatively easily and it also offered stable and predictable combustion, whereby the full capabilities of the valvetrain could be explored. The fuel that was used for all the SI testing was standard grade pump gasoline, which has an octane rating of 95 RON (Research Octane Number).

6.2.1 WOT Power and Torque

Figure 6.4 shows a graph of the WOT power and torque curves that were recorded for FVVA SI operation overlaid with the Hydra's standard power and torque curves for SI mode with the 9:1 cylinder head. The peak power for SI operation was 13.5 kW at 4000 rpm and the peak torque was 33 Nm at 3000 rpm. These values were recorded at wide open throttle (WOT), λ=1.0 and a spark timing of 16 CAD BTDC. Table 6.1 shows the inlet valve's opening and closing angles for the optimised engine performance.

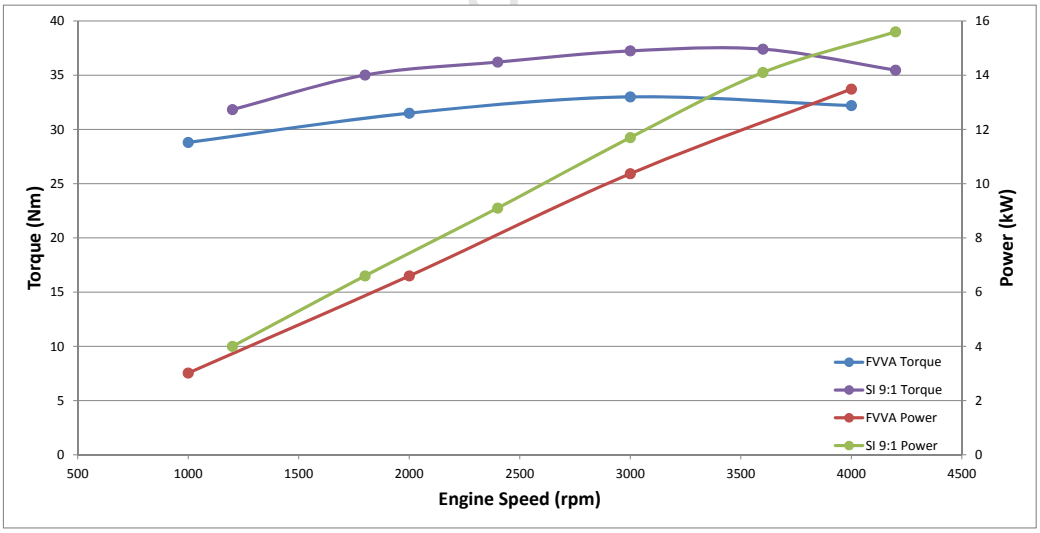

Figure 6.4: Torque and Power vs. Engine Speed for The SI Engine.

According to the Hydra's documentation the engine in SI mode was rated to produce 15 kW at 4000 rpm when using the 9:1 cylinder head. The spark timing was approximately 32 CAD BTDC and the fuel that was used was

"4 Star" gasoline. The fuel had an octane rating of 97 RON and contained tetraethyl lead, which boosted the fuel's octane rating and prevented knocking. It can also be assumed that this power was achieved with rich fuelling.

The torque produced by the FVVA engine was on average 5 Nm lower and the peak power was 1.5 kW lower than the SI Hydra engine with a fixed camshaft. It is difficult to compare the performance of the two engines because the setups and operating conditions were vastly different. However, considering that the compression ratio was lower, fuel octane rating was lower and the air/fuel ratio was stoichiometric, it can be said the FVVA engine's performance was acceptable.

Table 6.1: **Table of Optimised Inlet Valve Opening and Closing Angles for Maximum Torque.**

Engine Speed $[RPM]$	IVO $[CAD]$	IVC $[CAD]$
1000	358	605
2000	348	596
3000	343	592
4000	338	588

6.2.2 IVO Phasing

The inlet valve has the greatest effect on the engine's performance. Therefore, it was decided that the opening and closing points would be varied in order to investigate its effect. All of the experiments were performed at 2000 rpm, WOT, λ=1.0, standard valve timing and spark timing of 16 CAD BTDC.

Figure 6.5 shows how the engine's performance was affected when only the inlet valve's opening point was varied. IVO was incrementally varied by 10° with a maximum of 30° EIVO and 30° LIVO. The standard IVO timing of 348 CAD turned out to be the optimal point for IVO, which is understandable because 2000 rpm was close to the middle of the speed range and thus the standard valve timing would have been optimised for the mid-range speed, although compromising low and high speed operation. Even though IVO was already at its optimal point, this process and its results show that the timing of IVO has a significant effect on the engine's performance. It also highlights how easily the valve's timing can be manipulated in order to optimise and

increase the engine's performance, whether that being power output, fuel consumption or exhaust emissions.

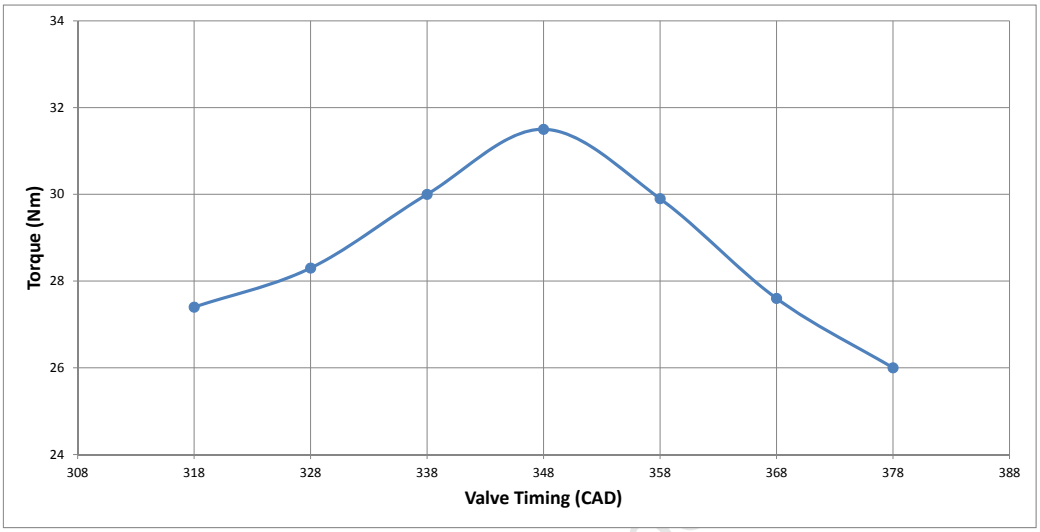

Figure 6.5: Torque vs. Valve Timing Showing IVO Phasing for The SI Engine.

It can be seen in Figure 6.5 that the torque drops off with EIVO. The reason for this is because some of the exhaust gas was expelled into the inlet manifold during compression and then re-breathed during the induction stroke. However, the exhaust gas takes up volume and heats the mixture. Therefore, less fuel has to be injected in order to maintain stoichiometry, and consequently less power was produced. LIVO increases in-cylinder turbulence and mixing, but it also limits the volume of air that is inducted into the cylinder since the overall open duration is reduced. As a result the amount of fuel that was injected had to be reduced so that a stoichiometric mixture was maintained.

6.2.3 IVC Phasing

The inlet valve's closing point was also varied in the same manner as the IVO point with a maximum of 30° EIVC and 30° LIVC. The results of this can be seen in Figure 6.6. As expected, the optimal IVC point was also at the standard valve timing of 596 CAD. The engine's torque dropped off with EIVC and LIVC, which can be attributed to some of the mixture being

exhausted during the compression stroke, and that the overall volume of inducted air and fuel mixture was reduced.

Although the torque was reduced with LIVC, it was observed that with a small amount of LIVC the specific fuel consumption improved from 277.4 g/kW.h at 596 CAD to 264.3 g/kW.h at 606 CAD LIVC, which is a 4.7% improvement in bsfc (brake specific fuel consumption). This is in line with a number of LIVC studies, which are noted in the Literature Review (Chapter 2).

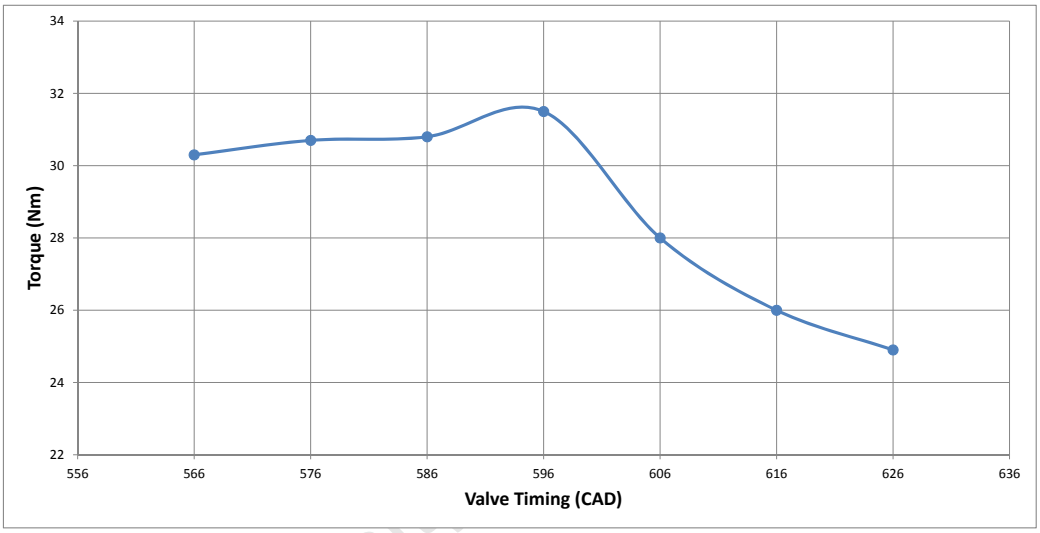

Figure 6.6: Torque vs. Valve Timing Showing IVC Phasing for The SI Engine.

6.2.4 Valve Profile Phasing

A common valve timing strategy, which was used in early automotive VVT systems, was to rotate the camshaft in relation to the drive gear. This could advance or retard the valve phasing of either the inlet or exhaust valves, and could also adjust the amount of overlap between the inlet and exhaust valves. The following experimentation was aimed at demonstrating this system and the Figure 6.7 shows the results.

The IVO and IVC points were gradually varied in small increments while their relative timing was kept constant. The engine's performance was noted after each increment. However, the data was only recorded in 10° steps to

show the general trend. The valve's phasing was advanced and retarded by a maximum of 30° in either direction. It was found that the standard inlet valve phasing at 2000 rpm provided the optimal valve timing with regard to engine torque. However, variable valve overlap is also used to control NOx and HC emissions. Therefore, this valvetrain could be used effectively for future emissions research.

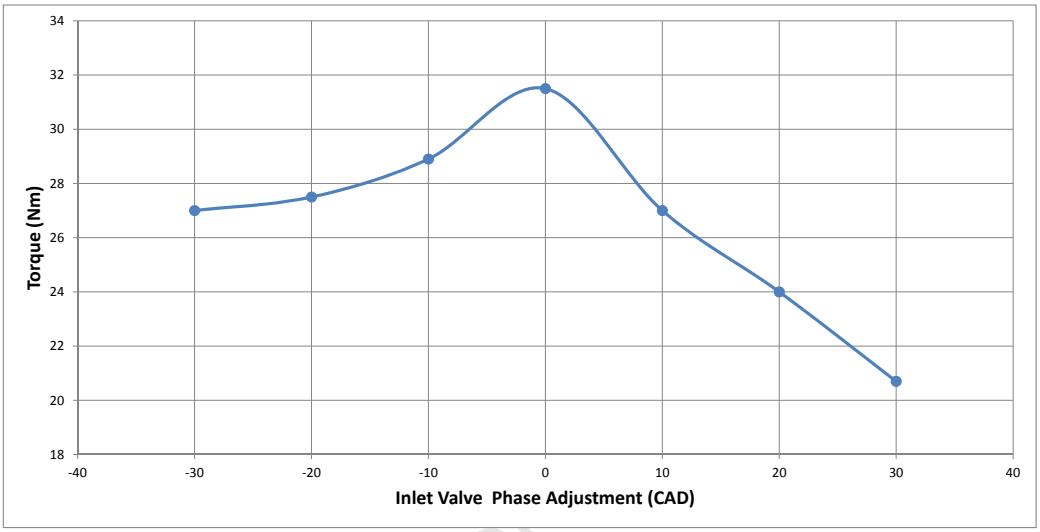

Figure 6.7: Torque vs. Valve Timing Adjustment Showing Inlet Valve Phasing for The SI Engine.

6.3 HCCI Testing

The aim of the HCCI testing was to establish a rough HCCI operating envelope with respect to engine speed and load, and to highlight the benefits of using the FVVA valvetrain to control HCCI combustion. In order to define an operating envelope, it is only required that the four corners be defined. Table 6.2 shows the four extremities of the envelope and the relevant settings that were required to induce HCCI combustion - namely Lambda value, Inlet Temperature and EVC point. All points were obtained at WOT, T_{water} = 89°C, T_{oil} = 78°C, P_{boost} = 15 psi and standard SI valve timing, except for when EIVC was employed. The section on the commissioning of the HCCI engine in Chapter 5 explains in detail how HCCI operation was achieved.

Table 6.2: **Test Results for HCCI Operating Envelope.**

Engine Speed $[RPM]$	Torque $[Nm]$	Power $[kW]$	Lambda $[\lambda]$	T_{Inlet} [°C]	EVC $[CAD]$
500	14.4	0.75	2.25	85	305
500	18.0	0.94	2.00	85	348
1000	17.0	1.78	1.80	96	332
1000	21.6	2.26	1.67	114	372

Figure 6.8 provides a visual comparison of the HCCI operating envelope with the FVVA SI torque curve. As can be seen, the maximum possible load for HCCI is significantly lower than what was achieved with SI combustion. The green dashed line shows a theoretical HCCI operating envelope that would have been expected for the engine. However, the actual operating speed range fell between 500 rpm and 1000 rpm. This is because the dyno struggled to maintain a constant speed below 500 rpm, which was caused by the physical limitations of the hardware. In addition, above 1000 rpm combustion became highly unstable and erratic, which was probably caused by combustion instabilities and cycle-to-cycle variations.

The engine's low load points were established by gradually increasing the fuel injection until combustion initiated. Once stable combustion was achieved the fuel injection duration was gradually decreased until just before the engine stalled. Therefore, the low load points signified the engine's lean misfire limit. The same method was used to establish the maximum load points whereby the fuel injection was gradually increased. The maximum

load points were limited by the combustion pressure rise rate, and therefore these points were on the verge of knocking.

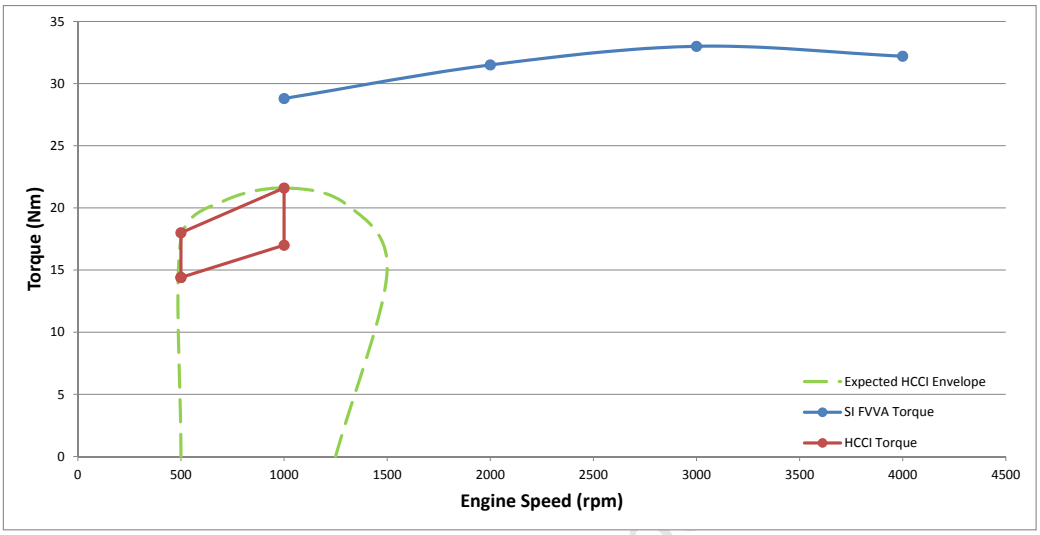

Figure 6.8: Comparison of The HCCI Operating Envelope and FVVA SI Torque Curve.

The figure below shows four pressure traces that were captured at each corner of the operating envelope and each trace was averaged over 64 engine cycles. However, the pressure traces could not be used for any significant calculations or comparisons because there was a large amount of uncertainty regarding the engine speed at which they were captured. As stated previously, the dyno could not maintain a constant speed at low rpm, and at higher rpm the combustion was very unstable. This caused the engine speed to fluctuate. At 500 rpm the engine speed fluctuated by as much as ± 35 rpm. This deviation in engine speed caused the pressure traces, which were recorded on the oscilloscope, to be either slightly stretched or squashed with respect to time. In other words, because the oscilloscope samples data at a set frequency, when the engine's speed changes, the time difference between each CAD changes.

The data that was captured around TDC was probably the most reliable portion of the pressure traces. This is because the TDC encoder was used as the trigger signal for capturing the pressure traces, which gave a stable reference point for that section of the pressure trace. Therefore, the stretching/squashing of the pressure trace around TDC can be assumed to be minimal.

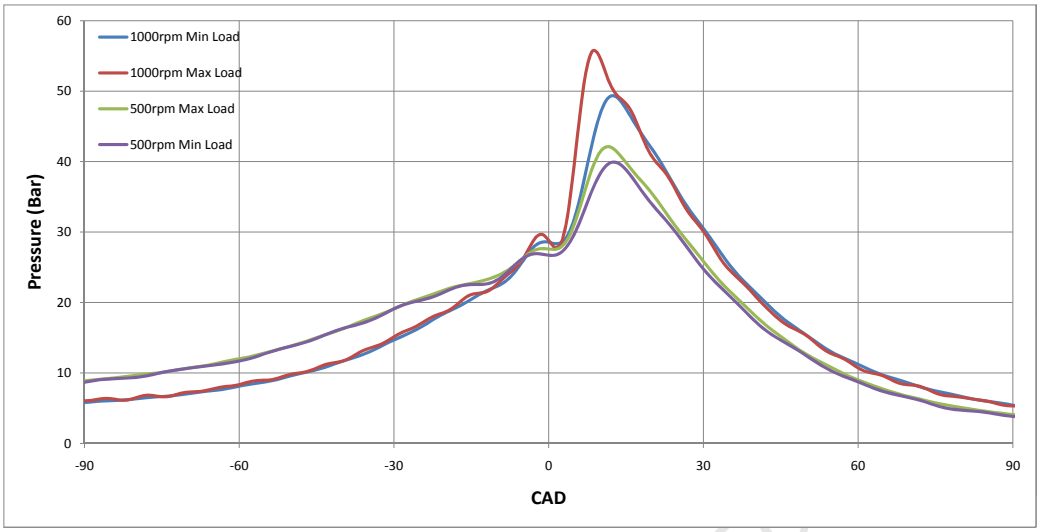

Figure 6.9: Comparison of The HCCI Operating Envelope Pressure Traces.

In Figure 6.9 the pressure traces for 1000 rpm and 500 rpm have significantly different compression strokes. This is probably caused by differences in their valve timing, which directly affects the cylinder pressure at the start of the compression stroke. In addition, the engine was designed to use a very small pressure transducer which was too small for water cooling. Consequently, this added a level of uncertainty to the pressure traces and could account for some of the deviation in the pressure traces.

The graph clearly shows the increase in cylinder pressure from the cool-flame temperature rise just before TDC. After a short delay, the main heat release occurred with the peak pressure between 8 CAD and 12 CAD ATDC. Figure 6.10 shows the heat release analysis of the pressure trace for 500 rpm at maximum load. The heat release analysis was performed according to the method described by Heywood [44]. A small cool flame reaction can be seen a few degrees before TDC, after which there is heat loss around TDC (3-5 J/CAD), and finally just after TDC the main heat release reaction occurs. The peak pressure varied between 49 bar and 56 bar depending on the engine speed and load. When the engine started to knock the cylinder pressure peaked as high as 100 bar, which can damage the engine and sensitive pressure transducer.

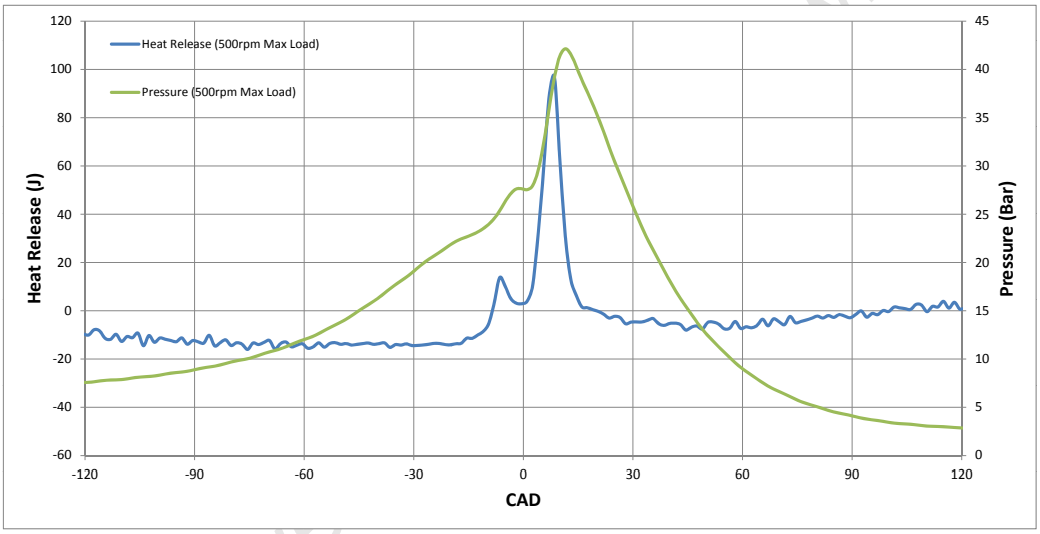

Figure 6.10: Heat Release Analysis for HCCI at Maximum Load and 500 rpm.

Chapter 7

Conclusions

This chapter lists the conclusions that can be drawn from the design and development of the FVVA valvetrain and the results of the experimentation and commissioning of the FVVA engine.

- The FVVA valvetrain and its subsystems were successfully implemented and incorporated with the single cylinder Ricardo Hydra engine as outlined in the primary objectives of project.
- The new FPGA ECU and control software were successfully designed, implemented and used to control the Hydra engine in diesel, spark ignition and HCCI operation. The custom ECU was also capable of controlling the various subsystems that were required to run the engine in the different operational modes.
- The FVVA valvetrain was effectively used to demonstrate some of the advantages of VVA technology through implementing different valve timing strategies, such as variable lift height, internal exhaust gas rebreathing and variable valve overlap. By varying the opening and closing timing of the inlet valve, it was demonstrated how significantly the inlet valve's timing affected the engine's torque output. The un-optimised IVO reduced the engine's torque by as much as 17% and the un-optimised IVC by 20%. The un-optimised inlet valve phasing reduced the engine's torque by 32%. Out-of-phase valve timing occurs when an engine with fixed timing camshafts operates in a speed range for which the camshafts where not designed/optimised.

- The FVVA valvetrain was effectively used to produce an optimised power and torque curve for the SI engine configuration. This demonstrated one of the important benefits of the FVVA valvetrain over fixed camshaft valvetrains.

- HCCI combustion was successfully achieved with the aid of the FVVA valvetrain and highlighted the benefits of the FVVA valvetrain. It showed that FVVA can successfully be used to implement EEVC in order to promote auto-ignition by internal exhaust gas re-breathing, which traps hot exhaust gas in order to increase the mixture's temperature. Even though the engine had a high propensity to knock excessively, and the combustion was too unstable to conduct any significant HCCI testing, a number of stable operating points were captured.

Chapter 8

Recommendations

The following is a list of recommendations for future work to be done regarding physical changes to the FVVA valvetrain, the control software and experimentation.

- During the operation of the actuators, pressurised air and a small amount of atomised oil escaped from the sides of the actuators and from underneath the solenoids. It is recommended that a special housing be designed which completely contains the actuators. If the engine's lubrication system is used to lubricate the actuators, there should be a drainage system that returns the oil to the engine's sump. Otherwise the oil should be drained into an external container which can then be used to refill the pressurised oil reservoir. The actuator housing should also have sufficient space so that large fittings can be used for the pneumatic supply, which will increase air flow to and from the actuators and improve the lift profiles at high engine speeds.
- During the testing phase of this project, it was discovered that a significant amount of wear occurred at the interface between the actuator pistons and valve shims. Cargine was contacted about this problem, and after inspecting the actuators, they concluded that the pistons had not been properly hardened. In addition, it was felt that there was insufficient lubrication even though Cargine stated in the actuator's manual that the oil leakage past the actuator piston provided enough oil for proper lubrication. It is recommended, therefore, that a separate oil circulation system is installed with nozzles that are positioned underneath the actuators and directed toward this interface.

- The NC-DVRT sensors that were used to measure the valve lift profiles only have a measurement range of 1.0 mm, which translates to a maximum of 12 mm of valve lift that can be measured. This causes the tops of the lift profiles to be cut off. Therefore, the sensors must be replaced with new sensors that have a measurement range of 1.5 mm that will ensure that the complete lift profiles are captured. The new sensors have a diameter which is 1.5 mm greater than the old sensors. Consequently, a new method will have to be devised to mount the sensors as they will not be able to fit into their original location on the actuators' collars.

- While performing the SI and HCCI testing, it was found that controlling the engine was very difficult and time consuming. There were simply too many variables and control parameters that needed to be supervised and adjusted, especially when changing the engine speed. The control system must be simplified so as to make it more user-friendly. This can be done by creating and populating more look-up tables and also by implementing a more advanced control system. Cargine has developed its own control system for the actuators which is capable of interfacing with an FPGA. Cargine should be contracted for assistance with upgrading the current control software or to implement the Cargine System.

- A large amount of data had to be passed between the FPGA and the host PC in order to analyse the pressure trace and the two lift traces. If the engine is upgraded to a four-valve engine, there will be two additional lift sensors that will need to be analysed. This will overload the FPGA's FIFO (First In, First Out) buffers and slow down the host PC as they will not be able to control the engine simultaneously and perform fast cycle-to-cycle analysis. A second PC and Indiset should be set up with the sole function of capturing and analysing the lift sensors and pressure traces. The Indiset is a multichannel data acquisition system, which is used for real time combustion and injection analysis. Once the data has been analysed, only the important information, such as actual valve opening and closing points, should be sent to the host PC that runs the LabVIEW and CalVIEW software.

- Various systems were not incorporated into the FPGA ECU and control software because they were not required to achieve the aims set out in this project. A few of the important systems that were not incorporated were the exhaust gas lambda sensor, laminar flow meter for the inlet air, and the fuel flow meter. However, a lambda sensor was used by

visually inspecting its output and manually adjusting the fuelling to maintain the correct lambda value. Control of the engine could be made significantly easier if look-up tables for throttle position, spark timing, fuel injection duration, injection timing, etc., versus engine speed and load, were populated and incorporated within the control software. The setup and population of look-up tables was not considered part of the scope for this project.

- The recommendations that have been proposed require expert knowledge of electrical systems and control theory. It is therefore highly recommended that whoever continues with this line of research has prior and expert knowledge of LabVIEW, control theory and electrical systems. If possible, a person with adequate knowledge of test cell systems and a mechanical engineering background should work in conjunction with an electrical expert so that all aspects of this research can be properly tackled.

References

[1] H. Hong, G. B. Parvate-Patil, and B. Gordon, "An asessment of intake and exhaust philosophies for variable valve timing," *SAE*, no. 2003-32-0078, 2003.

[2] S. Trajkovic, A. Milosavljevic, P. Tunestal, and B. Johansson, "Fpga controlled pneumatic variable valve actuation," *SAE*, no. 2006-01-0041, 2006.

[3] Wikipedia.org. (2011, January) Variable valve timing. [Online]. Available: http://en.wikipedia.org/wiki/Variable_valve_timing

[4] M. Wan. (2009) Autozine technical school. [Online]. Available: http://www.autozine.org/technical_school/tech_index.html

[5] J. B. Heywood, *Internal Combustion Engine Fundamentals*, 1st ed. Singapore: McGraw-Hill, 1988, p. 209.

[6] Mechadyne. (2006, December) The impact of valve events upon engine performance and emissions. [Online]. Available: http://www.mechadyne-int.com/vva- reference/papers/the-impact-of-variable-valve-actuation-on-engine- performance-and-emissions.pdf

[7] J. B. Heywood, *Internal Combustion Engine Fundamentals*, 1st ed., J. P. Holman, Ed. Singapore: McGraw-Hill, 1988.

[8] Y. Y. Ham and P. Park, "The effects of intake valve events on engine breathing capability," *In Proceedings of the Sixth International Pacific Conference on Automotive Engineering*, no. 912470, 1982.

[9] J. B. Heywood, *Internal Combustion Engine Fundamentals*, 1st ed. Singapore: McGraw-Hill, 1988, p. 218.

[10] Wikipedia.org. (2010, December) Continuous variable valve timing. [Online]. Available: http://en.wikipedia.org/wiki/Continuous_variable_valve_timing

[11] C. Menzel, C. Torresan, J. Knight, C. Raines, D. Sapp, M. Patel, R. Miles, N. Miles, and Z. Peng, "Electronic continuous variable valve timing for small si engines," *SAE*, no. 2008-01-1778, 2008.

[12] P. K. Wong and K. W. Mok, "Desing and modeling of a novel electromechanical fully variable valve system," *SAE*, no. 2008-01-1733, 2008.

[13] BMW-Sport. (2010) Bmw double vanos image. [Online]. Available: http://bmw-sport.net/linkedimages/double_vanos.jpg

[14] Wikipedia.org. (2010, November) Vtec. [Online]. Available: http://en.wikipedia.org/wiki/VTEC

[15] Wikipedia.org. (2010, November) Vvt-i. [Online]. Available: http://en.wikipedia.org/wiki/VVTL-i

[16] Honda. (2010) Honda vtec image. [Online]. Available: http://world.honda.com/automobile-technology/VTEC/

[17] Toyota. (2007, June) Toyota develops next-generation engine valve mechanism. [Online]. Available: http://www.toyota.co.jp/en/news/07/0612.html

[18] J. Allen and D. Law, "Production electro-hydraulic variable valve-train for a new generation of i.c. engines," *SAE*, 2002.

[19] W. Grueninger. (2010) Variable valve timing explained. [Online]. Available: http://www.motivemagazine.com/pub/feature/tech/Motive_Tech_Variable_Valve_Timing_Explained.shtml

[20] J. B. Heywood, *Internal Combustion Engine Fundamentals*, 1st ed. Singapore: McGraw-Hill, 1988, p. 206.

[21] T. W. Asmus, "Valve events and engine operation," *SAE*, 1982.

[22] F. Soderberg and B. Johansson, "Load control using late intake valve closing across flow cylinder head," *SAE*, no. 2001-01-3554, 2001.

[23] J. D. Haugen, P. L. Blackshear, M. J. Pipho, and J. W. Esler, "Modifications of a quad 4 engine to permit late intake valve closure," *SAE*, no. 921663, 1992.

[24] F. Soderberg and B. Johansson, "Fluid flow combustion and efficiency with early or late intake valve closing," *SAE*, no. 972937, 1997.

[25] M. Sellnau and R. Rask, "Two-step variable valve actuation for fuel economy, emissions and performance," *SAE*, no. 2003-01-0029, 2003.

[26] C. Gray, "A review of variable engine valve timing," *SAE*, no. 930820, 1988.

[27] R. M. Siewert, "How individual valve timing events affect exhaust emissions," *SAE*, no. 710609, 1971.

[28] R. A. Stein, K. M. Galietti, and T. G. Leone, "Dual equal vct - a variable camshaft timing strategy for improved fuel economy and emissions," *SAE*, no. 2008-01-1733, 1995.

[29] F. Zhao, N. Dennis, D. N. Assanis, P. M. Najt, J. E. Dec, J. A. Eng, and T. N. Asmus, "Homogeneous charge compression ignition (hcci) engines: key research and development issues." *SAE*, p. 327, 2003.

[30] R. Craknell, J. Ariztegui, K. Barnes, P. Bessonette, W. cannella, F. Douce, B. Kelecom, H. Kraft, I. Lampreia, D. Reckeard, M. Savarese, J. Williams, and K. D. Rose, "Advanced combustion for low emissions and high efficiency: A literature review of hcci combustion concepts," *CONCAWE*, no. 4/08, April 2008.

[31] J. B. Heywood, *Internal Combustion Engine Fundamentals*, 1st ed. Singapore: McGraw-Hill, 1988, p. 517.

[32] Blakeman, Chiffy, Phillips, Twigg, and Walker, "Development in diesel emissions aftertreatment technology," *SAE*, no. 2003-01-3753, 2003.

[33] U.S. Department of Energy Office of Transportation Technologies. (2001, April) Homogeneous charge compression ignition (hcci) technology, a report to the u.s. congress. [Online]. Available: http://www-erd.llnl.gov/FuelsoftheFuture/pdf_files/hccirtc.pdf

[34] R. Stanglmaier, "Homogeneous charge compression ignition (hcci): Benefits, compromises, and future engine applications," *SAE*, no. 1999-01-3682, 1999.

[35] S. M. Aceves, D. L. Flowers, F. Espinosa-Loza, J. Martinez-Frias, J. E. Dec, M. Sjberg, R. W. Dibble, and R. P. Hessel, "Spatial analysis of emissions sources for hcci combustion at low loads using a multi-zone model," *SAE*, no. 2004-01-1910, 2004.

[36] J. Martinez-Frias, S. M. Aceves, D. Flowers, J. R. Smith, and R. Dibble, "Hcci engine control by thermal management," *SAE International*, 2000.

[37] H. Kuzuyama, M. Machida, K. Akihama, K. Inagaki, and M. Ueda, "A study on natural gas fueled homogeneous charge compression ignition engine - expanding the operating range and combustion mode switching," *SAE*, no. 2007-01-0176, 2007.

[38] H. Hu, "The uk foresight vehicle research on extending hcci engine operating boundaries [presentation]." Lund: SAE HCCI Symposium, 2005.

[39] Wikipedia.org. (2010, November) Diesotto. [Online]. Available: http://en.wikipedia.org/wiki/DiesOtto

[40] B. AB. (2010, October) Cargine. [Online]. Available: http://www.brann.se/en/company/References/Referens_1/

[41] EVO.co.uk. (2007, April) Koenigsegg goes green. [Online]. Available: http://www.evo.co.uk/news/evonews/207928/koenigsegg.html

[42] NSK. (2011) Limiting speed. [Online]. Available: http://www.tec.nsk.com/handbook.asp?menu=4,0,0,0&PageID=/LimitingSpeed/IndexLimitingSpeed.html

[43] Wikipedia.org. (2010, November) Ground loop (electricity). [Online]. Available: http://en.wikipedia.org/wiki/Ground_loop_(electricity)

[44] J. B. Heywood, *Internal Combustion Engine Fundamentals*, 1st ed. Singapore: McGraw-Hill, 1988, p. 508.

[45] U. Carlson and A. Hoglund, "Cargine pneumatic actuator installation manual," 2009.

[46] U. Carlson, A. Hoglund, and M. Hedman, "Analysis and modeling of an electronically controlled pneumatic hydraulic valve for and automotive engine," *SAE*, no. 2006-01-0042, 2006.

[47] National Semiconductor Corporation. (2008, December) Lm1949 injector drive controller. [Online]. Available: http://www.national.com/ds/LM/LM1949.pdf

Appendices

Appendix A

Overview of Cargine Pneumatic Actuators

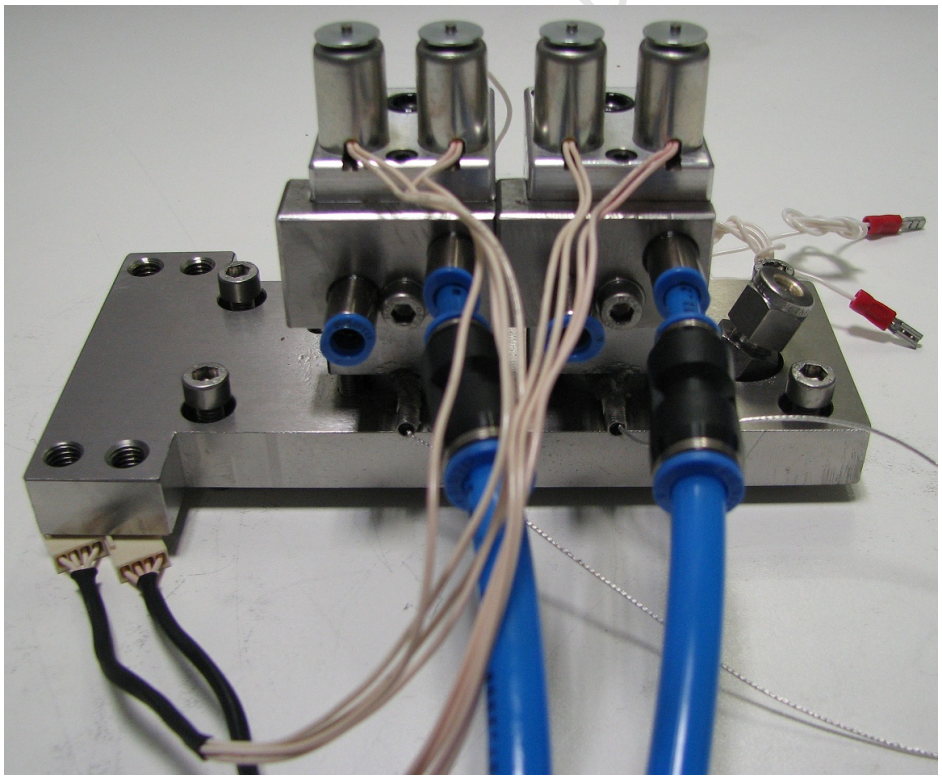

Figure A.1: The Cargine Pneumatic Actuator.

A.1 Introduction

Fully Variable Valve Actuation was accomplished by utilizing pneumatic-hydraulic actuators, which were electrically controlled via a FPGA ECU and computer. The actuators were supplied by Cargine Engineering AB, who have been researching free valve engines in conjunction with Lund University in Sweden. Solenoids were used to regulate pressurised air into the actuators, which allowed for the timing, open duration and lift height of the valves to be precisely controlled. This allowed for the valve events to be optimised over the entire speed and load range of the engine in order to achieve maximum power output in conjunction with significant reductions in fuel consumption and exhaust emissions. Figure A.1 on the previous page shows the actuators attached to their mounting plate, and the figure below is a diagram of an actuator with the critical components labelled.

The following appendix explains the internal operation of the actuators and their method of control. Details of the electrical control, lubrication and pneumatic systems are also to be found in this appendix. These systems were required for the actuators to function and were installed in the engine test cell.

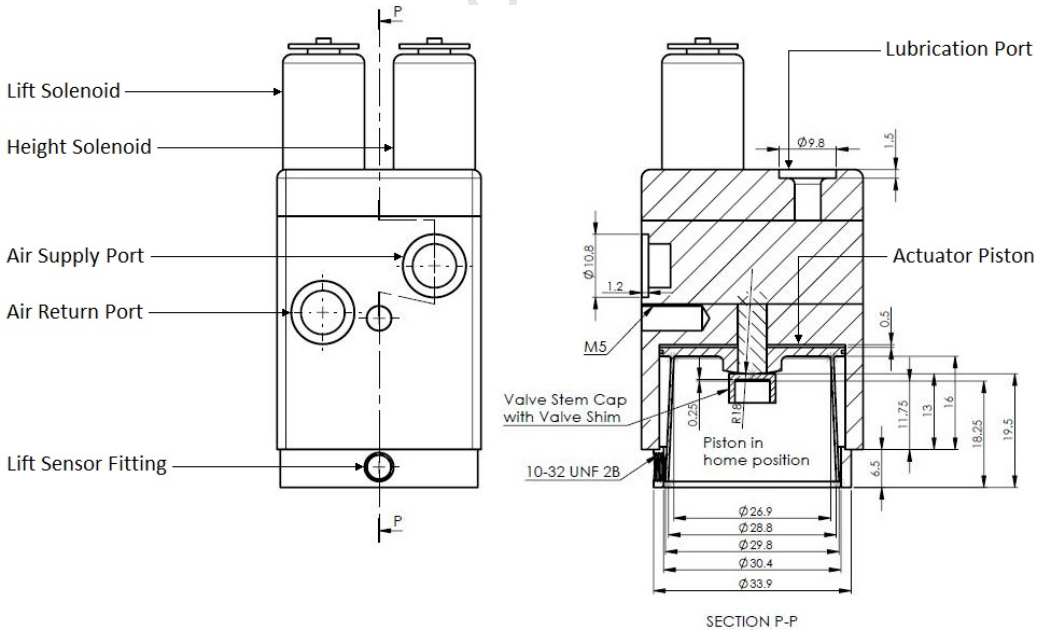

Figure A.2: Diagram of The Cargine Pneumatic Actuator [45].

A.2 System Dynamics and Operation

The actuators consist of two solenoids, two spool valves, two port valves, the actuator cylinder and piston, and a hydraulic latch/damper system. When the actuator is energised the actuator's piston opens the poppet valve by pushing on top of the valve stem. The actuator has no built-in mechanism to close the poppet valve and thus a conventional valve spring system is required to close the valve and return the actuator's piston to its home position.

The two push solenoids control the spool valves, which are used to control the air flow into and out of the actuator's cylinder. A hydraulic latch is used to hold the valve open at the desired height. This system allows for the maximum amount of work to be extracted from the air while also minimizing air and energy consumption. The hydraulic system is also used as a damper to reduce the valve's seating velocity in order to prevent valve seat recession.

The actuators operational cycle is divided into three distinct stages, which will be described in detail in the following three sections. The stages are as follows:

1. Air Charging
2. Expansion and Dwell
3. Air Discharging

The following table identifies the colours that are used to represent the air flow and pressures in the following diagrams, which are used to aid in the explanation of the system dynamics.

Table A.1: **Colours Table for System Pressures.**

Colour	System Pressure	Typical Pressure
Red	Supply Air/High Pressure	8 bar Gauge
Blue	Atmospheric Air/Low Pressure	1 bar Absolute
Yellow	Hydraulic Latch/Damper	8 bar Gauge

In the system diagrams there are two check-valves that are labelled *S1* and *S2*, which correspond to the timing solenoid (*Solenoid 1*) and the height solenoid (*Solenoid 2*) respectively. When a solenoid is energised it is coloured green and its corresponding check-valve functions as a one-way valve. When a solenoid is deactivated it is coloured blue and its corresponding check-valve is held off its seat, thus allowing two-way flow past the valve. A spring and damper system is shown in the two *port valves*. However, in reality the valve is a free moving cup without a spring or damper. Also, a damper is shown in the actuator piston, but this is just used to illustrate the damping effect of the hydraulic latch and friction.

A.2.1 Air Charging Stage

The system diagram for the *Air Charging Stage* can be seen in the figure below. The Air Charging Stage and the valve's motion is initiated by energizing the timing solenoid, which pushes *spool valve 1* slightly to the right. This allows high pressure air from the air supply to flow to the left side of *outlet port valve* and to the right side of *inlet port valve*. In addition, the high pressure air on the left side of the *inlet port valve* is allowed to exhaust to the atmosphere. The *outlet port valve* remains closed due to the difference in area between the two sides of the valve, even though both sides are supplied with high pressure air. Therefore, the high pressure air closes the *outlet port valve* and opens the *inlet port valve*. The high pressure air is now able to fill the actuator's cylinder, which starts moving the piston downwards and opens the poppet valve.

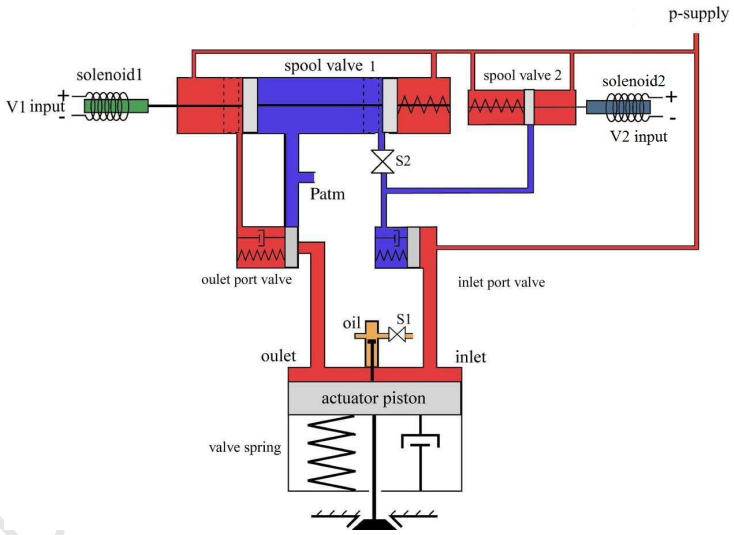

Figure A.3: Diagram of Air Charging Stage [46].

Check-valve *S1* is activated when the piston starts moving downwards. This allows oil to fill the hydraulic latch area, but prevents it from returning to the hydraulic reservoir.

A.2.2 Expansion and Dwell Stage

The system diagram for the *Expansion and Dwell Stage* can be seen in the figure below. The stage begins with *Solenoid 2* being energised. The maximum desired valve lift is determined by the time delay between the activation of the timing solenoid and the height solenoid. This is generally 2 ms to 5 ms, where a longer delay period will result in a greater lift.

The solenoid pushes *spool valve 2* slightly to the left, which sends high pressure air to the left of the *inlet port valve*. In actuality the *inlet port valve* is orientated vertically and because both sides of the valve are at high pressure, gravity closes the valve. The *inlet port valve* is then held closed due to the area difference between the two sides of the valve. Check-valve *S2* stops the high pressure air from escaping into the atmosphere through *spool valve 1*. *Solenoid 1* remains activated and therefore the *outlet port valve* remains closed and prevents the high pressure air inside the actuator cylinder from escaping into the atmosphere. The trapped air is now able to expand and the poppet valve and actuator piston will reach their prescribed maximum lift height.

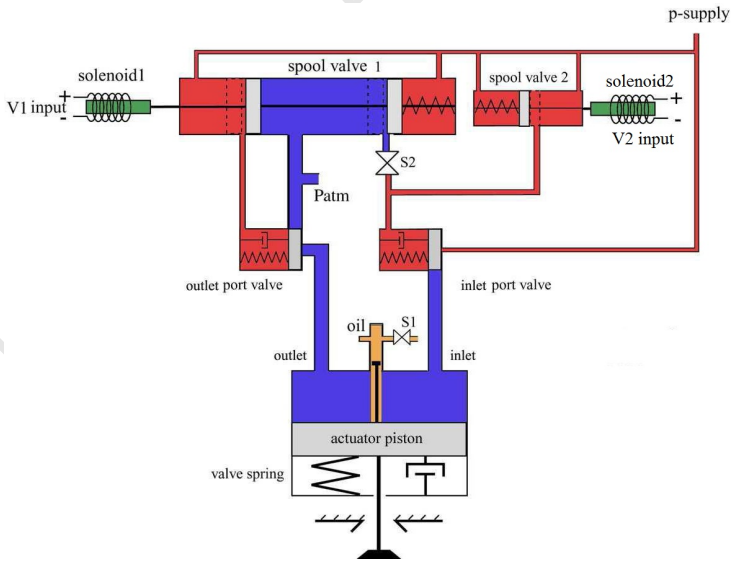

Figure A.4: Diagram of Expansion and Dwell Stage [46].

The high pressure oil trapped in the hydraulic latch balances the valve spring force and keeps the valve open at its prescribed lift height for as long as it is needed. This is the "energy saving mode", which allows the system to extract the full expansion work from the air that has entered the cylinder.

A.2.3 Air Discharging Stage

The system diagram for the Air Discharging Stage can be seen in the figure below. This is the final stage in the actuator's cycle where the air is expelled from the actuator's cylinder and the valve returns to its seat. In order to discharge the air and close the valve, both solenoids are deactivated, which consequently deactivates both check-valves *S1* and *S2*. This allows the oil and air to flow in either direction through *S1* and *S2* respectively. Once the solenoids are deactivated the springs inside the spool valves return them to their default positions. High pressure air on either side of the *inlet port valve* and the area difference between the two sides of the valve keeps the valve closed. Low pressure air is now on the left side of the *outlet port valve* and consequently the valve will open freely.

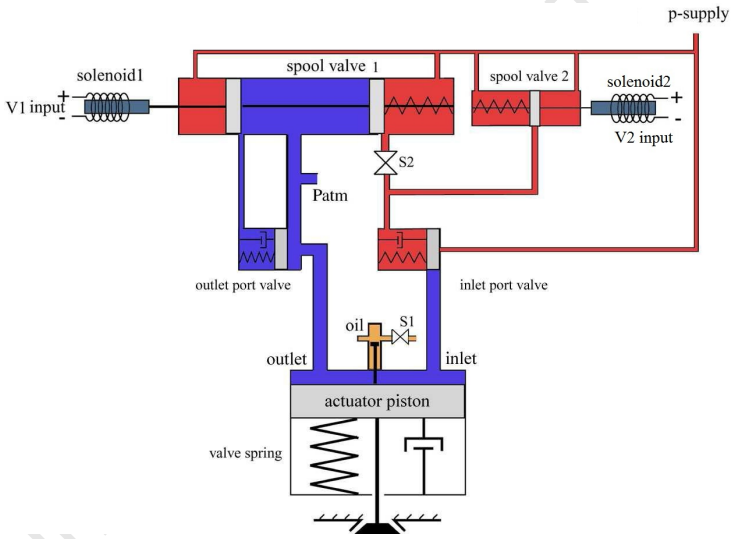

Figure A.5: Diagram of Air Discharging Stage [46].

When the hydraulic latch is deactivated it no longer resists the valve spring, and the actuator's piston and poppet valve are able to return to their home positions unhindered. The movement of the actuator's piston and the higher than atmospheric air pressure inside the actuator's cylinder opens the *outlet port valve* and the air inside the actuator's cylinder is able to discharge into the atmosphere. Also, the oil inside the hydraulic latch is discharged into the hydraulic lines. As the poppet valve nears its seated position, the rubber hydraulic lines expand slightly and function as a damper, which greatly reduces the valve's velocity and thus provides a smooth return and seating.

A.3 Solenoid Control Method

The pneumatic actuators were each controlled by two solenoids, which allowed the valve's timing and lift height to be fully controlled, thus enabling fully variable valve actuation. The following section lists the specifications of the actuator solenoids and details the control strategy employed.

A.3.1 Solenoid Specifications

Two small 3 V push-pull solenoids were used to actuate the spool valves and control the air flow into and out of the actuator. For optimal performance and low energy consumption the solenoids were activated with a peak and hold driver circuit. A diesel injector driver circuit was used to provide the optimal performance allowing for precise acceleration and retardation control.

It is also possible to control the solenoids with a simple square wave signal. However, this is not recommended because this will increase the heat load on the solenoids, reduce the performance, and increase energy consumption. If a square wave signal is used then the duty cycle must be less than 25% and the pulse length less than 1 second, otherwise the solenoids will overheat and be permanently damaged.

The following table lists the important specifications for the solenoids:

Table A.2: **3 V DC Solenoid Specifications.**

Item	Detail
Stroke	0.8 mm
Resistance	5 Ω
Peak Voltage	$\leq$ 14 V
Hold Voltage	$\approx$ 4.5 V
Peak Duration	3 ms @ 14 V peak

A.3.2 Control Circuit

A standard injector driver controller circuit was used to activate and control the timing and lift solenoids. The LM1949 linear integrated circuit (IC) was selected as the controller. The IC controls a Darlington transistor that drives the high current solenoid.

The current that is required to open a solenoid is significantly greater than the current that is needed to hold it open. Therefore, the IC controller directly senses the solenoid's current and saturates the solenoid until the peak current is four times the hold current, ensuring that the solenoid opens. Once the solenoid opens, the current drops to the hold level for the remainder of the input pulse. The peak and hold method greatly reduces the total energy consumption and also reduces the opening and closing delays.

Figure A.6 shows the recommended circuit diagram for the LM1949 IC controller which was used to control the actuator's solenoids.

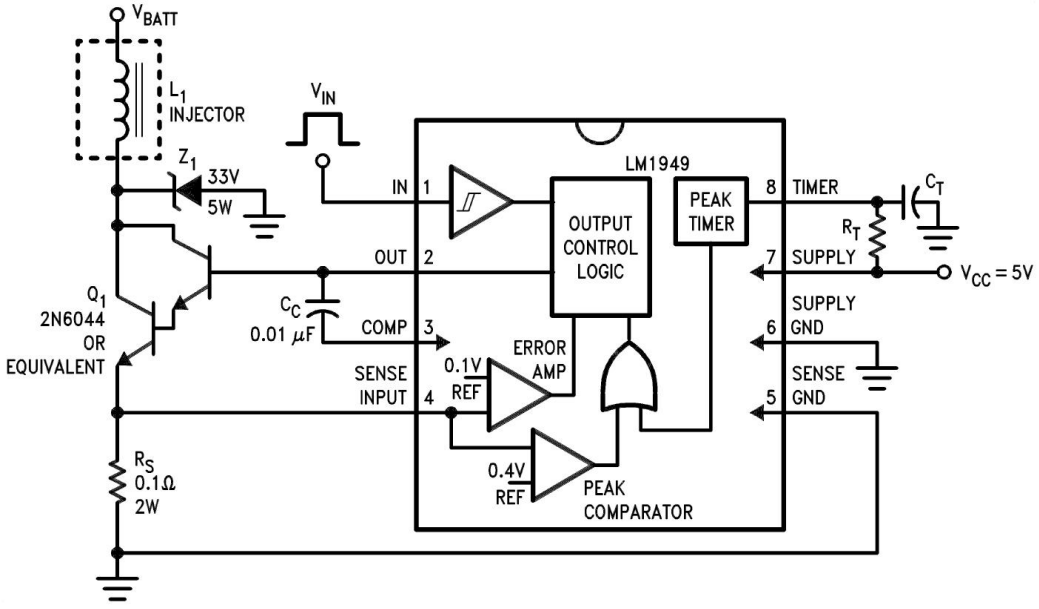

Figure A.6: Circuit Diagram of Solenoid Driver Circuit [47].

The peak and hold currents are determined by the applied voltage and the value of the sense resistor R_S. When a 5 V signal is sent to pin 1, the IC activates the Darlington transistor and consequently grounds the low-side of the solenoid.

A.3.3 Solenoid Control Signals

This section provides details on how the precise timing of the voltage pulses from the solenoid driver circuit controls the actuator's timing, open duration and lift height. There are five important timing stages/delays, which affect the motion of the actuator and they are as follows:

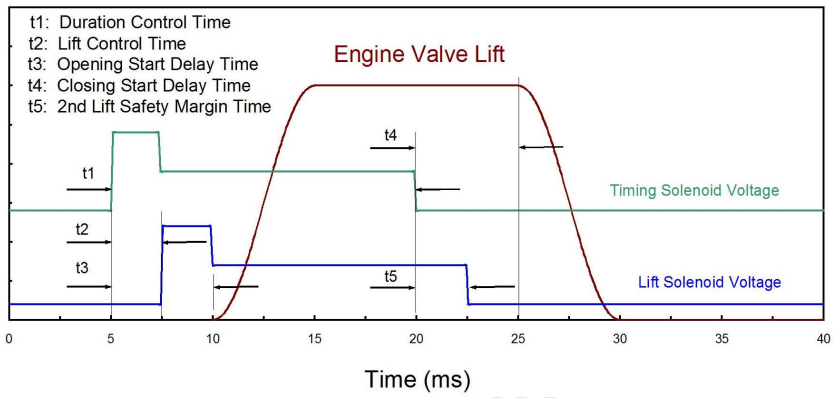

Figure A.7: Diagram of The Solenoid Control Signals [45].

Duration Control - t1: The start of the valve lift is initiated when the timing solenoid is energised and the duration of the valve lift is determined by the duration that the timing solenoid is energised.

Valve Lift Height - t2: The time delay between the activation of the timing solenoid and the lift solenoid determines the amount of high pressure air that enters the actuator cylinder and consequently, the valve's maximum lift height. The maximum lift height is also dependent on the supply pressure and the engine's cylinder pressure.

Opening Start Delay Time - t3: The typical *opening start delay time* between the start of the timing solenoid's voltage pulse and the poppet valve starting to open is between 4 ms and 5 ms.

Closing Start Delay Time - t4: The typical *closing start delay time* between the end of the timing solenoid's voltage pulse and the poppet valve starting to close, is between 4 ms and 5 ms. The closing start delay time depends on the air supply pressure and the hydraulic latch spring force. A higher air supply pressure or a weaker hydraulic latch spring force will both shorten the delay. However, if the spring force is too weak the hydraulic latch will not operate properly.

2nd Lift Safety Margin - t5: It is important that the lift solenoid's voltage pulse finishes after the timing solenoid's voltage pulse to ensure that the poppet valve does not reopen, which is possible at very short lift durations. It is recommended that the timing solenoid and lift solenoid have the same voltage pulse duration, which should give a sufficient *2nd lift safety margin*.

A.4 Pneumatic Supply System

The air supply is connected to the right hand port which is on the front of the actuator below the lift solenoid. The supply air line consists of a pressure regulator set to 8 bar, a water separation unit, an air lubrication unit and a 5 L reservoir that is located close to the actuators. Figure A.8 is a diagram of the pneumatic and hydraulic systems. It shows all the components in the systems and how they should be correctly assembled.

The lubricator provides lubrication for the spool valves and other internal components that are not lubricated by the hydraulic system. The lubricator is set to deliver 1 drop of oil per minute at the maximum air flow. The large volume air reservoir is required in order to reduce pressure fluctuations in the supply line, which are caused by the actuators' pulsating air usage. The pressure fluctuations could have a negative affect on the lift of the next actuator. The reservoir also ensures that there is a sufficient volume of high pressure air close to the actuators. Due to the high speed nature of the actuators' operation and low duty cycle (less than 40%), 8 mm hose was used for the air lines in order to maximise the volume of air that is available close to the actuator's inlet port. Therefore, the air that is close to the inlet port is able to be replaced quickly when it is used and guarantees that there will be sufficient air for the following cycle.

The air pressure that is required to open the poppet valve is dependent on the valve spring's preload and spring constant, and also the pressure difference across the valve during opening. The actuator's piston has a diameter of 32 mm and therefore it can produce a force of 80 N/bar of supply pressure. The actuators require a minimum supply pressure of 2 bar to overcome the spring's preload and an additional 3.5 bar to achieve the maximum possible lift height of 13 mm. However, a total pressure of 7 bar or greater is required in order to maintain the maximum valve lift throughout the engine's speed range.

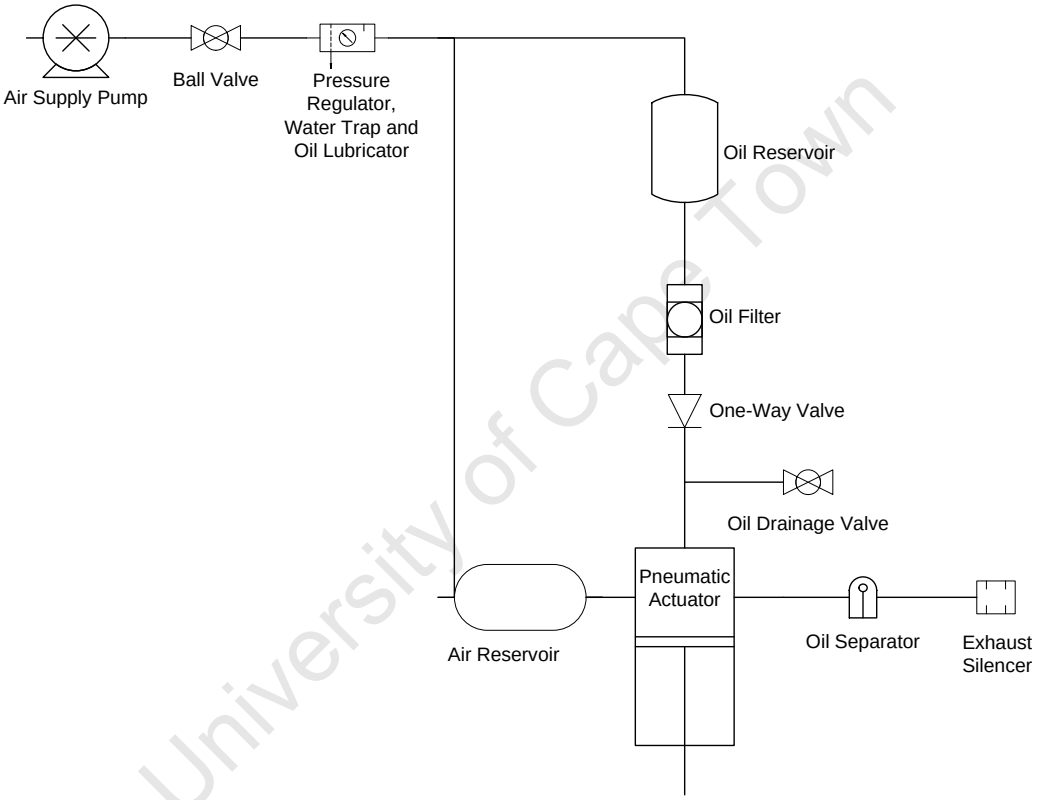

Figure A.8: Diagram of The Valvetrain's Pneumatic and Hydraulic Subsystems

The exhaust air system is connected to the left-hand port, which is on the front of the actuator below the timing solenoid. The exhaust air system requires an oil separator to remove the air lubrication that is added to the inlet air as well as the oil leakage from the hydraulic latch/damper. A silencer is also required to reduce the noise that is created by the high velocity exhaust air.

The actuators have a continuous leakage flow of 1-3 L/min per actuator, which escapes via venting ports on the left side of the actuators and from gaps underneath the solenoid wires at the front of the solenoids. The amount of air that the actuators consume is not directly proportional to amount of valve lift, but is closer to a quadratic relationship.

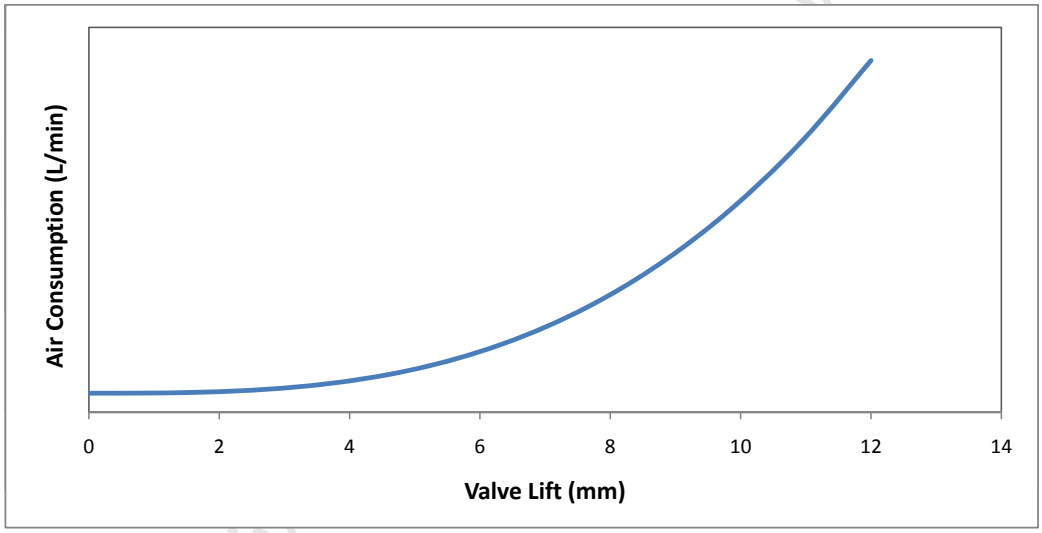

Figure A.9: Graph Illustrating The Actuator's Air Consumption vs. Valve Lift Height.

A.5 Lubrication System and Hydraulic Latch

The hydraulic system uses standard engine oil, in this case Shell 10W40, and consists of an oil reservoir, an oil filter, a check-valve and a rubber hose that is clamped to the top of the actuators and seals on an O-ring. These items must be assembled in the prescribed order, which can also be seen in Figure A.8. The oil reservoir is pressurised via the pneumatic supply system, which must be between 3 bar and 10 bar. If the oil pressure is less than the recommended level, then the hydraulic latch might only be partially filled, which will reduce the maximum sustainable lift. The oil filter must be able to remove particles greater than 10 μm. It is possible for the actuators to be damaged if particles greater than 10 μm travel through the actuators. The check valve is placed after the filter so that the filter does not act as a positive displacement pump when the valves are actuated, which can create a pressure build-up in the hydraulic lines and cause the valves to stay open. Additionally, the check-valve retains the oil in the rubber hose so that the hose can function as a damper when the actuator piston is returned.

When the actuator opens, pressurised oil is forced into the cavity above the stem of the actuator piston. When the poppet valve and actuator piston reach their prescribed lift height, the oil check-valve closes and the trapped oil maintains the set height. When the actuator solenoids are deactivated, the check-valve is opened and the poppet valve spring returns the actuator piston, which forces the oil inside the cavity back into the supply line. This causes the pressure to rise in the oil supply line and thus dampens the valve's seating velocity.

The hydraulic latch of one actuator requires 19.6 μl of oil per mm of valve lift. Therefore, at 12 mm of lift this corresponds to a volume of 0.255 ml.

The hydraulic lines that connect the check-valve to the lubrication port on top of the various actuators need to be flexible in order to accommodate the oil that is ejected from the hydraulic latch/damper when the piston is returned. The lines are made from standard rubber fuel hose with an internal diameter of 8 mm as this provides sufficient expansion in the lines to accommodate the oil. The length of the lines must be between 300 mm and 1500 mm for optimum performance. If the oil supply line is too stiff the poppet valve will not be able to close properly.

There is not a separate oil return line, and consequently oil that leaks out of the hydraulic latch goes into the air exhaust line. Therefore, an oil

separation unit is required in the air exhaust line. Some of the oil also leaks past the actuator piston and this leakage is used to lubricate the stems of the poppet valves. This flow is minimal, and over time, the valve spring compartment can become so full that the actuator piston will be obstructed. Therefore, an oil drain must be connected from the valve spring compartment to the engine's crank case. Under normal operating conditions (8 mm lift at 2000 rpm) the total leakage flow is between 0.1 ml/min and 0.3 ml/min per actuator.

The hydraulic system must be vented before the engine is first started up after assembly in order to remove any air in the system. After the lines have been vented, the actuators must be run at a low frequency ($\approx$ 5 Hz) until stable, and long duration valve lifts are established. If there is air in the system it will cause noticeable vibrations that could be several millimeters in amplitude. Under normal operating conditions there is a slight vibration measuring $\leq$ 0.25 mm, which is caused by the hydraulic latch when the valve reaches its prescribed lift height. An example of his can be seen in the Figure A.10.

Figure A.10: Graph of Characteristic Valve Vibration [45].

The grub screw that is between the two air ports on the front face of the actuator forms a part of the over-pressure safety valve. The safety valve is made up of a small ball bearing, twelve conical spring washers and a grub screw. It is important for the washers to be installed correctly and the grub screw properly torqued to ensure the system works properly. A diagram of the correct installation procedure can be seen in the figure below. The

washers must be installed with each pair of washers turned in the opposite direction so that they act as a spring. The grub screw must not be tightened excessively. The recommended maximum torque is about 1 Nm, which should fully compress the spring washers. The grub screw should then be unscrewed between 45° and 60° to achieve the correct compression. Another installation method that should ensure the best protection against valve piston contact and hydraulic overpressure is to run the actuator and simultaneously loosen the grub screw. When the valve lift begins to drop off, the correct point is found and the grub screw must be tightened by about 30° from that position.

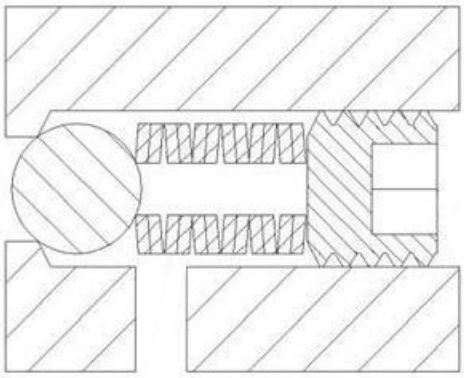

Figure A.11: Installation of Over-Pressure Relief Valve [45].

Appendix B

Control Software and LabVIEW Code

The custom ECU and FVVA control software were designed and implemented in a graphical programming language called LabVIEW (Laboratory Virtual Instrumentation Engineering Workbench). LabVIEW allows the user to develop programs rapidly that can control various devices and capture data which would otherwise be very difficult to do, and which would take significantly longer to construct.

These programs are known as virtual instruments (VIs) and generally consist of a front panel and a block diagram. The front panel is the Graphical User Interface (GUI), which has controls and indicators similar to those found in common laboratory equipment. The block diagram sits "behind" the front panel and is used for building the actual program. This is done by linking the virtual representations of laboratory equipment with connections akin to the wires on electrical circuit boards.

There are three program levels in a FPGA project; the Host VI, Real-Time VI and FPGA VI. Their names denote which section of hardware they operate on, with each level of the program having a very specific role and capability. Figure B.1 shows how these levels fit together in relation to the physical hardware.

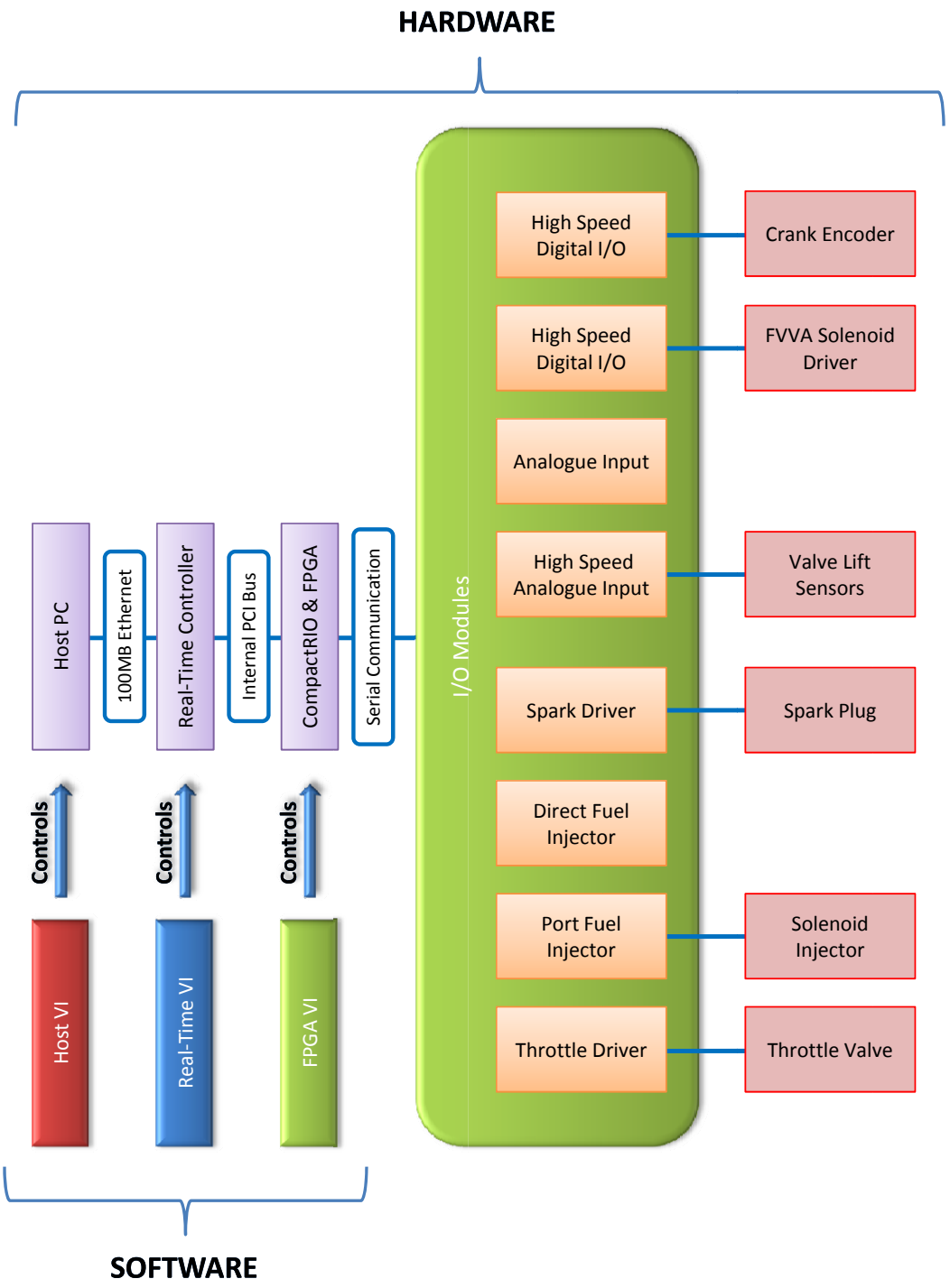

Figure B.1: Schematics of The Control System and I/O Devices.

B.1 Host PC and User Interface

CalVIEW software was used to create the user interface and communicate data between the Real-Time Controller and the Host PC via an Ethernet connection. CalVIEW was developed by Drivven Inc., which was the same company that made some of the I/O (Input/Ouput) modules that were used. Use of CalVIEW greatly simplifies the process of creating the communication link between the Host PC and the Real-Time Controller. Once the layout of the GUI has been constructed, with all the necessary controls and indicators that the user would require, CalVIEW is used to pair the controls, indicators, variables and look-up tables on the Host VI with their partners on Real-Time controller VI. The data buffering, data transfer, timing and synchronization are all controlled by CalVIEW. The primary advantage is that this is a more efficient method of communication between the devices and it also frees up development time for the programmer.

The following table lists the main variables that were transferred between the Host VI and RT VI and were used to control the engine and FVVA valvetrain. These variables are common throughout the Host VI, RT VI and FPGA VI.

Table B.1: **List of LabVIEW Control Variables.**

Variable	Unit
Spark Enable	Boolean
Spark Timing	DBTDC
Fuel Enable	Boolean
Fuel Timing	DBTDC
Fuel Injection Duration	ms
Throttle Tilt Angle	Degrees
Inlet/Exh Valve Enable	Boolean
Inlet/Exh Open	CAD
Inlet/Exh Open Offset	CAD
Inlet/Exh Close	CAD
Inlet/Exh Close Offset	CAD
Inlet/Exh Height Timing	us
Inlet/Exh Height Duration	CAD
Inlet/Exh PID	Boolean

Figure B.2 shows the User Interface (Front Panel) on the Host PC, which

is used to control the engine and valvetrain. The various switches and variables for controlling spark timing, fuel injection, throttle position and the FVVA settings can all be see on the Main Engine Control tab. The engine speed and fault lights are also visible.

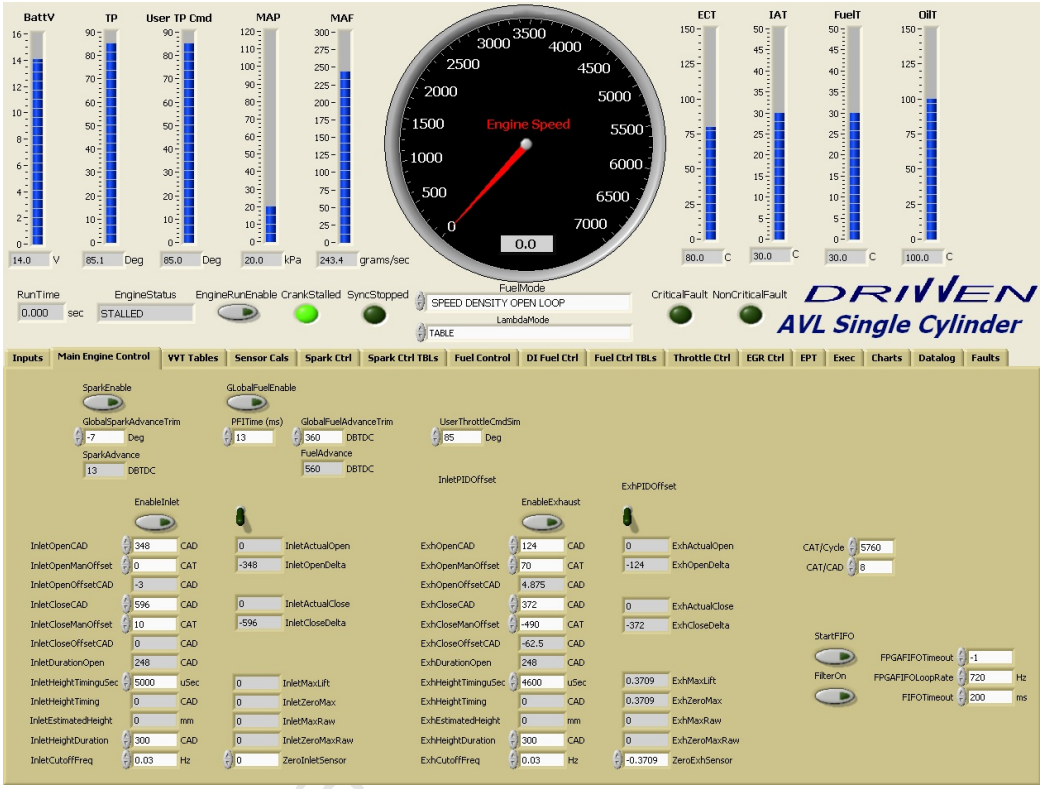

Figure B.2: CalVIEW User Interface on The Host PC.

B.2 Real-Time Controller

The front panel of the Real-Time (RT) VI is shown in Figure B.3. This VI has all the controls and indicators that are required to operate the engine. However, they are only used for programming purposes and not for the actual engine control. The following functions are performed by the RT VI:

1. Read Data from the FPGA.
2. Write Data to the FPGA.

3. Interface with CalVIEW.

4. Maintain synchronization and perform tasks in discreet time intervals.

5. Perform control strategies, such as PID (Proportional-Integral-Derivative) control loops, and multitask the various operations/loops.

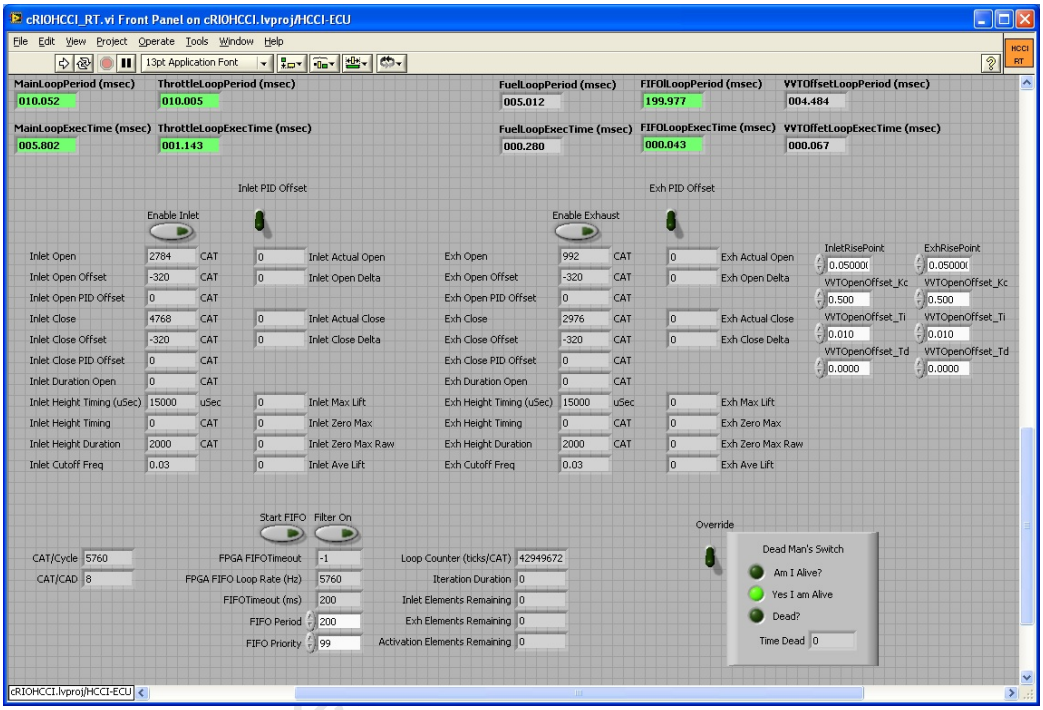

Figure B.3: Real-Time Controller VI Front Panel.

There are a number of programme loops in the RT VI that must run simultaneously and according to a specific cadence. The first loop is the main control loop in the RT VI, which performs the reading and writing of data to/from the FPGA. This loop is divided into the following sequence of events: Read data from the FPGA, perform minor calculations for FVVA control, and write data to the FPGA. This loop also contains most of the CalVIEW variables for interfacing with the Host VI.

The next four loops in the RT VI perform the following separate functions:

1. Manipulation of crank angle encoder signal for the control of the other systems and calculation of the engine's speed.

2. Control of the throttle using a PID (closed loop control via potentiometer).
3. Control of fuel injection duration using look-up tables and the lambda sensor.
4. Control of the spark timing using look-up tables.

The last two control loops in the RT VI were specially designed for the FVVA valvetrain. The first loop reads the raw lift sensor data from the FPGA, and then two calculations are performed on the data to convert the raw voltage signal into a lift trace in millimetres with respect to the engine's CAD. The second loop determines the maximum valve lift that was achieved for each valve actuation using a user-defined look-up table to update the valves' opening and closing offset values, which depended on the engine's speed. This ensures that as the engine's speed is increased the timing of the valve's opening and closing points remain constant. This is achieved by advancing the timing of when the solenoid is energised, or retarding the timing when the speed is decreased. The look-up table was manually populated by motoring the engine through the operational speed range, and then capturing the offset values.

A number of safety features are employed on the RT VI to ensure the user cannot damage the engine, and also to keep the engine running should communication with the Host PC be lost. A typical example of safety circuitry is the "Engine Run Enable" button, which disables all the controls on the Host VI so that nothing can be accidentally enabled. Another example that is specific to the FVVA system is that the valve opening and closing points are checked before the valve is actuated to ensure that the valves will not strike the piston when they open.

An important aspect of controlling the valvetrain's actuators is the timing of the solenoids in relation to the engine's rotation. The engine and valvetrain effectively function independently and therefore need to be synchronised by some method. The difficulty with this is that there are a number of formats for measuring the engine's rotation and time intervals. The user controlling the engine needs the engine's speed and angle to be displayed in RPM and CAD respectively. The crankshaft encoder outputs the angle of the crankshaft in Crank Angle Ticks (CAT), which has a range from 0 to 5760 CAT. Each CAT represents one eighth of a CAD from 0 to 720 CAD. The valve's timing and height is determined by how long each solenoid is energised, which is controlled in microseconds. The FPGA's 40 MHz processor

gives a resolution of 25 nanoseconds per processor clock tick, which is used to synchronise the software. These conversions therefore require very fast and precise calculations. As a result, all of the unit conversions were performed on the Real-Time Controller before they were transferred to either the Host PC or FPGA.

B.3 Field-Programmable Gate Array

The FPGA VI was the last level of the control software and was used to perform the reading and writing of data to the analogue and digital modules. This VI was more simple than the Real-Time VI because there were no calculations or data manipulation that needed to be performed; only the communication between the FPGA and I/O modules.

There were four communication loops in this VI, the largest of which was the Drivven loop which reads and writes specific values to the Drivven modules. These functions were encrypted by Drivven so that the way they operate and their actual communication methods were not known.

The other three communication loops were specifically designed for the FVVA system. The first FVVA loop controlled the timing of the solenoids. It did this by keeping track of the engine's crank angle, and only energised the solenoids between the opening and closing points and once the valve had been enabled. The solenoids were energised by sending a true boolean value to the high speed digital I/O module and de-energised by sending a false boolean value.

The second FVVA loop read in the raw lift sensor data for both the valves. Each data point was concatenated with its respective crank angle so that the lift height could be related to the correct crank position. This was a large amount of data that needed to be sent to the Real-Time controller and had to be done at a very high speed. Therefore, all the data was fed into a FIFO buffer which managed the transfer to the RT VI and also ensured that no data was lost.

The last loop on the FPGA calculated the valves' opening and closing points. This was originally performed on the Real-Time Controller, but it required too much processing time causing the RT VI to crash. The loop determined these points by initially calculating the lift sensor's average value

during the portion of the cycle when the valve was closed. Then, by using a number of flag variables, and comparing the average value to the rest of the valve's cycle, the valve was determined to be open or closed when the lift height crossed a certain threshold. This provided an accurate and dynamic way to determine these points, which were crucial in controlling the FVVA system.

The following figure shows the front panel of the FPGA VI and the various control and indicator variables that were used to operate the FVVA I/O modules.

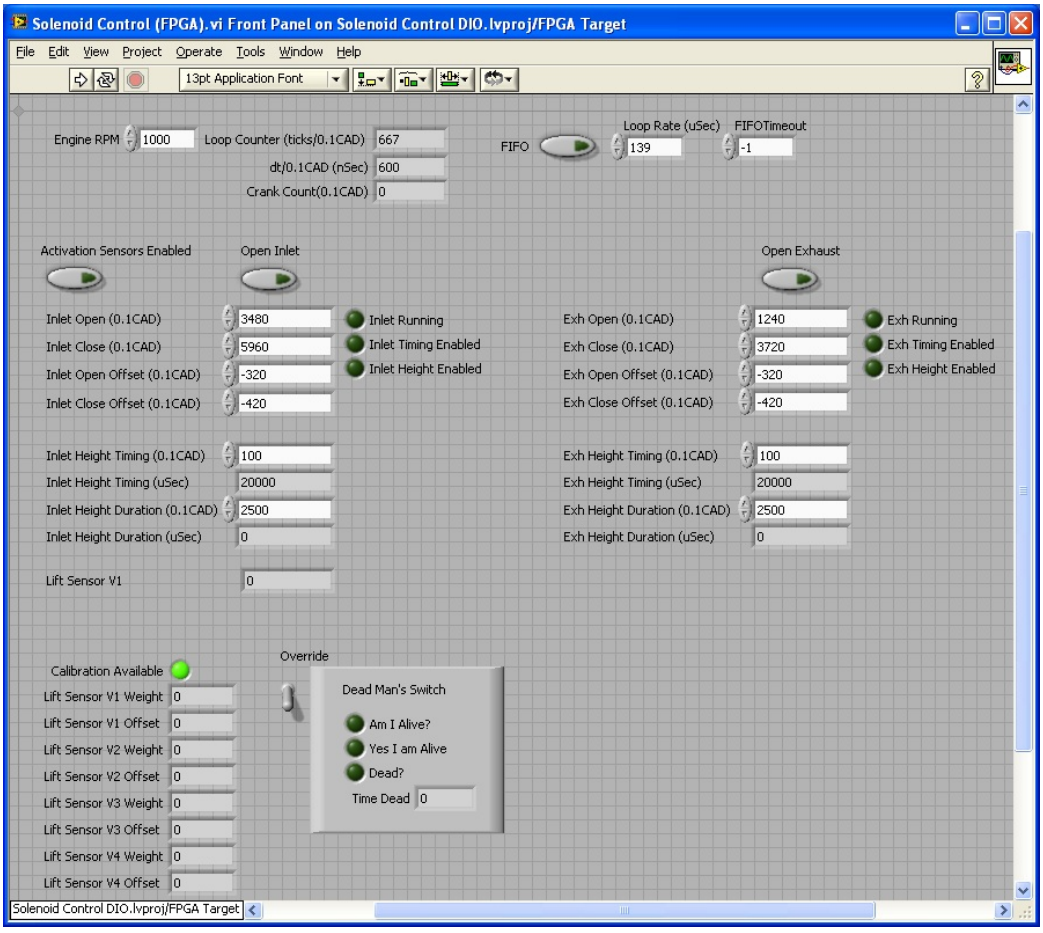

Figure B.4: FPGA VI Front Panel.

Figure B.5 is an extract from the FPGA VI's block diagram. It shows the loop that controls the opening and closing of the exhaust valve actuator.

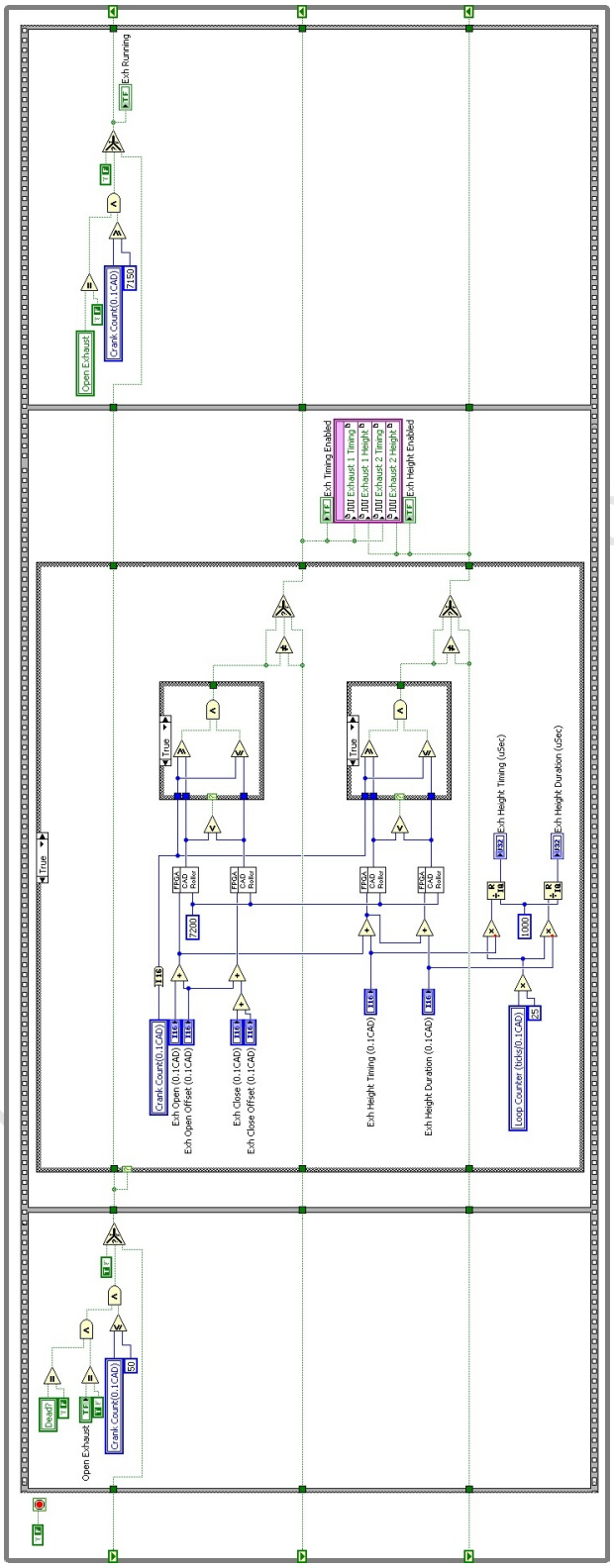

Figure B.5: FPGA VI Block Diagram.

Appendix C

Subsystems of the Experimental Apparatus

The following appendix covers the various subsystems that make up the test cell and experimental apparatus.

C.1 Cooling System

The engine cooling system was a water-to-water closed-loop system. The engine's primary cooling water was stored in an external reservoir that was situated between the engine and the dynamometer. The primary cooling water was pumped through the engine and then through a water-to-water heat exchanger which was cooled via a secondary external chilled water system. The secondary cooling water circulated through all the engine test cells in the facility. The temperature of the primary cooling water was manually controlled by a mechanical thermostat, which was located on top of the reservoir, and regulated the amount of water that was allowed to flow through the heat exchanger.

Cooling for the engine lubrication system was also controlled in the same manner as the cooling system, where the temperature was manually set by a mechanical thermostat. The oil was cooled via a heat exchanger, which used the facility's chilled water system. The following figure shows the oil and water cooling systems.

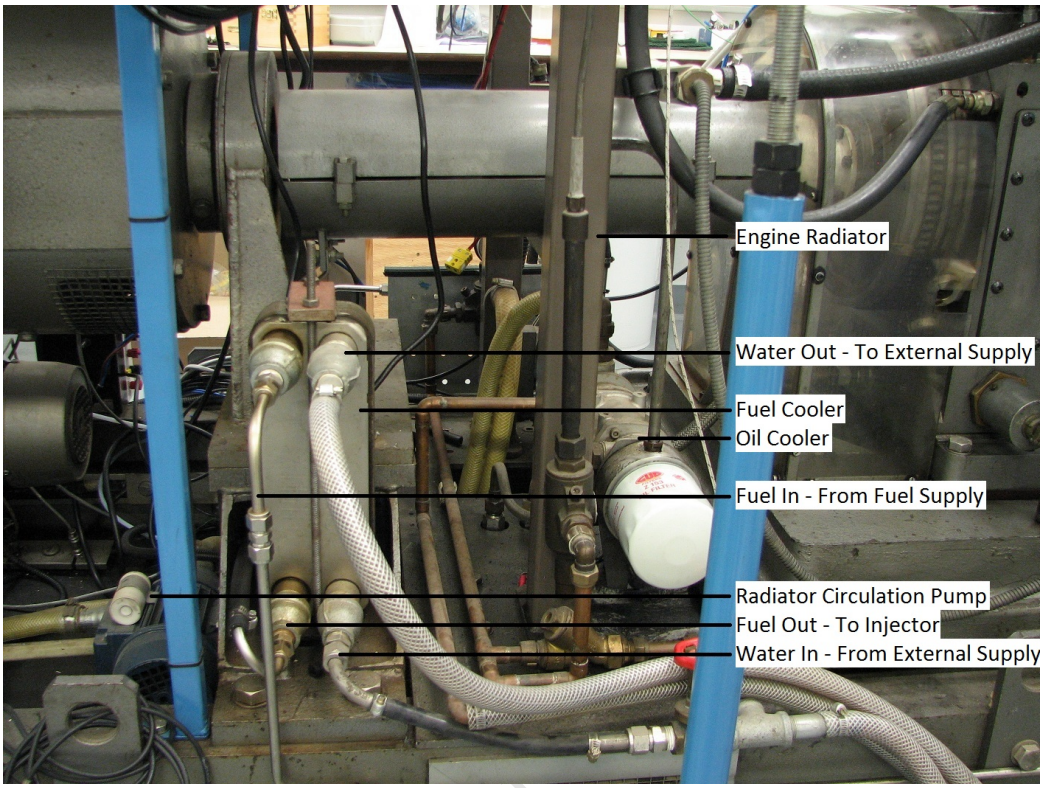

Figure C.1: Engine Water and Oil Cooling System.

C.2 Inlet Air Preparation

The test cell was equipped with systems to control the temperature and pressure of the engine's air supply. These systems were used for maintaining stable combustion and consistent operating conditions. They were also important for operating the engine in HCCI mode and provided accurate control of the autoignition point and combustion phasing.

A heater element, similar to that found in a hot water kettle, was used to heat the air supply, and it was located just before the bellows in the air supply system. The temperature was controlled via an external temperature control unit which used a relay switch to turn the heater element on and off in order to maintain the desired temperature. A thermocouple was situated in the inlet plenum, which provided closed-loop feedback for the temperature controller. This allowed the controller to compare the actual inlet air temperature with the set point temperature and regulate the heater element accordingly. A thermocouple on the heat element provided a safety signal to prevent the

heater element from over-heating and burning out.

The inlet air pressure was boosted by a roots blower and reservoir, which could provide a maximum boost pressure of 8 bar. The pressure was manually set with a control valve and pressure gauge. A Cussons P7200 Laminar Flow Meter was connected between the roots blower and reservoir, which allowed for accurate air mass flow measurements. There was also a fan-cooled heat exchanger that could be turned on to cool the compressed air. The following figure shows the inlet air preparation system.

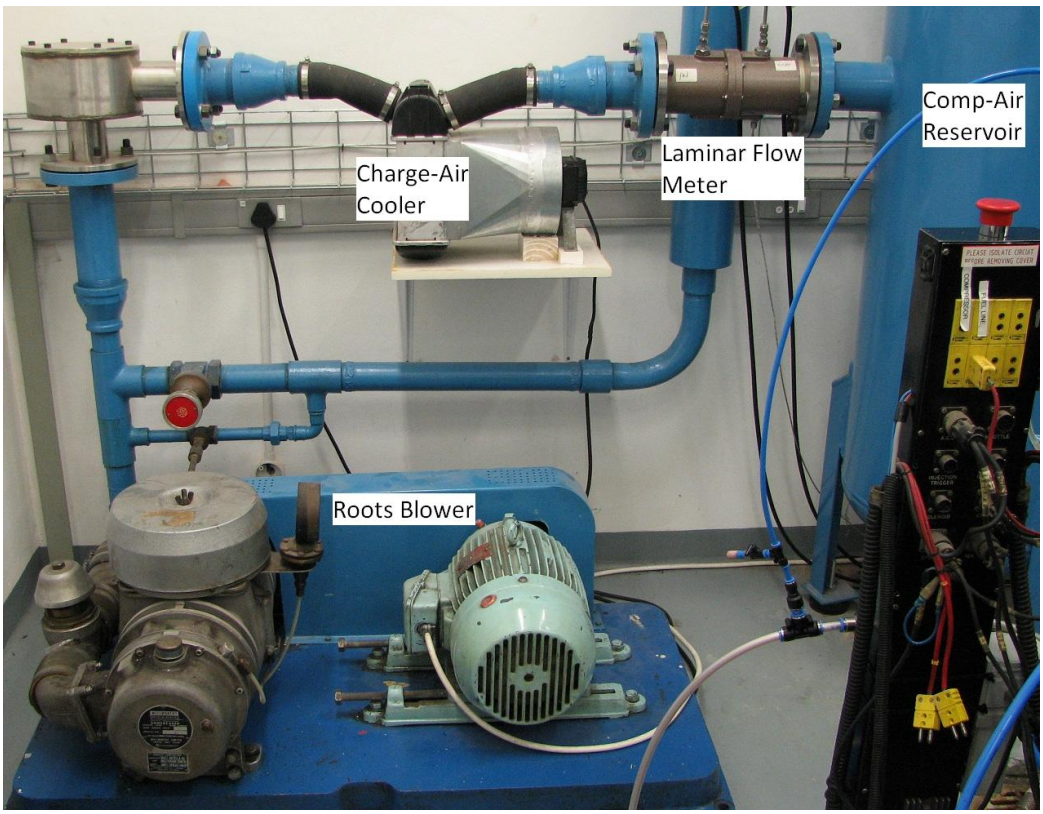

Figure C.2: Inlet Air Supply System.

C.3 Fuel System

Figure C.3 below is a close up photo of the Hydra's fuel system. The figure shows the various pumps and filters in the system. Figure C.4 shows the whole fuel system, including fuel tank and mass flow meter. The fuel system for this test cell operated independently from the system that runs through the rest of the facility. Hence, a 20 L fuel drum had to be brought into the test cell whenever the engine was run.

Figure C.3: Fuel System: Pumps, Filters and Air Mass-Flow Meter.

The fuel pump was activated via a button on the dyno controller in the control-room. However the dyno's thyristor drive did not have to be on in order for the fuel to circulate. When the pumps were activated, the low pressure pump sucked in fuel through a small in-line filter. Once the fuel

passed through the pump, it was pumped into a de-aeration unit to remove any air in the fuel. The fuel then entered the AVL mass flow meter which had an internal beaker that collected the fuel and weighs it. The fuel then went through another fuel pump which was at a slightly higher pressure of 6 bar. The fuel was then pumped through the final large in-line filter before it was sent to the fuel heat exchanger. This was located on the dyno base frame and maintained the fuel at a set temperature. After passing through the heat exchanger the fuel was sent to the fuel injector and into the engine. A fuel return pipe ran between the injector and AVL mass flow meter to allow any excess fuel to circulate through the system.

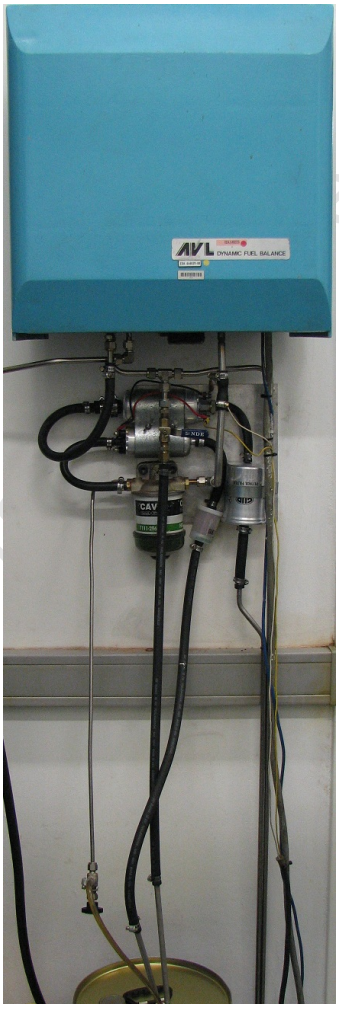

Figure C.4: Engine Fuel Supply System

Appendix D

Operational Procedures

The following procedures must be followed when starting up or shutting down the engine.

D.1 Engine Startup Procedure

1. Visually inspect the engine and subsystems for any loose connections, loose pipes, leaking fluids and possible short circuits.

2. Empty any excess oil in the valvetrain's oil separation unit and top up the valvetrain's oil reservoir. If this is not done, oil will eventually spill out of the silencer.

3. Fetch a 20 L fuel container (with the required fuel) from the fuel store. Place the container onto the tray underneath the fuel pumps next-to the thyristor drive and insert the suction and return lines into the container. For safety precautions, fuel should always be returned to the fuel store when testing for the day has been completed.

4. Turn on the thyristor drive with the handle at the base of the unit, which is situated in the corner of the test cell.

5. Open the shut-off valve for the valvetrain's pneumatic system which is located on the wall next to the thyristor drive. Check the pressure gauge to ensure that the valvetrain is supplied with the correct air pressure, which should be 8 bar.

6. Open the shut-off valve for the building's chilled water circulation system, which is located on the floor next to the thyristor drive. Make sure that water is flowing into the test cell's drain. If there is no water flowing then the facility's water pumps must be turned on. The switches for the pumps are located on the facility's main control board in the control room.

7. Turn on the switch for the radiator's water circulation pump, which is beneath the electronics table that is located above the dyno.

8. Turn on the 12 V car battery at the junction box, which is located on the side of the electronics table.

9. Turn on the following items which are on the electronics table: FPGA 24 V power supply, 12 V DC power supply, pressure transducer charge amplifier and solenoid controller box.

10. Open the air extraction vent that is above the exhaust pipe. Close the exhaust vent for the Ignition Quality Tester (IQT), which is located in the corner next to the thyristor drive. This will ensure that all exhaust gas is properly evacuated from the test cell and the engine is supplied with fresh air.

11. Close all the test cell doors. This is important for the ventilation system to function properly and to contain the engine noise.

12. If the control PC is off, turn it on and load the LabVIEW and CalVIEW software.

13. Turn on the AVL Indiset using the switch located on the back panel. The Indiset is situated on top of the dyno controller. If the Indiset is not switched on, the crank encoder will not have power and the FPGA and control software will be unable to pickup the crank encoder's signal.

14. Turn on the ventilation system for the test cell at the facility's main control board. This particular test cell does not have a dedicated ventilation/extraction system and has to use the Heavy Duty (HD) test cell's system. Therefore, the switches must be turned on for the AHU1 (Auxiliary Handling Unit), the extraction fan and HD test cell.

15. On the dyno controller, turn on the water and oil heaters and the water, oil and fuel pumps. Wait 15 min for the water and oil to reach at least 60°C before starting the engine. Once the engine has reached its operating temperature, both heaters can be turned off.

16. Open the HCCI ECU program in LabVIEW and start the real-time VI.

17. Ensure that CalVIEW has connected to the target and then launch the host VI by clicking the play button.

18. Press the red "RESET" button on the dyno controller to reset the safety circuits and warning lights. The dyno will not start without first being reset. Once it has been running for a few seconds, the "RESET" light will turn off and the dyno will switch to "AUTO".

19. Set the speed dial on the dyno controller to zero to ensure that the dyno will not suddenly start at full speed. Then, turn the dial slightly forward so that the dyno's direction of rotation is positive. If this is not carried out, the dyno's rotational direction will be unknown and it could shake violently.

20. Set the dyno controller switch to the "off" position. This will allow the dyno to automatically alternate between motoring the engine and absorbing torque. Once the engine is operational, the dyno can be switched to absorb, which will prevent the dyno from attempting to motor the engine should the speed fluctuate, and will also give a better torque reading.

21. Press the green button on the dyno controller to begin motoring the engine and use the speed dial to adjust the engine's speed to the desired value.

22. The CalVIEW host VI should now be reading the engine speed, and the engine should be ready to start. If any of the warning lights on the front panel indicate a fault ("Crank Stalled", "Sync Stopped", "Critical Fault" or "Non Critical Fault"), flip to the "Faults" tab or the "EPT" tab and click on the appropriate "Clear Faults" button to reset them.

23. When you are ready to start the engine and you are certain that everything is in order, click the "Engine Run Enable" button. This is a safety switch to ensure that nothing is accidentally turned on. If the "Engine Run Enable" button is not enabled, then all switches and controls will be disabled and you will be unable to engage any of the systems.

24. Flip to the "Main Engine Control" tab. This tab allows the user to control the FVVA valvetrain, the throttle position, spark timing and fuel injection variables.

25. Enable the inlet and exhaust valves. Next, make sure the throttle valve is open by increasing its angle and then enable the fuel injection.

26. Finally, enable the spark plug and slowly increase the fuel injection duration until combustion begins.

D.2 Engine Shutdown Procedure

1. On the CalVIEW front panel disable the fuel injection and then the spark plug.

2. To stop the dyno, press the red button on the dyno controller, which is next to the control PC in the control room. The dyno will gradually slow until it stops.

3. Disable the inlet and exhaust valves, and then turn off the "Engine Run Enable" button. CalVIEW and LabVIEW can be closed and the computer shut down if testing for the day has been completed.

4. Turn off the water and oil heaters and the fuel pump on the dyno controller. However, the oil and water pumps should be left on to circulate and assist in cooling the engine.

5. Turn off the Indiset using the switch on its back panel. The Indiset is located above the dyno controller, which is next to the control PC.

6. Turn off all of the devices on the electronics table. The electronics table is located above the dyno. These devices are: FPGA 24 V power supply, 12 V DC power supply, pressure transducer charge amplifier and solenoid controller box.

7. Turn off the 12 V car battery at the junction box next to the dyno controller.

8. Close the shut-off valve for the valvetrain's pneumatic system, which is located on the wall next to the thyristor drive.

9. Turn off the ventilation system for the test cell, which is located on the main control board in the control room. The AHU1, the extraction fan and HD test cell control switches must all be turned off.

10. Remove the suction and return pipes from the fuel container. Make sure that the pipes are drained before removing them completely to ensure that fuel does not spill onto the floor. Close the fuel container and return it to the fuel store.

11. Once the engine has cooled down, turn off the thyristor drive and the water pump that is located under the electronics table. Then disengage the switches on the dyno controller for the oil and water pumps.

12. Close the shut-off valve for the facility's chilled water circulation system, which is located on the floor next to the thyristor drive. Turn off the pumps for the circulation system at the facility's main control board.

13. Visually inspect the engine and subsystems for any loose connections, loose pipes, leaking fluids and possible short circuits in order to make sure that nothing has been damaged or has failed during testing. Walk around the test cell and double check that everything is off.

14. Turn off the lights and close the test cell doors.

Appendix E

Hazards and Precautions

E.1 Fuels and Lubricants

Whenever one is working with flammable liquids there is a risk of fire or hazardous spillages. Care must be taken when transporting and moving fuel containers so that spillage does not occur. When the test cell is not being utilised or testing being performed, all fuel and hazardous liquids should be kept in the fuel store. If spillage should occur, then there are cleaning kits and instructions located throughout the lab, and fuels and lubricants should be disposed of as specified in the instructions.

Certain hydro-carbons are easily absorbed through the skin and are known to be highly carcinogenic. It is therefore extremely important that gloves and other protective equipment are used when handling any oil or fuel, no matter how small a volume. Isopropyl nitrate, which was used as a cetane improver, is known to be highly toxic and extra care must be taken when working with it. Should a person working with hazardous liquid experience a splash in his/her eyes, there are clear signs to special eye irrigation kits which are located around the facility.

Before and after testing, fuel lines should be checked to make sure that all fittings and pipes are intact and are not leaking. This is due to the danger of fire from the heat of the engine and surrounding surfaces when operating. In addition, it is important to ensure that the fuel lines do not come in contact with anything hot that could melt them and cause a fire. In the event of a fire breaking out, the facility is equipped with smoke detectors,

fire extinguishers with all exits clearly demarcated. A fire should never be tackled single-handedly, and the facility's emergency procedures should be read and understood before the use of any flammable substance or dangerous equipment.

E.2 Exhaust Gas

Combustion products of the internal combustion engine include CO_2, CO and other gases. Prolonged inhalation of these gases can quickly lead to poisoning and asphyxiation. The test cell has a powerful ventilation system with an extraction fan (to remove exhaust gas from the test cell) as well as an inlet fan to supply fresh air. There is also a smoke detector in case of fire or if the ventilation system should fail. The test cell has special doors that seal and allow the ventilation system to form a negative pressure within the test cell. This prevents exhaust gases from escaping into the control room.

E.3 High Pressure Air

High pressure air is used to power the FVVA valvetrain and pressurise its lubrication system. If one of the air lines should break, there is a possibility of the operator being injured. Because pressurised air would cause the air line to whip, with possible injury to the eyes, it is important for operators always to wear eye protection when working with compressed air and the FVVA valvetrain.

E.4 Hot Surfaces

Not all energy released from fuel combustion in an internal combustion engine is converted into work. Excess energy is either removed through the exhaust, or via cooling system. The result of this energy release is that the engine and surrounding surfaces become extremely hot. These hot surfaces pose a significant risk to the operator of burns, as well as a risk of the electrical wiring and equipment melting. The exhaust system poses the greatest risk because it is the hottest surface as well as being the most exposed. To

protect against burns from the exhaust, certain parts are covered with protective shielding. To alert the operator to this danger, signage is displayed throughout the facility warning of hot surfaces. However, to encase the entire exhaust system is impractical, and therefore it is the operator's responsibility to be aware of hot surfaces and to take the necessary precautions.

E.5 Tripping

There are a number of hazards in the vicinity of the test cell which can cause injury that an operator or visitor should be aware of. These include drains, piping for the facility's chilled water circulatory system, electrical cabling and open trenches. Wherever possible, all wires should be tied down or enclosed in trenches, and tripping hazards should be clearly marked to alert those persons unfamiliar with the test cell. Notwithstanding this, all persons entering the test cell should always take precautions by being alert to their immediate surroundings, and by taking care as they move about the facility.

E.6 Hearing Protection

The engine and FVVA valvetrain create a high level of noise whilst running, which can damage a person's hearing. This risk is significantly increased as the engine operates within an enclosed area inside a building. Because of this, if the engine or valvetrain are running, everyone inside the test cell should wear hearing protection. Signs to this effect are clearly visible in the test facility. Because of the noise, the doors to the test cell should also be kept closed so as not to disturb people working in other areas of the facility.

E.7 Electrocution

Most of the electrical systems require electrical power from the mains supply. As a result, there is always the risk of electrocution when working in the test cell. All electrical systems and wiring are insulated and have the correct insulating terminals to minimise the risk. As a result, all sources of electrical power are clearly labelled with their output voltages to prevent the

incorrect power source from being used. Notwithstanding these precautions, all electrical systems must be isolated with their power source disconnected when being worked on.

Appendix F

Technical Drawings

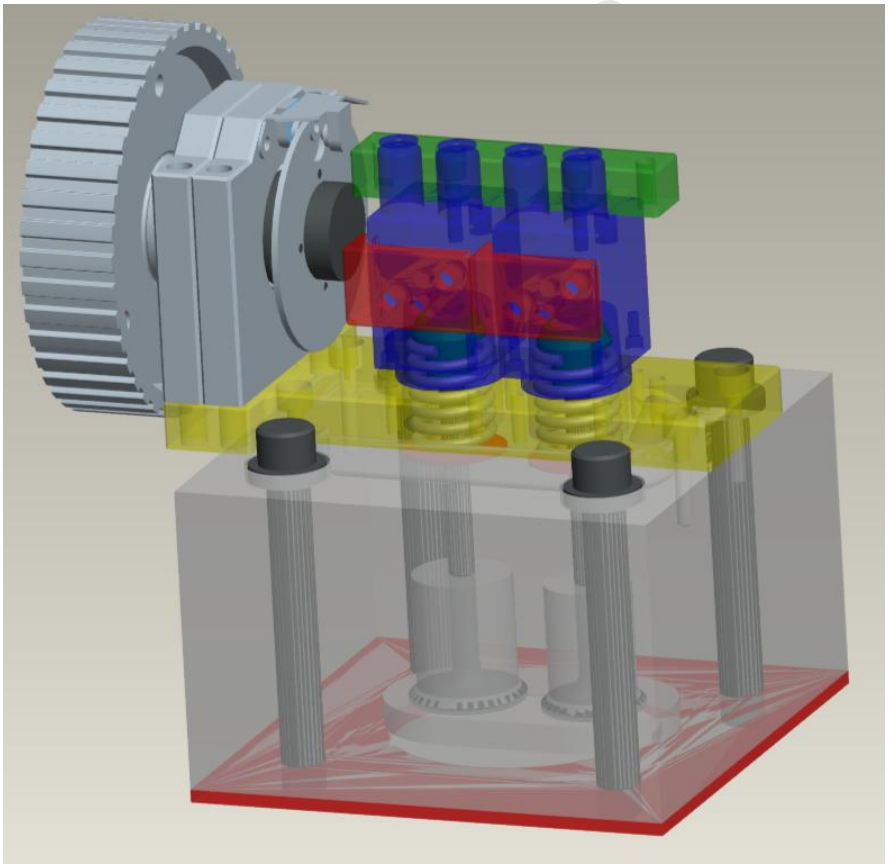

Figure F.1: Pro Engineer Rendering of The FVVA Valvetrain Assembly.

F.1 Manufacturing Drawings

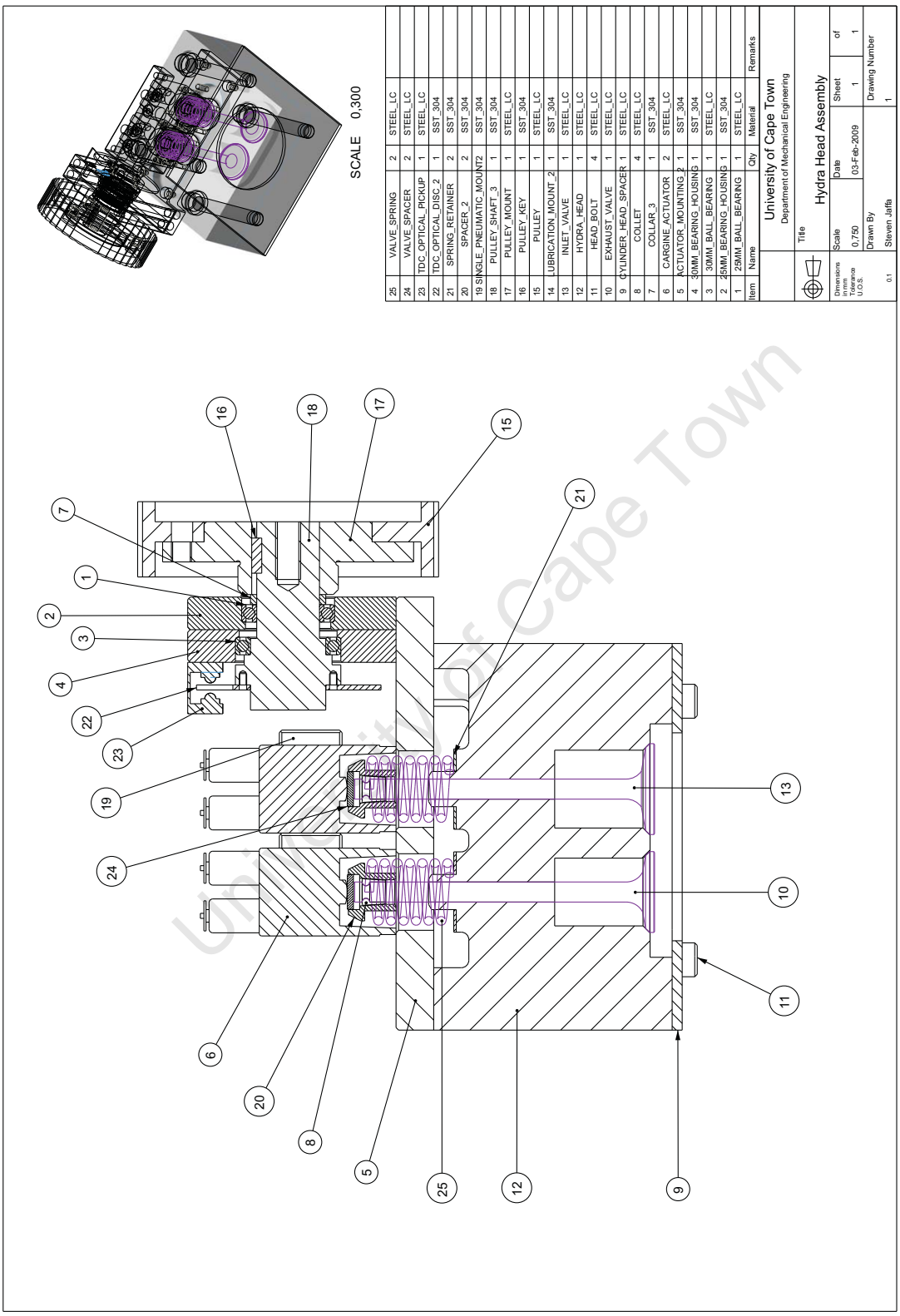

Figure F.2: Manufacturing Drawing: Hydra Head Assembly.

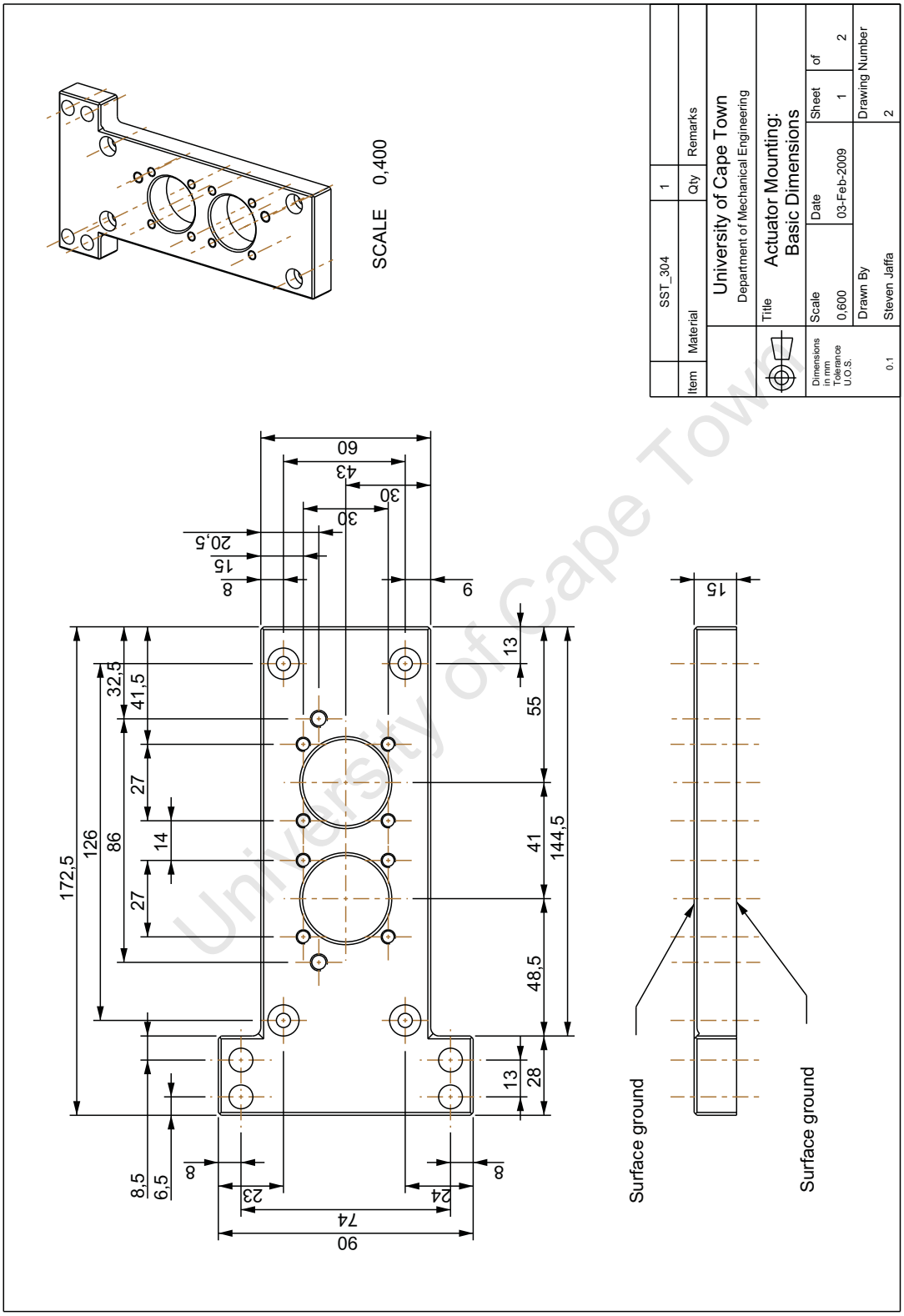

Figure F.3: Manufacturing Drawing: Actuator Mounting Drawing 1 – Basic Dimensions.

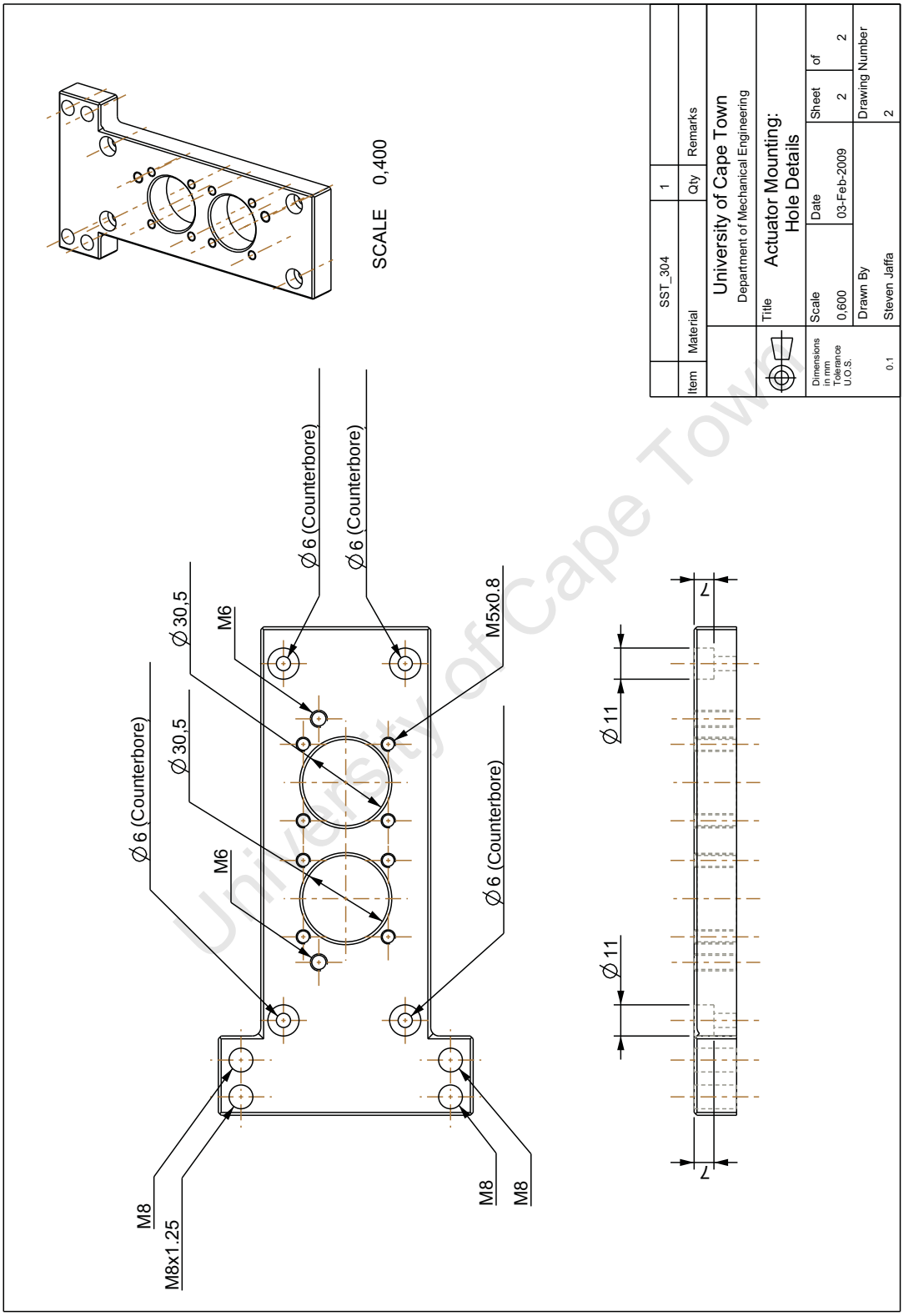

Figure F.4: Manufacturing Drawing: Actuator Mounting Drawing 2 – Hole Dimensions.

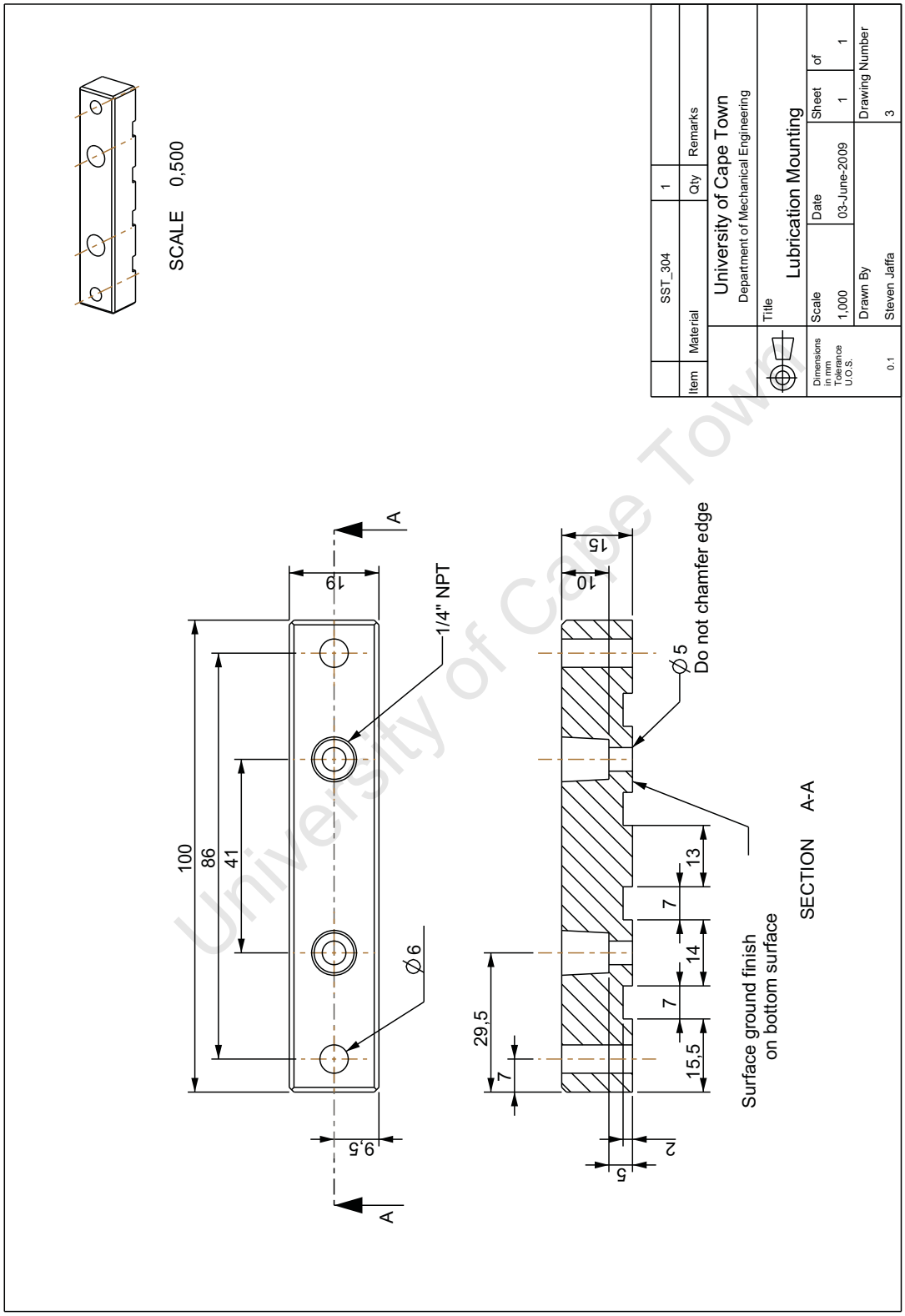

Figure F.5: Manufacturing Drawing: Lubrication Mounting.

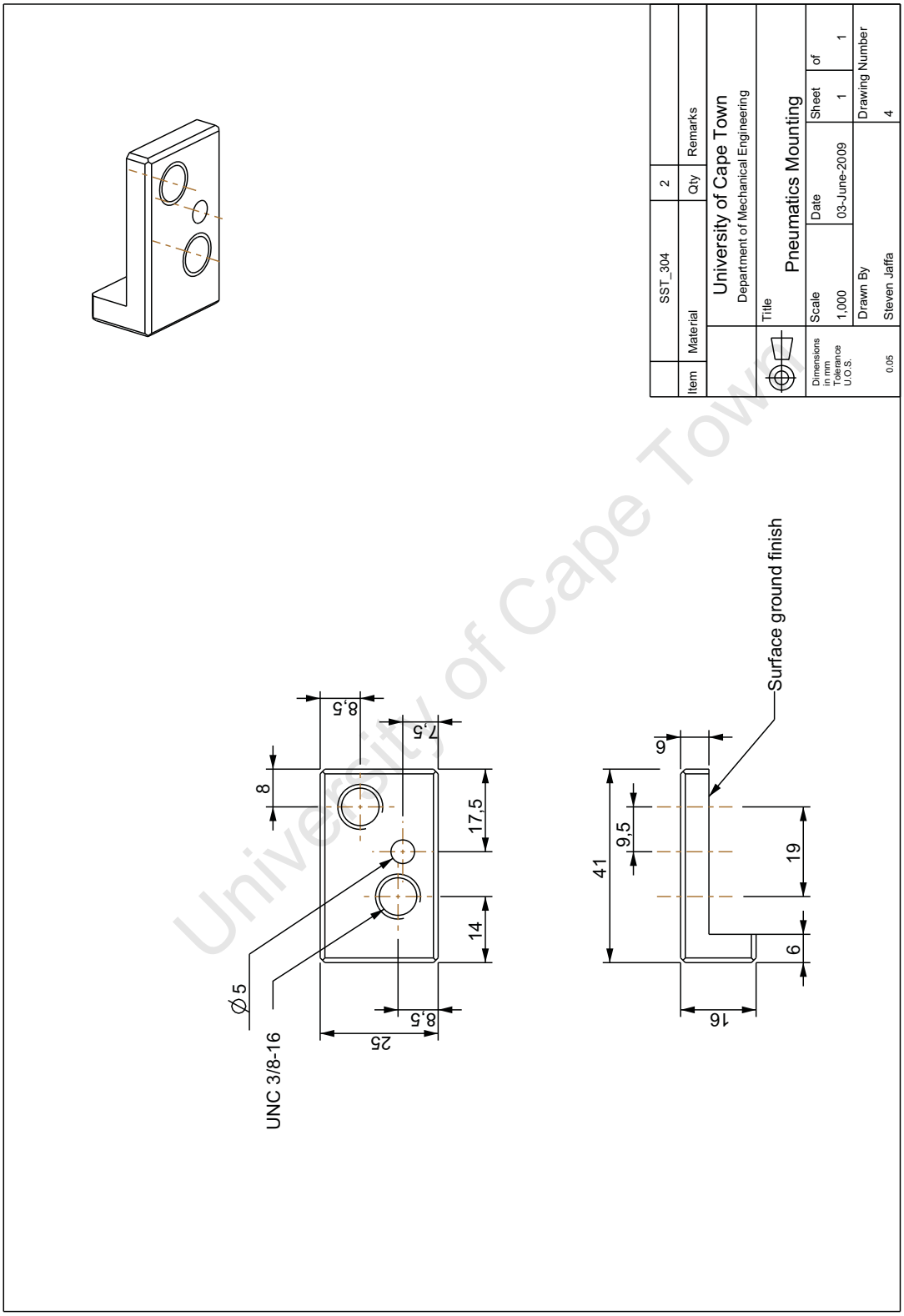

Figure F.6: Manufacturing Drawing: Pneumatics Mounting.

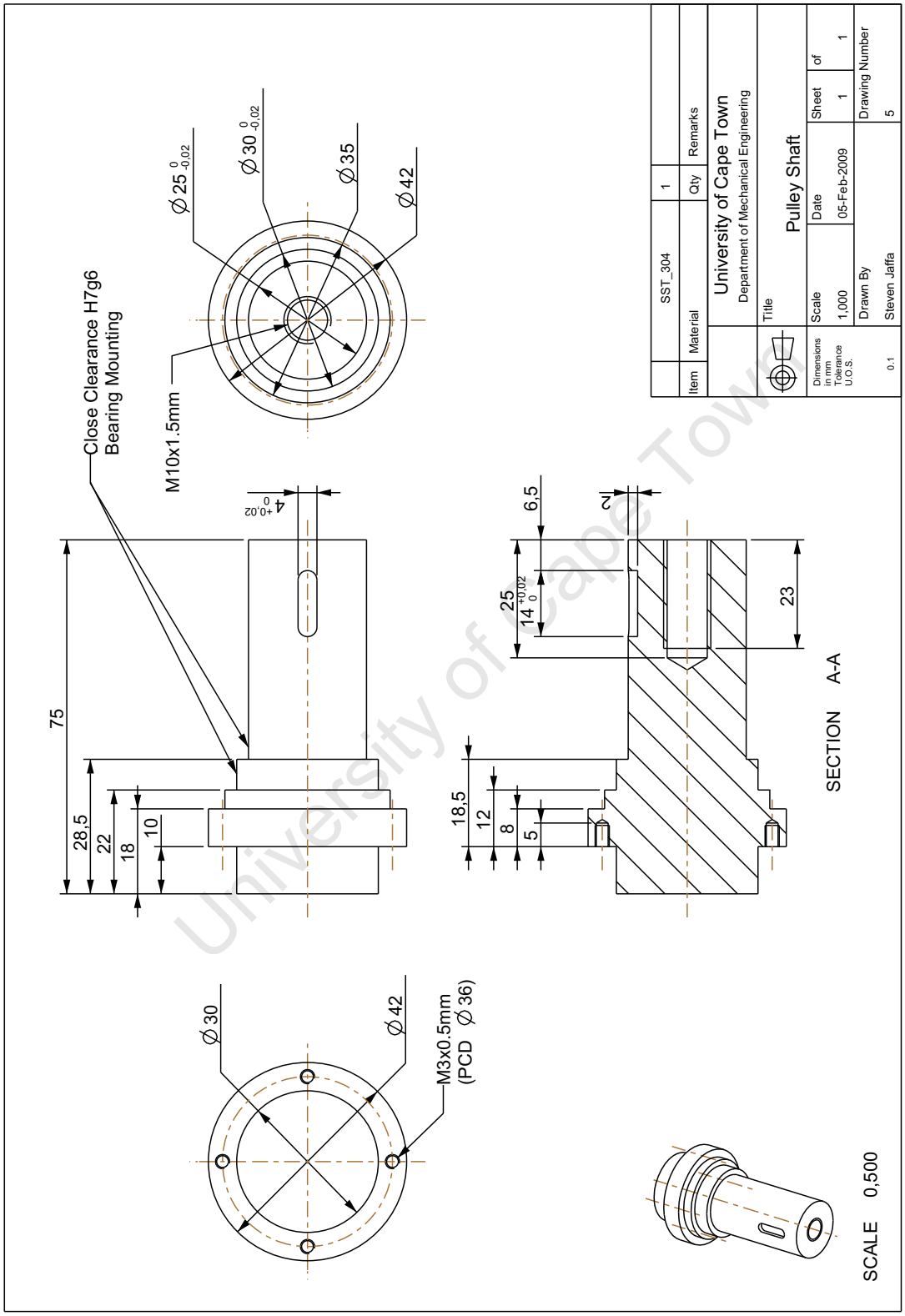

Figure F.7: Manufacturing Drawing: Pulley Shaft.

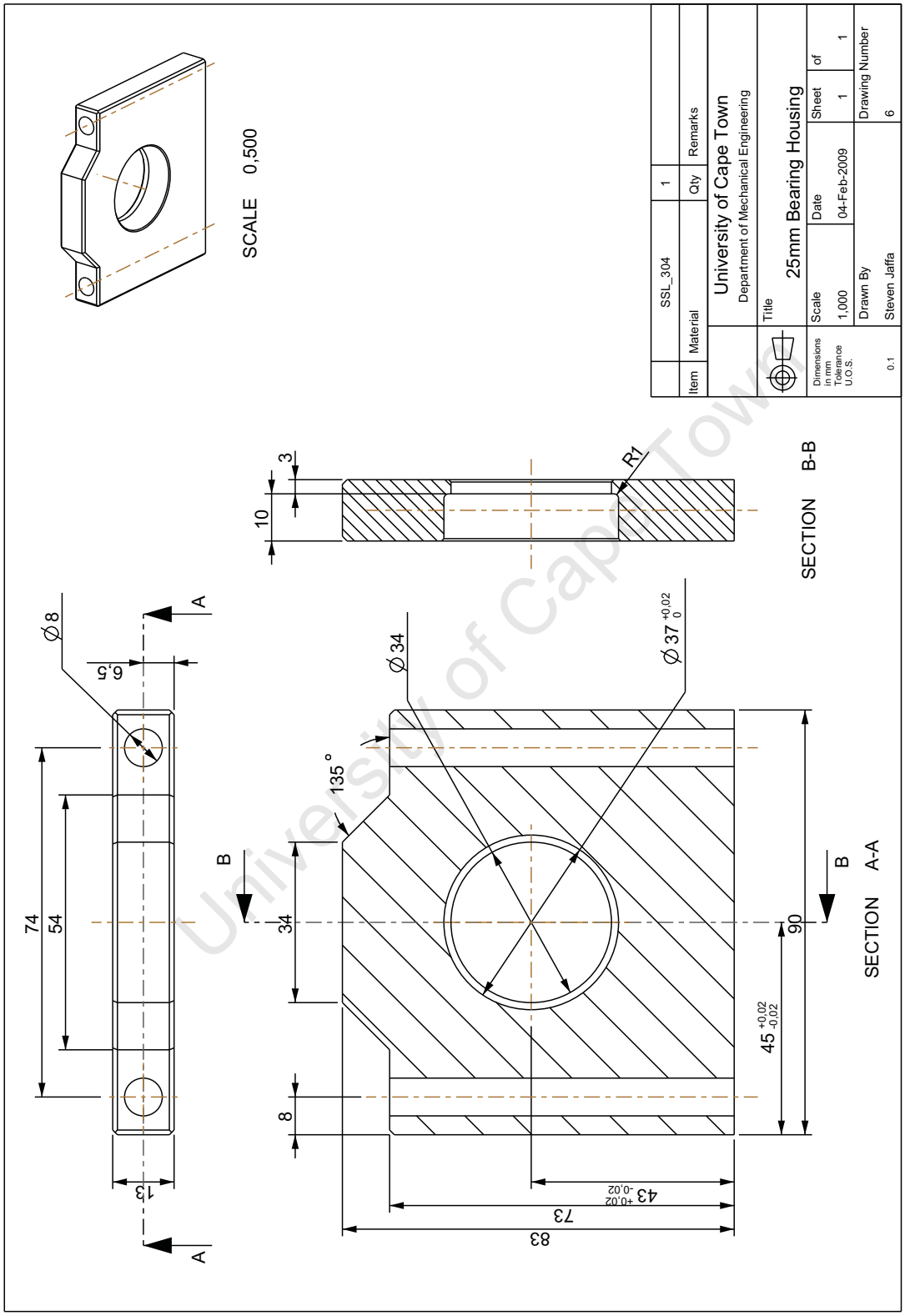

Figure F.8: Manufacturing Drawing: 25mm Bearing Housing.

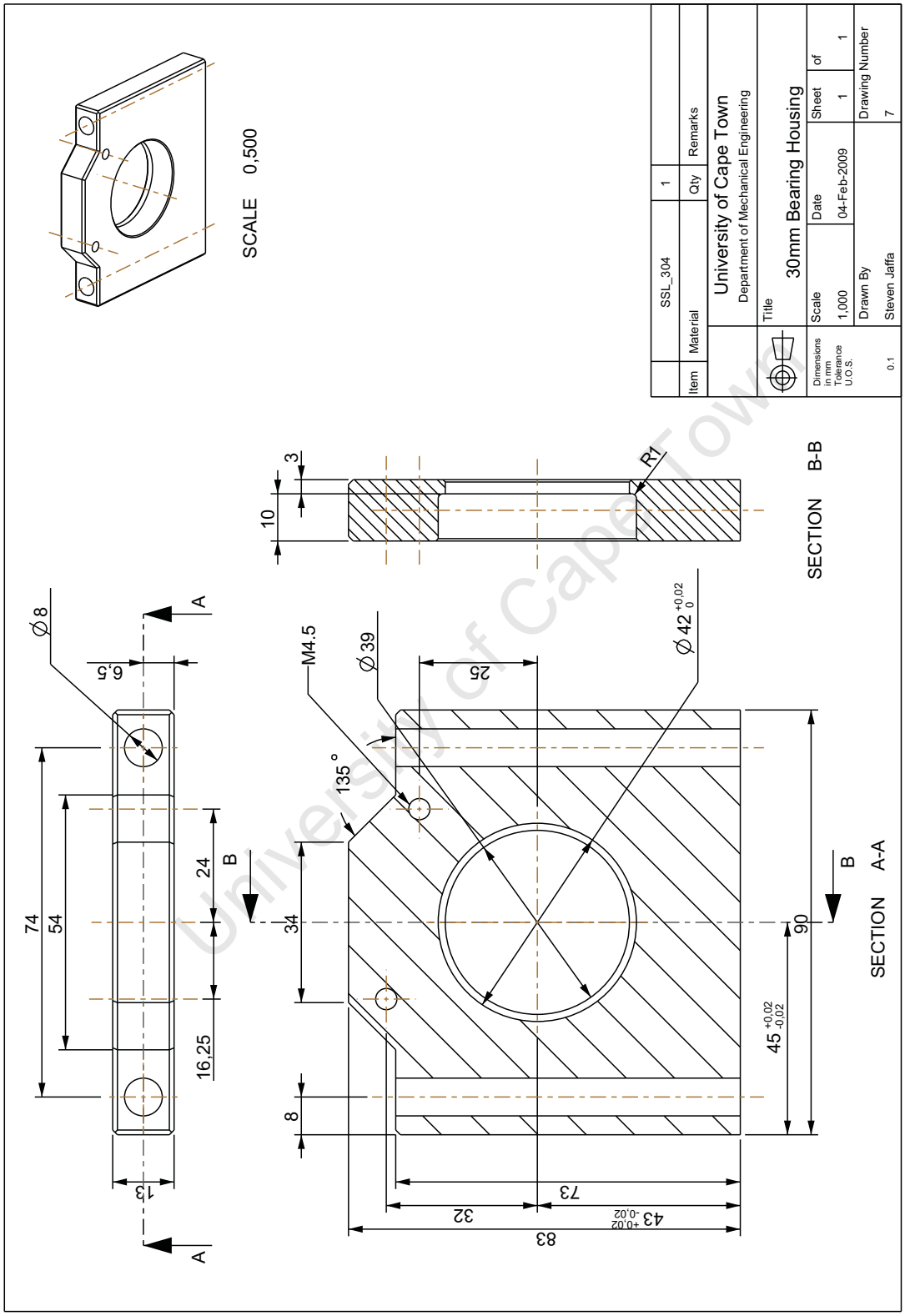

Figure F.9: Manufacturing Drawing: 30mm Bearing Housing.

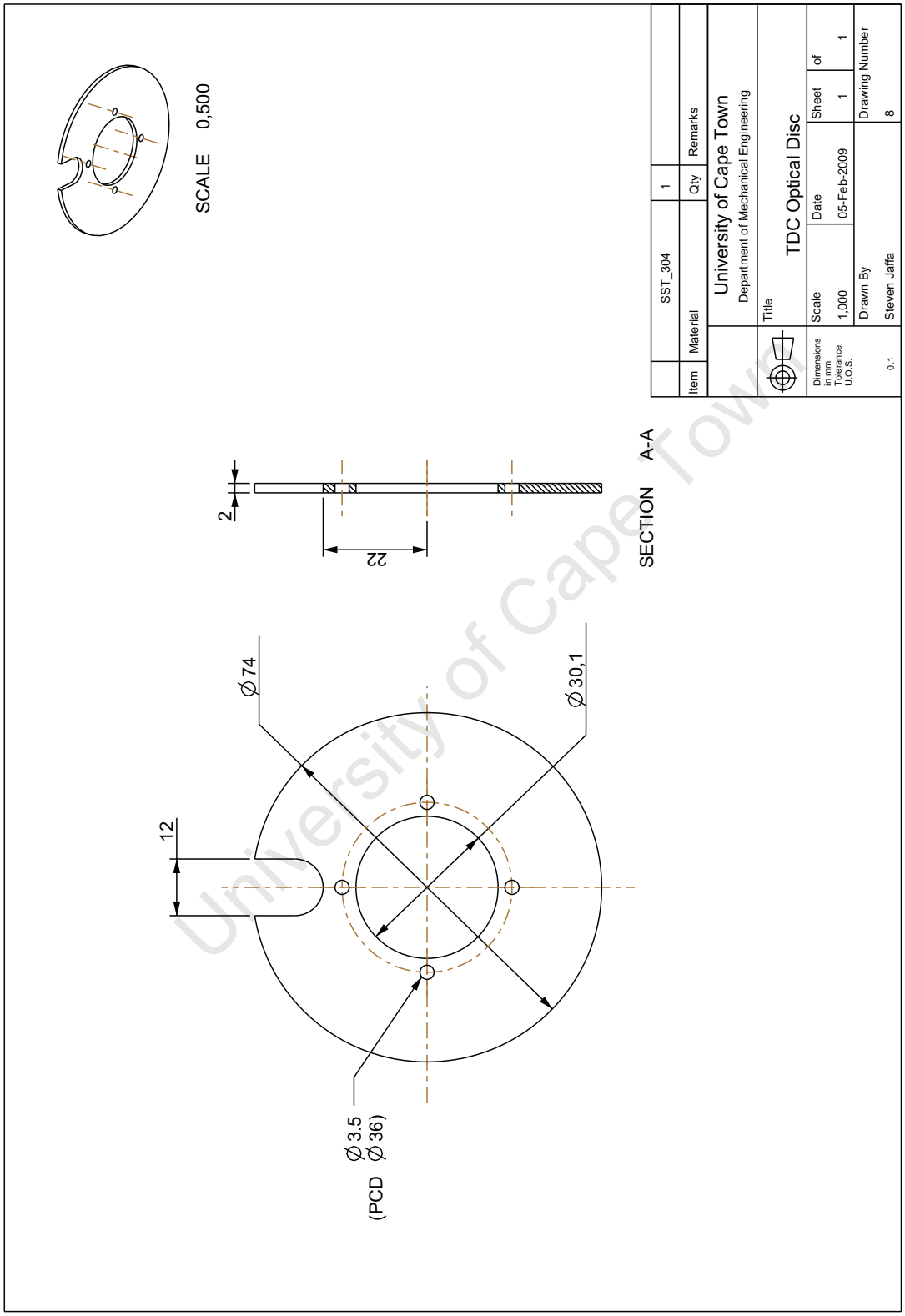

Figure F.10: Manufacturing Drawing: TDC Optical Disc.

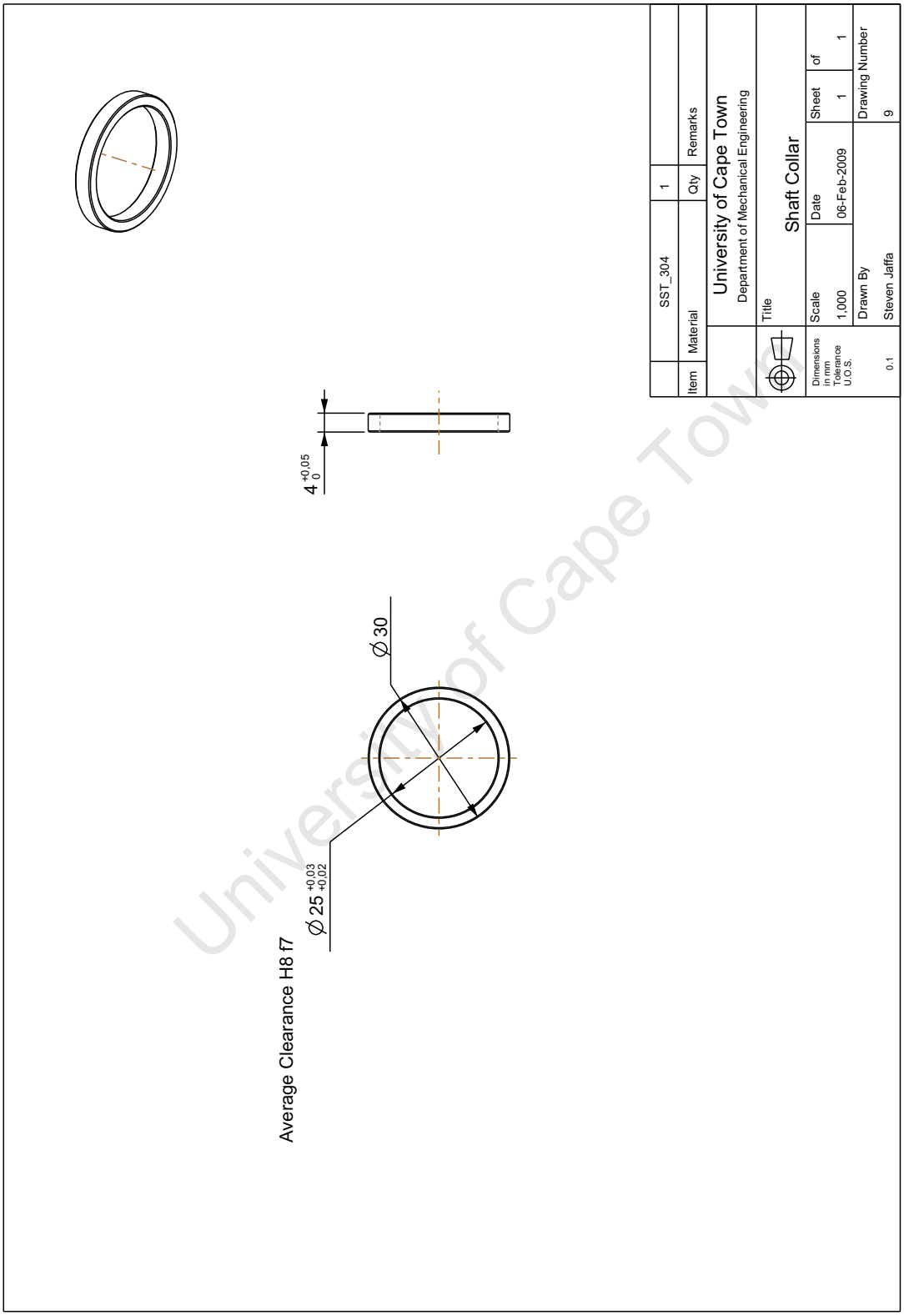

Figure F.11: Manufacturing Drawing: Pulley Shaft Collar.

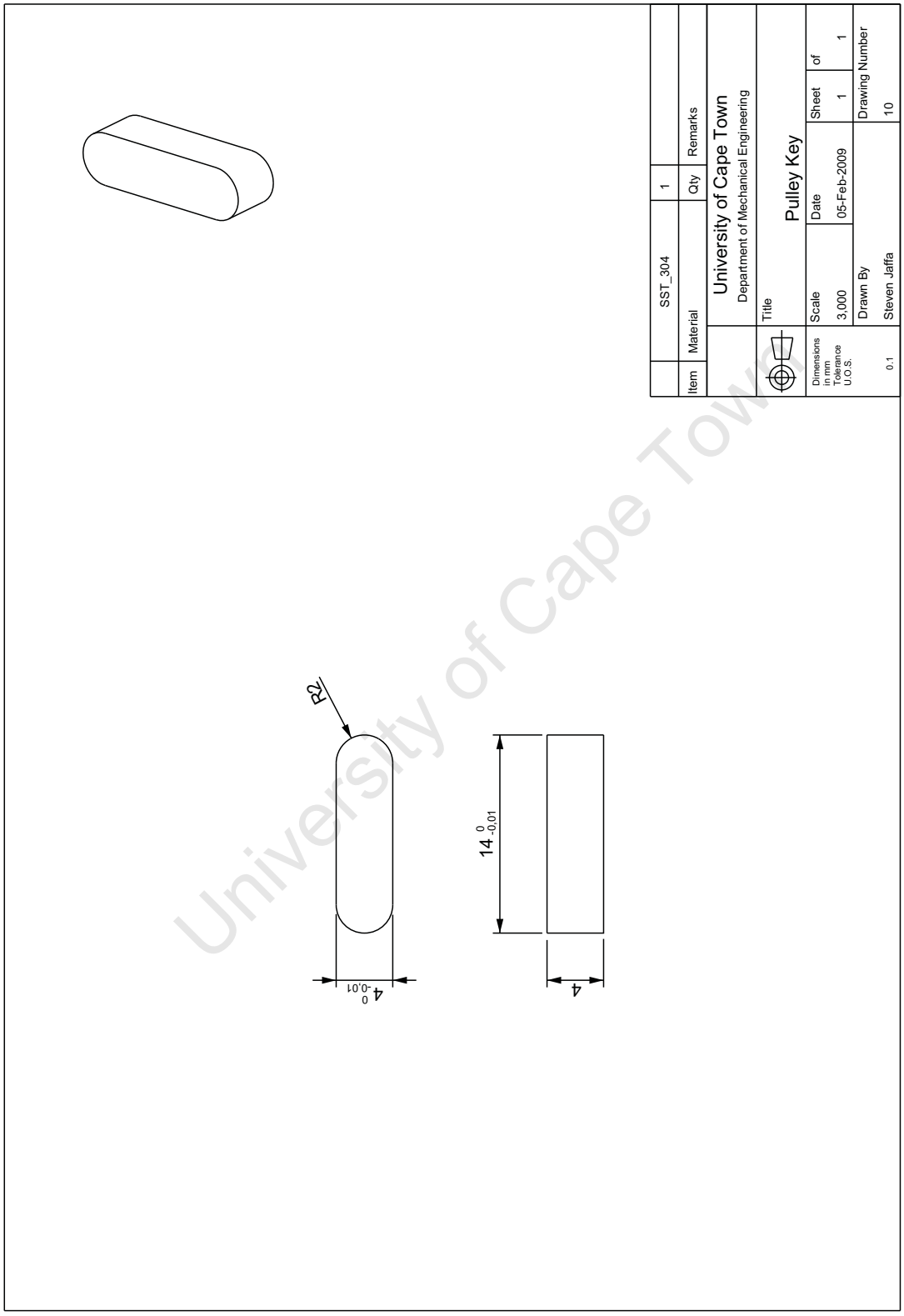

Figure F.12: Manufacturing Drawing: Pulley Key.

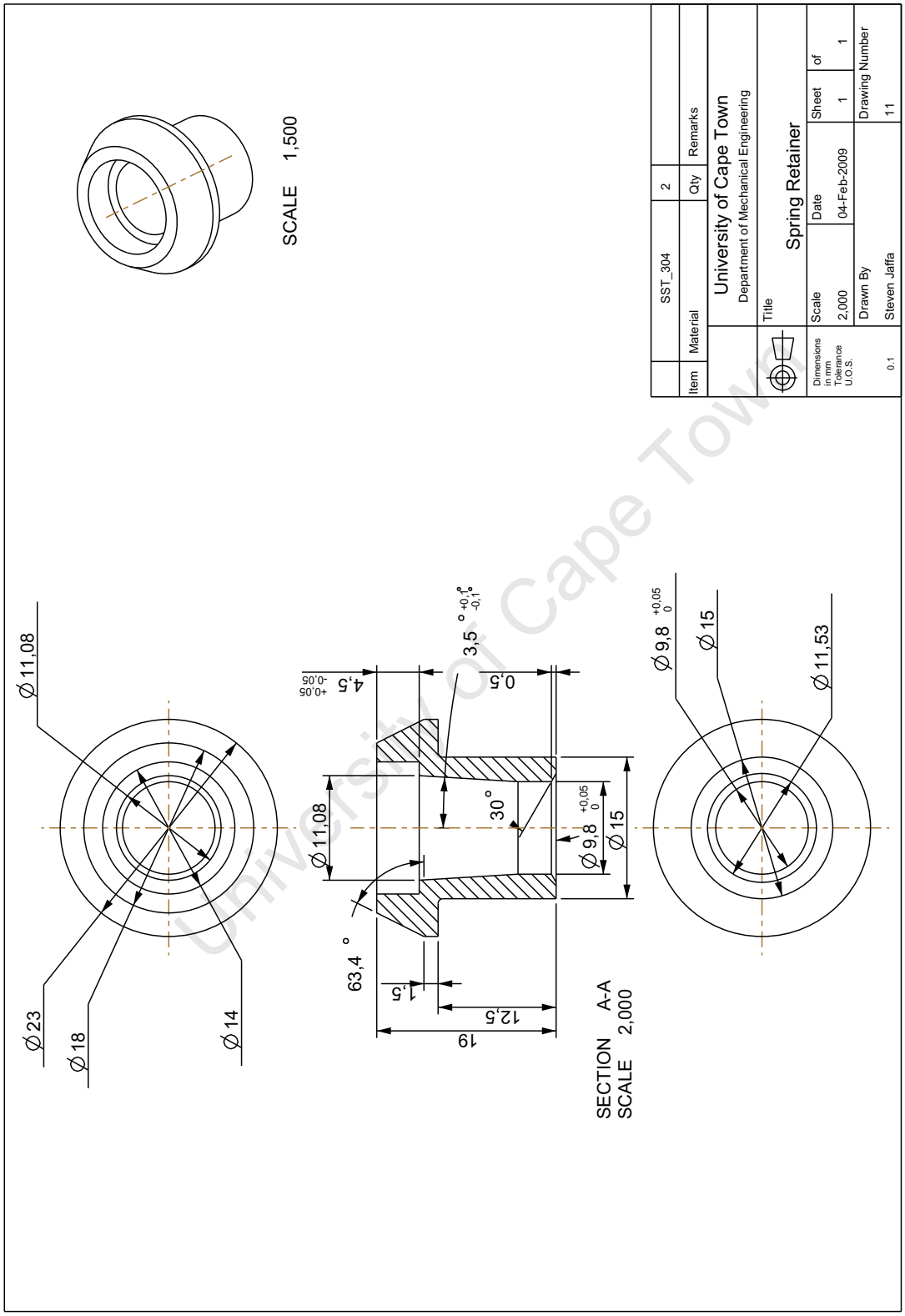

Figure F.13: Manufacturing Drawing: Spring Retainer.

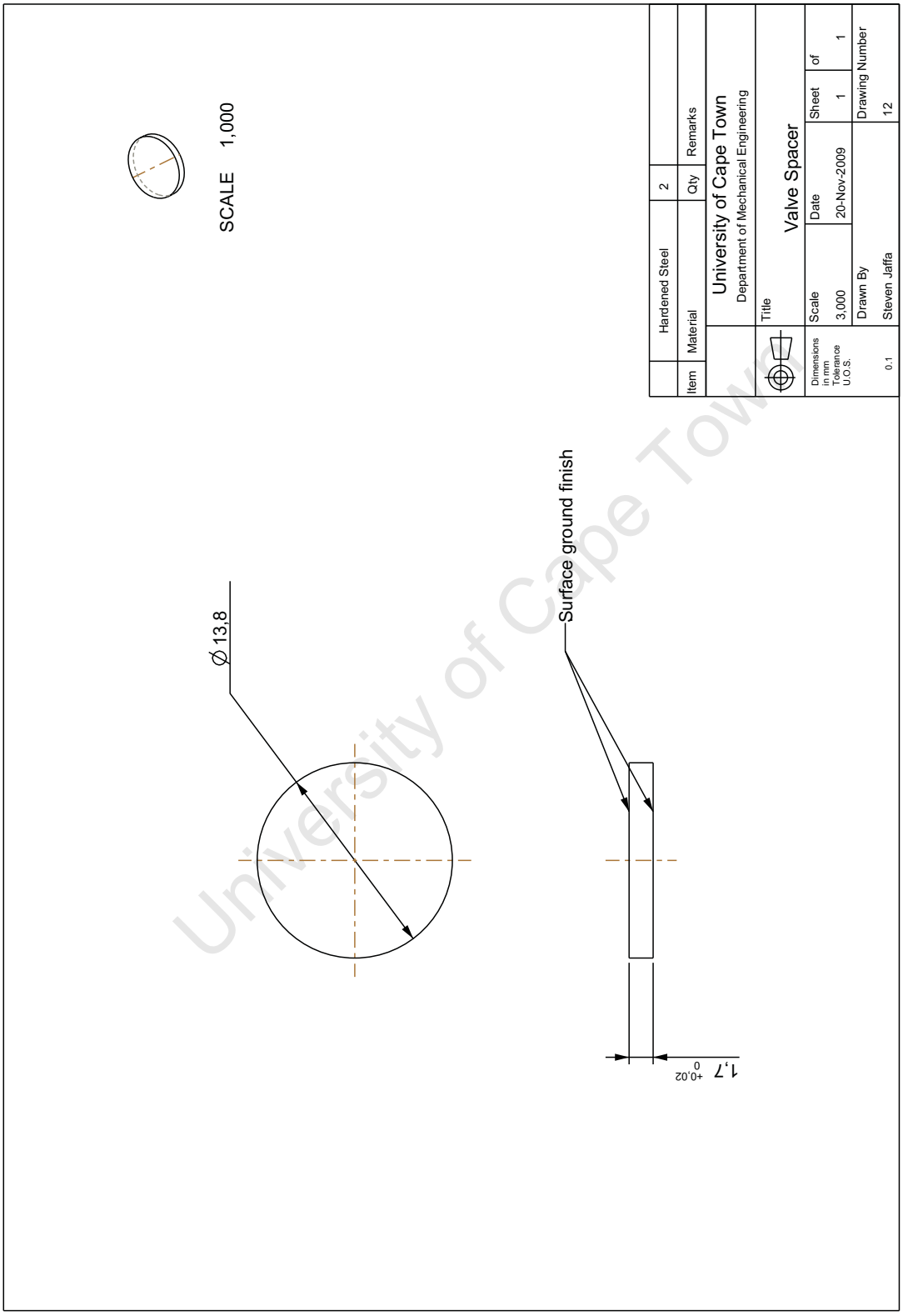

Figure F.14: Manufacturing Drawing: Valve Spacer.

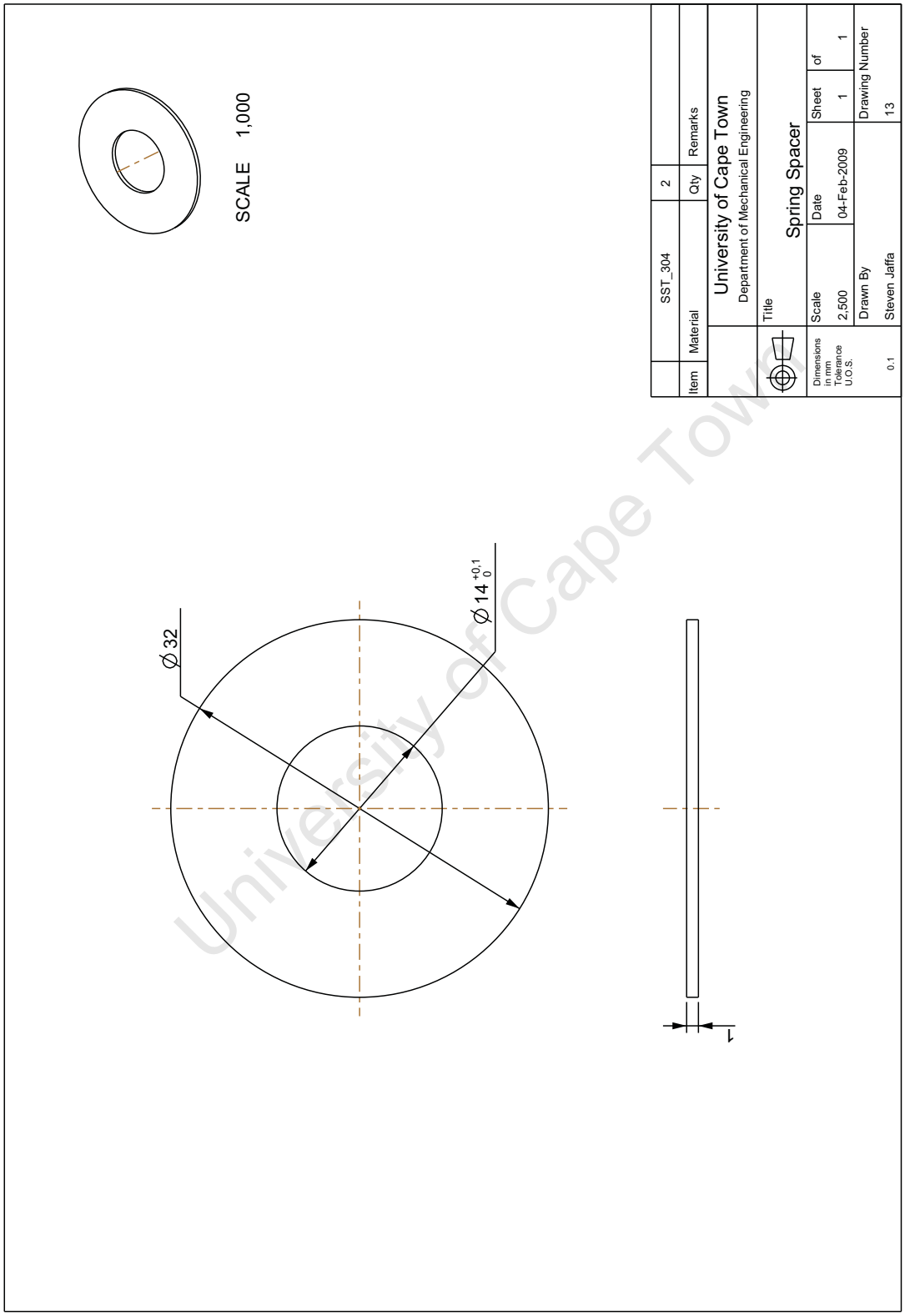

Figure F.15: Manufacturing Drawing: Spring Spacer.

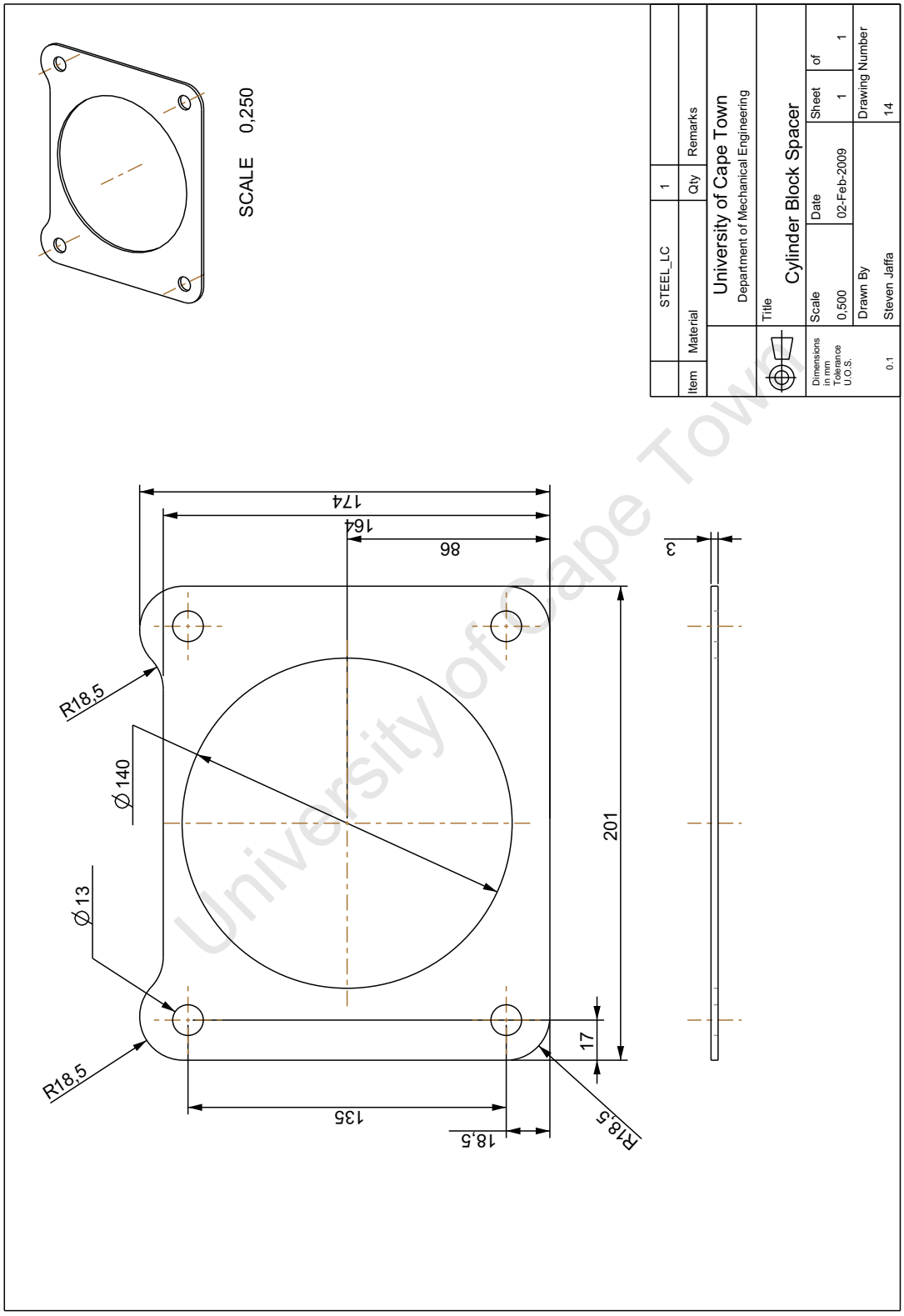

Figure F.16: Manufacturing Drawing: Cylinder Block Spacer.

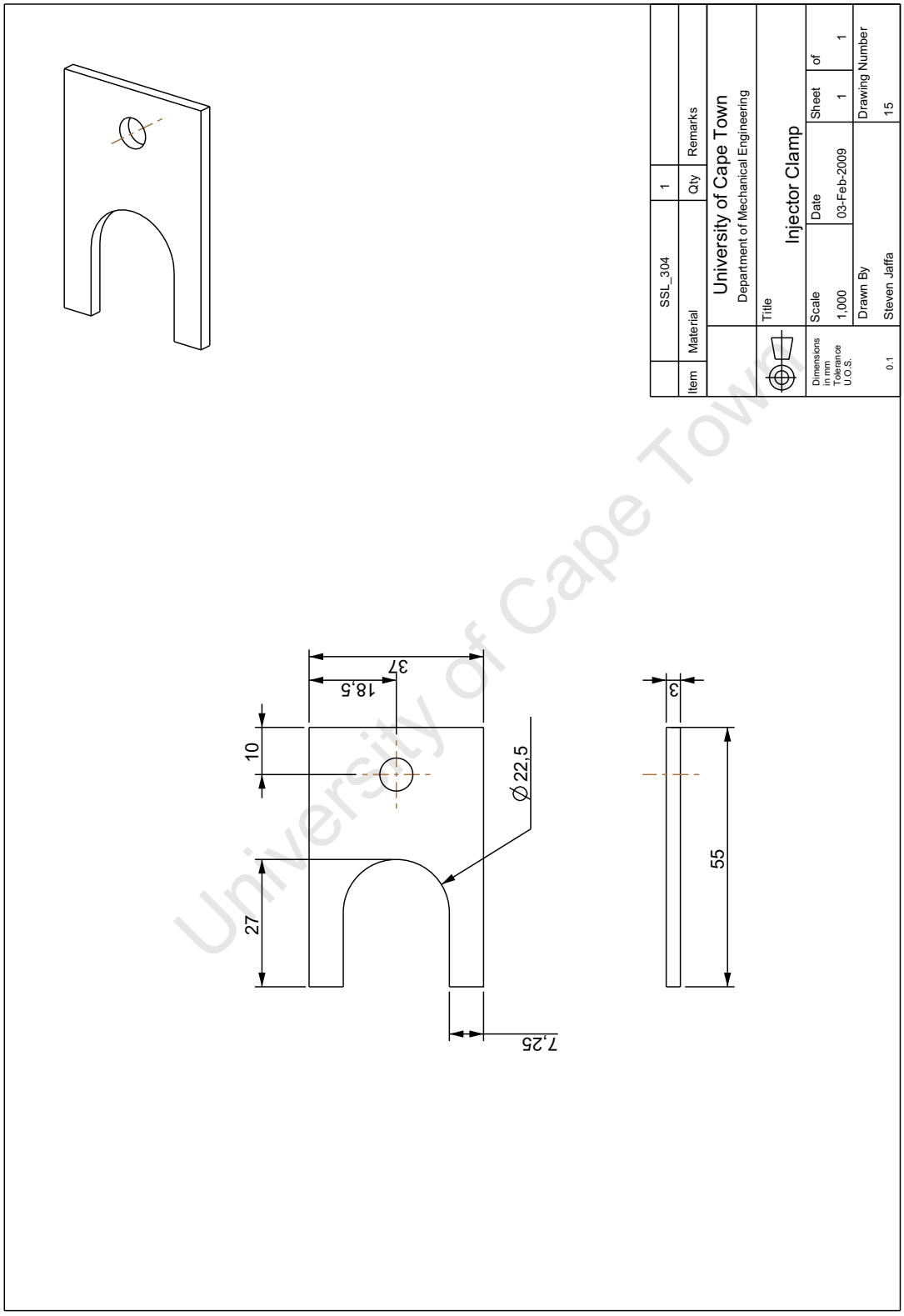

Figure F.17: Manufacturing Drawing: Injector Clamp.

F.2 Cargine Drawings

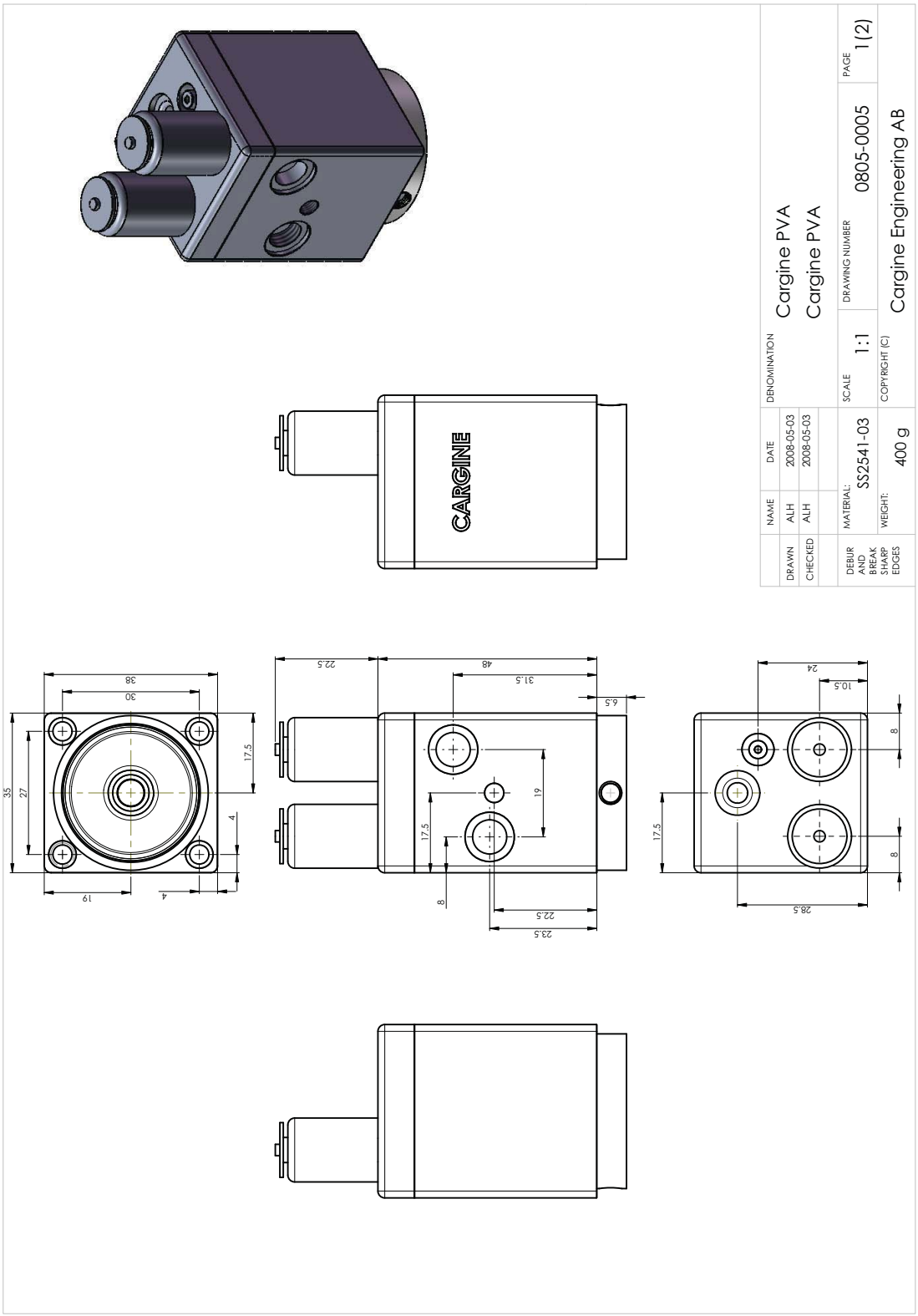

Figure F.18: Technical Drawing: Cargine Pneumatic Actuator – Part 1 [45].

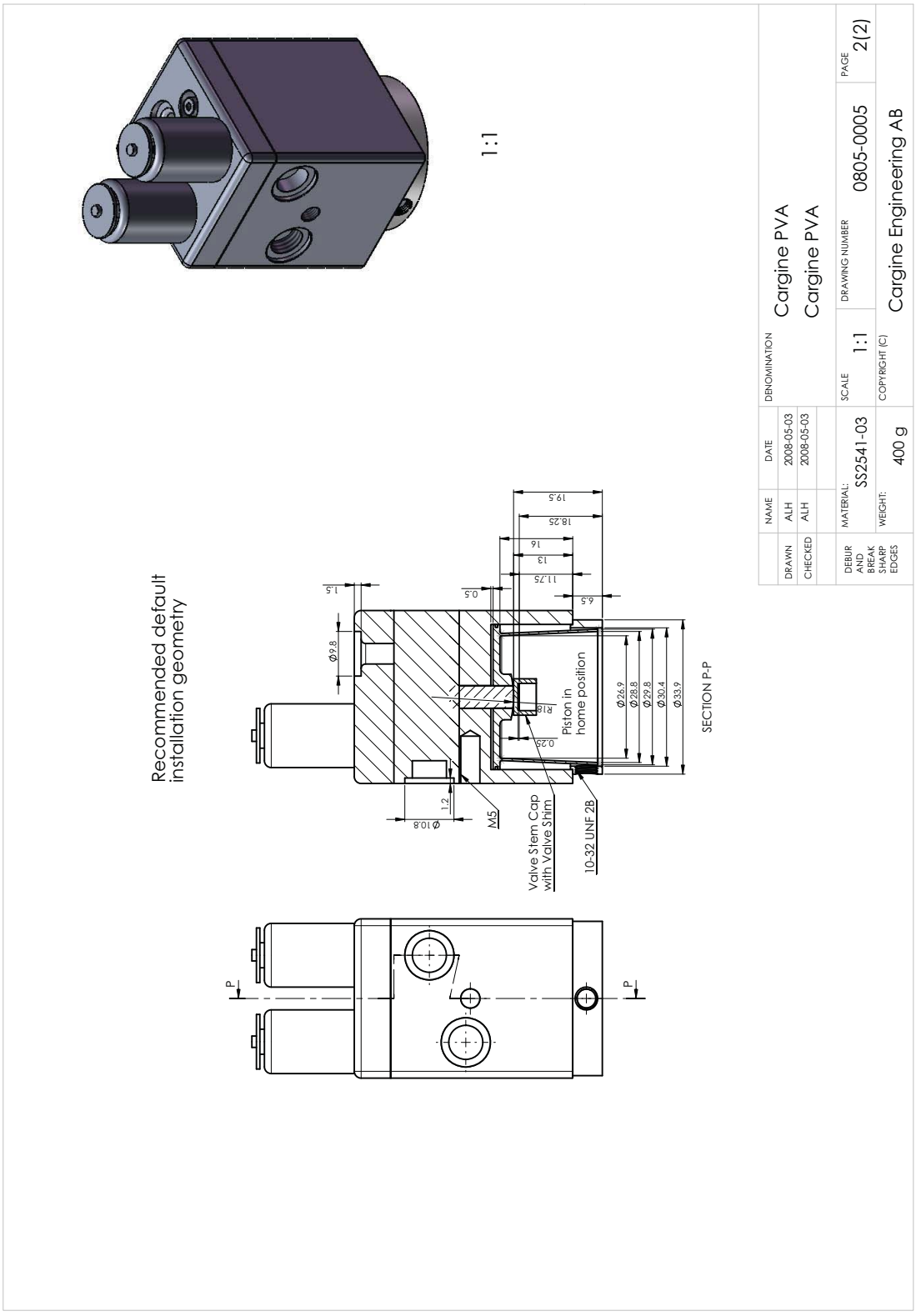

Figure F.19: Technical Drawing: Cargine Pneumatic Actuator – Part 2 [45].

F.3 MicroStrain Drawings

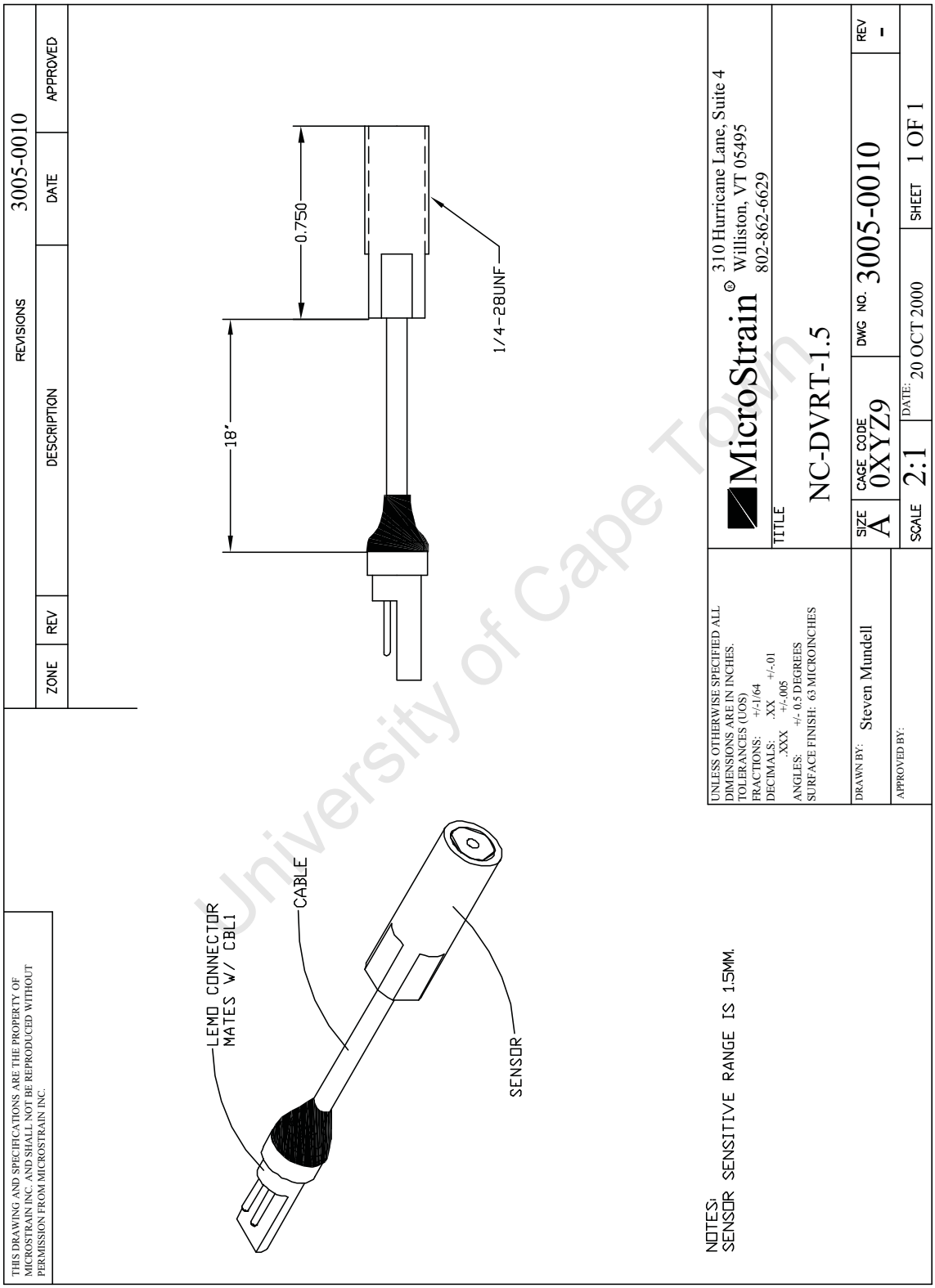

Figure F.20: Technical Drawing: Microstrain Sensor NC-DVRT-1.5.

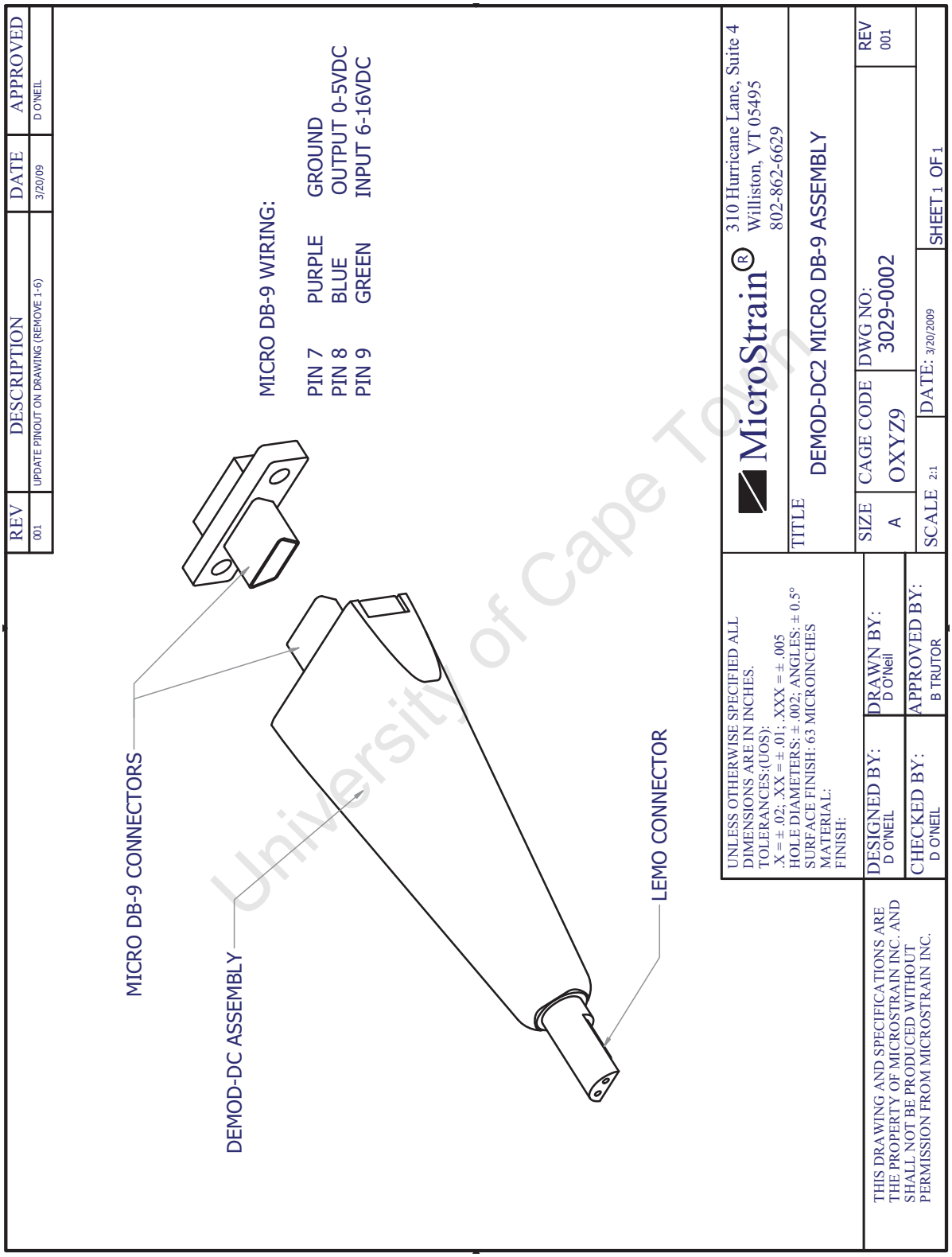

Figure F.21: Technical Drawing: Microstrain Signal Conditioner DEMOD-DC.